

Patch Loading Resistance of Plated Girders
-Ultimate and serviceability limit state-

Jonas Gozzi

Luleå University of Technology
Department of Civil, Mining and Environmental Engineering
Division of Structural Engineering - Steel Structures

Doctoral Thesis 2007:30

Patch Loading Resistance of Plated Girders

-Ultimate and serviceability limit state-

Jonas Gozzi

Luleå University of Technology
Department of Civil and Environmental Engineering
Division of Structural Engineering - Steel Structures
SE - 971 87 Luleå, Sweden
www.ltu.se

June 2007

PREFACE

After almost three years of work regarding constitutive models and mechanical behaviour of steel, which ended up in my Licentiate thesis, my supervisor Professor **Ove Lagerqvist** asked me if I could picture myself working with patch loading the next couple of years. Since I was rather tired of material modelling, which by the way isn't that related to the other research conducted at the division, I said yes without any doubts. If that was the right answer I still don't know but it clearly was inspiring to focus on something else, and further, it brought Ove closer to my research which has been a pleasure for me. Not to mention his invaluable knowledge in the field, his ideas and his inventive jokes. Thanks for these years!

The change of research subject also involved the newly retired Professor **Bernt Johansson** in my project. I am sincerely grateful for your engagement, your ideas and your comments on the content in this thesis!

However, none of this would have been possible without the financial support from the Research Fund for Coal and Steel, RFCS, who sponsored the project ComBri, "*Competitive Steel and Composite Bridges by Improved Steel Plated Structures*", in which most of the work in this thesis was conducted. Further, also the Development Fund of the Swedish Construction Industry, SBUF, and Luleå University of Technology have contributed financially to this work. They are all hereby thankfully acknowledged.

My professional collaboration with Dr. **Anders Olsson** ended with the Licentiate thesis but you stayed as a friend and sounding-board even afterwards. Thanks for careful reading of the manuscript and I look forward to late-night Dry Martinis on your terrace now that we are almost neighbours!

Friends and colleagues at the Division of Structural Engineering in general and the research group for Steel Structures in particular, headed by associate professor **Milan Veljkovic** who always have interesting ideas when it comes to FEM, are hereby deeply acknowledged. I will really miss you now when my journey continues elsewhere.

The experimental work carried out in this thesis would not have been possible without the qualified personnel at Complab, especially **Georg Danielsson, Lars Åström** and **Claes Fahleson** deserves an acknowledgement.

Further, also my science partner **Mattias Clarin** was deeply involved in the experimental part of this work as well as in the finite element studies of the tested girders. We have experienced a lot during the years, from hunted by a crazy lady in Shanghai and skiing trips to the “Country boarder” to early and heavy field trips after “Stålbyggnadsdagen” and several discussions late at nights both related to work but mostly not. I am very grateful for your support and collaboration, thanks mate!

In January 2007 me and my family left Luleå for new adventures. I got a job opportunity at SSAB Tunnpått and I am very thankful to **Joachim Larsson** and **Janne Kuoppa** who gave me the chance to finish this thesis here in Borlänge! Also the rest of the Design group are acknowledged for treating me as a team member even though I have mostly focused on this thesis.

Last but definitely not least, the persons who really supported me and made me finish the thesis without spending too many late nights and weekends at work, my wife **Lina** and our daughter **Elsa**. I give you all my love!

Borlänge, June 2007

Jonas Gozzi

SUMMARY

Patch loading or partial edge loading of steel girder webs is a load case where a concentrated force is introduced perpendicular to the flange of a girder. This usually induces a local failure of the girder web in the vicinity of the loaded flange. In structural applications concentrated forces are a common load case for girders introduced for example; at supports, by purlins, from crane wheels and during launching of bridges. For fixed loads, the problem of concentrated forces are usually solved by transverse stiffeners but for moving loads this is not practically possible neither an economical solution. Further, it would be possible to use longitudinal stiffeners when the load is moving but stiffeners are expensive to fit and for girders with web depth below 3 m longitudinally stiffeners are not economically justified. Instead, the girder web itself has to resist the applied load in such cases.

From the fifties and later a large amount of studies on this subject have been performed, starting with investigations on the elastic buckling of plates where only a part of the edge was loaded and followed by many test series and resistance functions. The earlier proposed resistance models were usually divided into two separate checks, one for yielding and one for instability. However, the test results do not show of any clear distinction between those two cases.

This thesis deals with patch loading of plated girders without longitudinal stiffeners in both the ultimate and the serviceability limit state. A resistance model in the ultimate limit state is proposed, that have a continuous transition from yielding to buckling and hence, that is harmonized with the procedure for other buckling problems. The model contains three significant parts; the yield resistance, the elastic buckling load used to establish the slenderness and a reduction factor that relates the slenderness to the actual resistance. The advantage with the design model presented herein, which is a modification of the work presented by Lagerqvist (1994) and later introduced in EN 1993-1-5 (2006), is that the same equations are used irrespective of failure mode. The in this thesis proposed design procedure for patch loading gives a better accuracy of the predicted resistance compared to the design rule in EN 1993-1-5.

Most of the experimental studies performed by others contain tests with very short loaded lengths, i.e. very concentrated loads. In order to gain more knowledge of the influence of the loaded length, three patch load tests were conducted where only the loaded length was varied. By means of the test results and a parametric study with the finite element method it was concluded that the variation in loaded length could be well described by the design procedure proposed in this thesis.

For a bridge girder, the problem concerning resistance to patch loading usually occurs during launching. Bridge launching is a common method to erect steel and composite bridges and means that the bridge girders are assembled on ground behind the abutment and then pushed out over launching shoes into the final position. The launching shoe on which the girder travels will introduce a concentrated force to the girder, which can be of a magnitude that governs the web thickness and even a small increase of the web thickness can add a substantial amount of steel. Therefore, it is important to find a suitable criterion for the serviceability limit state for patch loading, i.e. for bridge launching. Compared to the ultimate resistance the amount of available research considering the serviceability limit state is very limited. In fact, only one serviceability limit criterion proposed by Granath (2000), which was developed for stationary loadings, was found.

A number of FE-analyses of the launching process were carried out to investigate at what loads different girder cross sections will have a repeatable behaviour. A girder section of a bridge girder was subjected to several repeated travelling loads corresponding to a long bridge girder launched over several supports together with a co-existing bending moment. By means of these FE-analyses a serviceability criterion is established with a limit criterion not allowing any effective plastic membrane strains. The bridge designer can beneficially use the proposed serviceability criterion for bridge launching.

SAMMANFATTNING

I flertalet praktiska fall belastas stålbalkar av koncentrerade laster. Detta lastfall kallas lokal intryckning och det ger upphov till vertikala tryckspänningar i balklivet som är störst under den belastade flänsen och avtar sedan till den motsatta flänsen. Koncentrerade laster kan t ex uppträda vid stöd, under åsar, som hjultryck på kranbanebalkar och vid lansering av brobalkar. För laster som har ett bestämt läge, som t ex vid stöd, löses problemet oftast med tväravstyvningar. När rörliga laster är aktuella är det dock lite svårare. För det första är avstyvningar generellt sett dyra att montera och för det andra är det naturligtvis inte möjligt att ha avstyvningar överallt när lasten förflyttas. Ett annat alternativ är längsgående avstyvningar som höjer bärförmågan med avseende på lokal intryckning men dessa är förstås också dyra att montera. För höga balkar, över 3 m, behövs ofta längsgående avstyvningar av andra skäl men för balkar under 3 m är det inte ekonomiskt försvarbart. Med andra ord måste rörliga laster för balkar med en livhöjd under 3 m bäras av livet självt och för det krävs tillförlitliga dimensioneringsregler.

Föreliggande avhandling behandlar lokal intryckning av svetsade balkar utan längsgående avstyvningar i brott- och bruksgränstillstånd. När det gäller brottgränstillstånd finns det stora mängder publicerat material från provning och inom områdena kritisk bucklingslast samt bärförmågefunktioner. Tidigare var ofta bärförmågefunktionerna uppdelade på två funktioner, en för flytning och en för instabilitet. Det är dock svårt att separera dessa och inga försök visar på en klar skillnad mellan flytning och instabilitet. Lagerqvist (1994) tog ett stort steg i detta avseende och föreslog en bärförmågefunktion harmoniserad med de modeller som används vid andra bucklings- och stabilitetsproblem. Det innebär att modellen har en gradvis övergång mellan flytning och buckling. Beräkningsmodellen består av tre olika delar, ett uttryck för den plastiska bärförmågan, den kritiska bucklingslasten och en reduktionsfaktor som är empiriskt kalibrerad mot försöksdata. Lagerqvists modell har senare blivit implementerad i Eurokod 3 del 1.5, EN 1993-1-5 (2006). I denna avhandling föreslås en modifierad variant av bärförmågefunktionen i Eurokod 3 som ger mindre spridning jämfört med försöksdata och dessutom avlägsnar den diskontinuitet som finns i beräkningsmodellen idag.

Vidare har nästan all tidigare forskning fokuserats på mycket koncentrerade laster, d v s korta lastlängder. För att öka förståelsen för lastlängdens inverkan på bärförmågan och för att fylla luckorna i försöksdatabasen har tre försök utförts i detta arbete. Försöken genomfördes på tre identiska svetsade balkar med tre olika lastlängder. Utifrån försöksresultaten och en efterföljande parameterstudie med hjälp av finita elementmetoden kunde det konstateras att den

föreslagna bärförmågefunktionen också kan användas för långa lastlängder. Upp till 1,2 gånger livhöjden kontrollerades med tillfredställande resultat.

När det gäller bruksgränstillstånd finns det betydligt färre publicerade artiklar. Det enda egentliga kriteriet föreslogs av Granath (2000) för balkar utsatta för en stationär koncentrerad last. En brobalk utsätts normalt endast för intryckning under själva produktionen, d v s om den lanseras. Lansering av stålbroar och samverkansbroar är vanligt, speciellt långa broar som är för tunga att lyftas på plats. Vidare är det en bra metod om bron skall sträcka sig över vatten eller vägar/järnvägar och området under bron ej kan användas. Under lanseringen sammanfogas brobalkar bakom ena landfästet och skjuts sedan ut över lanseringslager till dess slutliga position. Vid lanseringen utsätts stålbalkarna för relativt stora koncentrerade laster från stöden som balken glider på. Dessa laster är alltså inte stationära utan rörliga och kan vara så stora att de bestämmer livtjockleken. Eftersom en liten ökning i livtjocklek skulle öka mängden stål avsevärt är det därför viktigt att på ett bra sätt kunna uppskatta livets bärförmåga i ett sådant fall. Eftersom detta kan ses som ett bruksgränstillstånd och inte är det lastfall som brobalken är dimensionerad för primärt, bör kravet vara att balken ej ska få kvarstående deformationer under lanseringen. Om brobalken dessutom lanseras över många stöd och om kvarstående deformationer uppstår som växer vid varje ny passage kan det bli problem att bära de laster som balken egentligen var dimensionerad för. Vidare har det blivit vanligare att lansera brobalkar där betongfarbanan gjuts innan lanseringen. Detta ökar förstås egentytngden och därigenom också de koncentrerade lasterna från lanseringslagren.

I denna avhandling har detta studerats med hjälp av finita elementanalyser av broelement. Ett antal olika tvärsnitt har utsatts för ett konstant böjande moment och en koncentrerad last som vandrar längs flänsen. Detta har upprepats tre gånger och en last har bestämts när inga effektiva plastiska membrantöjningar har utvecklats i livet vilket i sin tur innebär att de kvarstående deformationerna ej växer för varje ny lastpassage. Utifrån dessa laster har ett bruksgränskriterium etablerats för brolansering, d v s för rörliga laster.

NOTATIONS AND SYMBOLS

Notations and symbols used in this thesis are listed and explained here in alphabetical order.

a	width of web panel between transverse stiffeners
α	distance between yield lines in the web
α, α_F	imperfection factor
b	correction factor
b	width
b_{eff}	effective width
b_f	flange width
β	$\frac{G \cdot K}{D \cdot h_w}$
β, β_1, β_2	distance between plastic hinges in the flange
c_u	half of the length of the web resisting the applied force
D	plate stiffness
δ	error term
δ	web imperfection
δ_i	observed error term for test specimen i obtained from a comparison of r_{e_i} and $b \cdot r_{t_i}$
δ_w	vertical displacement of flange under load
E	Young's modulus
ε	strain
$\varepsilon_{\text{yield}}$	total strain at yield point
f^*	reference yield strength taken as 300 MPa
f_u	ultimate tensile strength
f_y	yield strength
$f_{y,\text{nom}}$	nominal yield strength

f_{yw}	yield strength of the web material
f_{yf}	yield strength of the flange material
F	safety factor
F	applied force in test
F_E	applied transverse force or patch load
F_{FE}	applied transverse force in finite element simulations in the serviceability limit state
$F_{FE,sls}$	level of applied transverse force that gave reversible behaviour according to finite element simulations
F_{FEM}	load where no effective stresses above the yield strength appear at the web surface from finite element analysis
F_{cr}	elastic critical buckling load
F_R	patch loading resistance
F_{Rc}	patch loading resistance, crippling or buckling
F_{Rd}	design resistance
F_{Ry}	patch loading resistance, yielding
$F_{R,int}$	patch loading resistance recalculated to fulfil the interaction equation with bending moment
$F_{R,sls}$	patch loading resistance in the serviceability limit state
$F_{slender}$	patch loading resistance in the serviceability limit state, slender girders
F_{stocky}	patch loading resistance in the serviceability limit state, stocky girders
F_u	ultimate load from test
$F_{u,FE}$	ultimate load from finite element analysis
F_y	yield resistance
$g_{rt}(X)$	resistance function of the basic variables used as design model
$G \cdot K$	torsional stiffness of the flange
γ	distance from loaded flange to first yield line in the web
γ_M	partial factor for the resistance
γ_M^*	corrected partial factor for resistance

γ_{M1}	partial factor for members susceptible to instability
h_w	web depth
η	yielded length of the web not offering any resistance to bending deformations
η	generalized imperfection factor, $\eta = \alpha \cdot (\bar{\lambda} - \bar{\lambda}_0)$
I_f	second moment of area, flange
χ	reduction factor
χ_F	reduction factor for patch loading
$\chi_{F,sls}$	reduction factor for the serviceability limit state that reduces the ultimate resistance to a serviceability resistance
$k_{d,n}$	design fractile factor
k_n	characteristic fractile factor
k_σ	buckling coefficient for plate buckling
k_F	buckling coefficient for patch loading
k_{Fs}	buckling coefficient for a simply supported plate
k_{Fc}	buckling coefficient for a plate with clamped longitudinal edges
K	numerical constant
l_y	effective loaded length
$l_{y,FE}$	effective loaded length obtained from finite element analysis
$\bar{l}_{y,FE}$	normalized effective loaded length from finite element analysis
\bar{l}_{y,m_1+m_2}	effective loaded length, including both m_1 and m_2 , normalized with $l_{y,FE}$
\bar{l}_{y,m_1}	effective loaded length, including only m_1 , normalized with $l_{y,FE}$
L_{eff}	effective length for resistance to transverse forces, $L_{eff} = \chi_F \cdot l_y$
λ	correction factor taking into account the influence from a/h_w on k_F
λ	a function of the girder dimensions and material properties
$\bar{\lambda}$	slenderness parameter
$\bar{\lambda}_0, \bar{\lambda}_{F0}$	plateau length
$\bar{\lambda}_F$	slenderness parameter for patch loading
m	average

M_0	initially applied external bending moment in finite element analysis
M_E	applied bending moment
M_i	plastic moment resistance, inner plastic hinge
M_o	plastic moment resistance, outer plastic hinge
M_{pf}	plastic moment resistance, flange
M_{pw}	plastic moment resistance, web
M_R	bending moment resistance according to EN 1993-1-5
$M_{u,FE}$	ultimate bending moment from finite element analysis
μ	friction coefficient
ν	Poisson's ratio
r	resistance value
r_d	design value of the resistance
r_e	experimental resistance value
r_{ei}	experimental resistance value for specimen i
r_k	characteristic value of the resistance
r_m	resistance value calculated using the mean values \underline{X}_m of the basic variables
r_n	nominal value of the resistance
r_t	theoretical resistance determined from the resistance function $g_{rt}(\underline{X})$
r_{ti}	theoretical resistance determined using the measured parameters \underline{X} for specimen i
s	standard deviation
s_s	loaded length
s_y	distance between plastic hinges in the flange
σ	stress
$\bar{\sigma}$	mean stress
σ_c	compression stress
σ_{cr}	critical stress
σ_{max}	maximum stress

σ_{\min}	minimum stress
σ_w	stress in the web
t	thickness
t^*	reference web thickness taken as 2,5 mm
t_i	idealized flange thickness
t_{nom}	nominal web thickness
t_f	flange thickness
t_w	web thickness
θ	angle defining the deformation of the web at the yield lines
V	coefficient of variation
V_δ	estimator for the coefficient of variation of the error term δ
V_E	applied shear
V_R	shear resistance
V_r	$V_r = \sqrt{V_\delta^2 + V_{rt}^2}$
V_{rt}	coefficient of variation of the basic variables, $V_{rt} = 0,08$
W	section modulus
W_{eff}	effective section modulus according to EN 1993-1-5
W_{el}	elastic section modulus
\bar{x}_{error}	mean deviation from 1
\underline{X}	basic variables X_1, \dots, X_j
\underline{X}_m	mean values of the basic variables

TABLE OF CONTENTS

PREFACE	I
SUMMARY	III
SAMMANFATTNING	V
NOTATIONS AND SYMBOLS	VII
TABLE OF CONTENTS	XIII
1 INTRODUCTION	1
1.1 Background	1
1.2 Scope and limitations	3
1.3 Outline and content	4
2 REVIEW OF EARLIER WORK	5
2.1 General	5
2.1.1 Approach for design of structural elements subjected to buckling	6
2.2 Elastic critical buckling load	9
2.3 Ultimate resistance	18
2.3.1 Empirical models and other non-mechanism models	18
2.3.2 Mechanism models	22
2.3.3 Interaction with bending moment	39
2.3.4 Interaction with shear	42
2.3.5 Review of experimental investigations	43
2.4 Serviceability limit state	43
2.5 Summary of the review	48

3	EXPERIMENTAL WORK	51
3.1	General	51
3.2	Uniaxial coupon tests	51
3.3	Patch loading tests	52
3.3.1	Geometry and test set-up	52
3.3.2	Measurements	55
3.4	Test results	58
3.4.1	P200	58
3.4.2	P700	64
3.4.3	P1440	69
3.5	Concluding remarks from the experimental work	74
4	NUMERICAL STUDY	77
4.1	General	77
4.2	Finite element model	77
4.3	Calibration	79
4.4	Parametric study	82
4.5	Concluding remarks from the numerical study	83
5	PATCH LOADING RESISTANCE	85
5.1	General	85
5.2	Yield resistance	85
5.3	Proposed design procedure	92
5.4	Statistical evaluation of the proposed design procedure	101
5.5	Comparison with other models	102
5.6	Concluding remarks	104
6	BRIDGE LAUNCHING - A SERVICEABILITY LIMIT STATE	107
6.1	General	107
6.2	Bridge launching	108
6.3	Numerical study	110
6.3.1	Finite element model and method	111
6.3.2	Results from the numerical study	115
6.4	Proposed criteria for bridge launching	121
6.5	Concluding remarks	124

7	DISCUSSION AND CONCLUSIONS	127
7.1	Discussion	127
7.2	Conclusions	131
7.3	Future work	132
	REFERENCES	133
	APPENDIX A UNIAXIAL COUPON TESTS	139
	APPENDIX B PATCH LOADING TESTS	143
B.1	Measured girder dimensions	143
B.2	Strain gauge layout on girder webs	143
B.3	Force - strain curves for the P200 test	144
B.4	Force - strain curves for the P700 test	147
B.5	Force - strain curves for the P1440 test	149
	APPENDIX C DATA FROM TESTS BY OTHERS	151
	APPENDIX D INFLUENCE OF VARIOUS PARAMETERS	169
	APPENDIX E ANNEX D OF EN 1990 (2002)	173

1 INTRODUCTION

1.1 Background

It is common that steel girders in structures are subjected to concentrated transverse forces. Such concentrated forces acting perpendicular to the flange is denoted patch loading. In general structures such problems are usually solved by transverse stiffeners. This solution works well when the load is fixed at a position for example at supports. However, stiffeners are expensive to fit and if the load is moving, e.g. crane wheels, it is difficult to solve the problem in this way. Another example which also is difficult to solve by transverse stiffeners is launching of bridges. This is a common method to erect steel and composite bridges to heavy to lift into position. Instead, the bridge sections are assembled on ground behind the abutment and then pushed out over launching shoes or rollers into position. In this case concentrated forces are introduced to the girders from the launching shoe. Further, as the girder is launched the support reactions from the launching shoes are introduced to the girders at various positions along the girder. These concentrated forces can be of the magnitude that governs the web thickness and even a small increase of the web thickness may add a substantial amount of steel. Moreover, there is a trend in construction of composite bridges to cast the concrete bridge deck before launching, which obviously increases the self weight and consequently also the concentrated forces from the launching shoes.

For large bridges with long spans it is common that longitudinal stiffeners are attached to the web for different reasons, e.g. buckling due to bending. It was early established that such longitudinal stiffeners also increase the patch loading resistance to some extent. Generally, for girders with web depth below 3 m such longitudinally stiffeners should not be used for economical reasons but for deeper girders they might be necessary. Several studies considering the patch loading resistance of longitudinally stiffened girder webs have been carried out, e.g. by Graciano and Johansson (2003), Kuhlmann and Seitz (2004), Davaine and Aribert (2005) and recently Clarin (2007).

Between 2003 and 2006 the RFCS (Research Fund for Coal and Steel) sponsored research project ComBri (2007) “*Competitive Steel and Composite Bridges by Improved Steel Plated Structures*”, was carried out. The objective was to promote the wider use of steel plated structures in bridges and to improve steel plated cross sections in steel and composite bridges for the final and execution state. The project was divided into different work packages considering for example shear resistance, bending resistance and patch loading resistance. Most of the work presented in this thesis was conducted within the ComBri project.

This thesis deals with patch loading resistance of plated girders without longitudinal stiffeners in both the ultimate and serviceability limit state. Considering the ultimate limit state the amount of published research is substantial and there are a great number of different proposals for how to determine the resistance. Lagerqvist (1994) took a great step forward introducing a design procedure not only valid for the three different cases, i.e. patch loading, opposite patch loading and end patch loading, but also harmonized with the design rules for other kinds of buckling problems. Before this it was common to have two criteria for the resistance, one based on yielding and one based on instability. However, the test results do not show any clear distinction between those two cases. At the end it is always a buckle in the web under the load, which size increases with increasing web slenderness. Therefore, it is concluded that there is a gradual transition between yielding and buckling as for other instability problems and this was covered in a good manner by the design procedure by Lagerqvist.

The work concerning patch loading resistance in the ultimate limit state presented herein is a continuation and modification of the procedure presented by Lagerqvist. The main focus was on two areas. First, the yield resistance which have been up for discussion several times, for example within the ComBri project, and secondly, the simplest way to increase the resistance of the web for instance when it comes to launching of bridges is to increase the length of the launching device. It is therefore of interest to investigate how this influence the resistance and a study concerning the loaded length was carried out in this thesis both by means of tests and numerical analyses.

Considering the serviceability limit state, on the other hand, the amount of published research is very limited. The only actual criterion found was presented by Granath (2000), which was a criterion based on stationary loadings. The criterion proposed herein is focused on the loadings that are introduced to a steel girder during bridge launching, i.e. including a travelling or moving patch load. The criterion itself are defined by the demand that the deformations during launching should be reversible. For simplicity, the criterion is based on the ultimate patch loading resistance multiplied with a function depending on the slenderness of the girder. It is shown by finite element analyses that the demand of a reversible behaviour gave a decreased serviceability load compared to the ultimate resistance with decreasing slenderness.

1.2 Scope and limitations

The scope of the work presented in this thesis was:

- To obtain test results with respect to patch loading with varied loaded length.
- To perform a parametric study by means of a numerical study considering the influence from the loaded length on the patch loading resistance.
- To investigate whether the mechanism model developed for the yield resistance proposed by Lagerqvist (1994) is relevant or not.
- To formulate a design procedure for patch loading of plated girders in the ultimate limit state.
- To establish a serviceability limit state criterion developed for bridge launching, i.e. for travelling loads.

The following limitations were imposed on the work:

- The patch loading resistance was calibrated against a data base including I-girders only.
- The patch loading resistance was derived for plated girders only.
- Only the patch loading resistance was considered, i.e. not opposite or end patch loading.
- Only girders made of structural steel was included in the calibration of the patch loading resistance, i.e. not stainless steel girders.
- The serviceability limit state criterion for bridge launching was developed only by means of FE-results.

To the best of the authors knowledge the features that are original in this thesis are:

- The results from the tests considering the variation in loaded length.
- The design procedure considering patch loading resistance in the ultimate limit state.
- The serviceability limit state criterion developed for bridge launching.

1.3 Outline and content

Section 2 gives a review over the most important work found in the literature considering patch loading of girders without longitudinal stiffeners. It is divided into elastic critical buckling loads, resistance to patch loading in the ultimate limit state and serviceability limit state.

Sections 3 - 6 are the central parts of the thesis. In Section 3 the experimental work considering patch loading tests of girders with varying loaded length are presented. The uniaxial tensile tests performed on the plate material used in the tested girders are also described in Section 3. The calibration of the numerical model as well as a parametric study regarding the loaded length can be found in Section 4.

Section 5 contains the proposed design procedure regarding patch loading resistance in the ultimate limit state. It includes a numerical study considering the yield resistance and consequently the modified yield resistance. Further, Section 5 also includes the calibration of the new reduction factor as well as a statistical evaluation according to Annex D of EN 1990 (2002) aiming at determination of the partial safety factor, γ_{M1} . Finally, Section 5 comprises a comparison with other proposed design procedures.

A serviceability limit state criterion for bridge launching is presented in Section 6, which apart from the criterion itself also includes a large numerical study on girder sections subjected to a travelling patch load and a coexisting bending moment.

Section 7 comprises a general discussion and the conclusions from the work in this thesis together with some proposals for future work.

Additional test data which was decided to take up to much space in the body of this thesis are displayed in Appendix A and B. Appendix C includes the full test data base collected by Lagerqvist (1994) and complemented with the available work performed after that. Appendix D comprises graphs showing what influence different variables have on the patch loading resistance proposed here. Finally, Appendix E contains the procedure for determination of the partial safety factor that should be applied to the resistance according to Annex D of EN 1990 (2002).

2 REVIEW OF EARLIER WORK

2.1 General

Patch loading or partial edge loading of steel girder webs is an area studied by many researchers over the years. From the fifties and later a large amount of studies on the subject have been performed, starting with investigations on the elastic buckling of plates where only a part of the edge was loaded and was followed by many test series and resistance functions. The resistance functions were mainly fully empirical in the beginning but from the seventies and later also semi-empirical methods were presented. Those methods were based on some kind of mechanical model, which was adjusted to fit the experimental results. However, most of the resistance models developed were divided into two separate checks, one for yielding and one for web buckling or crippling, i.e. partial buckling of the web. Though, the test results do not show of any clear distinction between direct yielding and web buckling. Further, it was early established that the web thickness and the yield strength of the web are the most important parameters when predicting the ultimate resistance of a girder subjected to patch loading.

In the mid nineties a thorough review of the work performed in the field of patch loading until then was conducted by Lagerqvist (1994). The review contained a large amount of tests, work on the elastic critical buckling load for partial edge loading and various references concerning ultimate resistance formula for patch loading. Lagerqvist came up with a method for determining the ultimate resistance for patch loading and opposite patch loading as well as end patch loading. The method of Lagerqvist was harmonized with the methods for other buckling problems, see Section 2.1.1, i.e. the method was based on three parts; the yield resistance, a slenderness parameter and a reduction factor that relates the resistance to the slenderness. A slightly modified version of this method was also implemented in Eurocode 3 for plated structural elements, EN 1993-1-5 (2006), and will be thoroughly described later in this review.

Further, as the review by Lagerqvist includes a large number of references it was decided herein to only focus on the most important contributions, in the author's opinion, related to the work in this thesis. However, the data base of test results collected by Lagerqvist will be used for calibration of the herein proposed design model for patch loading.

In addition to the tests performed and found in the literature by Lagerqvist, other tests carried out after 1994 by others and by the author of this thesis are added to the data base. The new tests found in the literature are presented in Section 2.3.5 and the tests performed by the author are presented in Section 3.

Regarding serviceability limit state for girders subjected to patch loading there are a very limited amount of research available. The only proposed design model for serviceability limit state was presented by Granath (2000), which is described later in Section 2.4.

This review is divided into five parts starting with the elastic critical buckling load for a plate subjected to a partial edge load in Section 2.2. Section 2.3 describes the most important contributions regarding resistance functions for patch loading in the ultimate limit state. Section 2.3 also includes interaction between patch loading and bending moment, interaction between patch loading and shear and the last contributions to the test data base. Further, Section 2.4 deals with the somewhat limited work on serviceability limit state for girders subjected to patch loading. The review is then summarized in Section 2.5.

2.1.1 Approach for design of structural elements subjected to buckling

During the last 40 years a standard approach has been developed describing the resistance of structural elements subjected to various forms of buckling, see Figure 2.1. The approach includes a uniform transition between yielding and instability through three significant parts. First, a prediction of the yield resistance, F_y , that usually is taken as the maximum resistance ignoring strain hardening. Secondly, the theoretical elastic critical buckling load, F_{cr} , which is determined according to classical elastic buckling theory. F_{cr} is only used for the definition of the slenderness parameter

$$\lambda = \sqrt{\frac{F_y}{F_{cr}}} \quad (2.1)$$

The third element in the model is a function relating the resistance to the slenderness parameter

$$\chi = \frac{F_R}{F_y} = f(\lambda) \quad (2.2)$$

In Figure 2.1 it can be seen that different buckling problems are described by quite different χ -functions. If F_R would be equal to F_{cr} then together with Equation (2.1) we have

$$\chi = \frac{F_{cr}}{F_y} = \frac{1}{\lambda^2} \quad (2.3)$$

As can be seen in Figure 2.1 this function overestimates the resistance for column buckling except for high slenderness values.

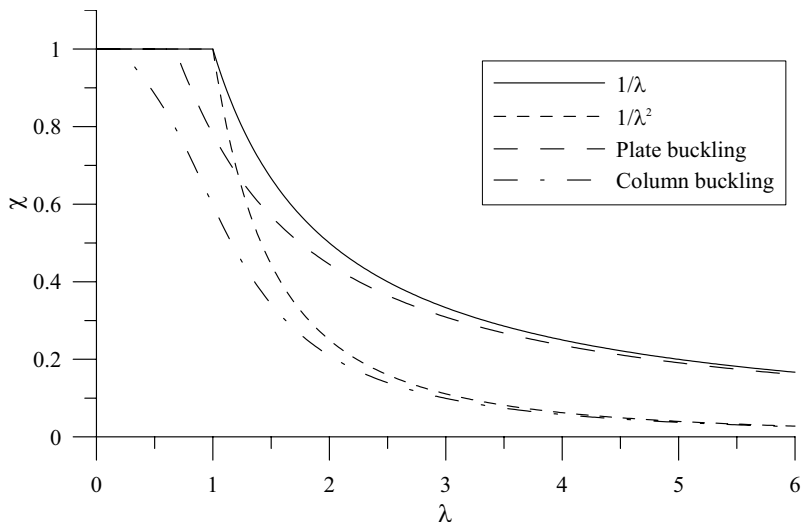


Figure 2.1 Different χ -functions for structural elements subjected to buckling.

It is well known that for plate buckling problems the classical critical load is not describing the ultimate resistance of a plate in compression. The resistance is very much influenced by the redistribution of stresses in the post critical range for plates supported along the edges. The effective width approach is one way of dealing with this phenomena.

In the effective width approach it is assumed that the ultimate load is reached when the maximum edge membrane stresses are equal to the yield strength of the material, f_y . As the buckle form in the middle of the plate, the stresses are redistributed as shown in Figure 2.2 for a simply supported plate uniformly compressed along two opposite edges.

This stress distribution is approximated by letting the maximum edge stress act uniformly over two strips of the plate while the middle part of the plate is neglected. If the width of each strip is $b_{\text{eff}}/2$ and if collapse occurs when the maximum edge stress reach f_y then

$$b_{\text{eff}} \cdot f_y = b \cdot \bar{\sigma} \tag{2.4}$$

von Kármán et al. (1932) proposed that the two strips with the total width of b_{eff} would fail when the critical buckling stress is equal to f_y , i.e.

$$f_y = \sigma_{\text{cr}} = k_{\sigma} \cdot \frac{\pi^2 \cdot E}{12 \cdot (1 - \nu^2)} \cdot \left(\frac{t}{b_{\text{eff}}}\right)^2 \tag{2.5}$$

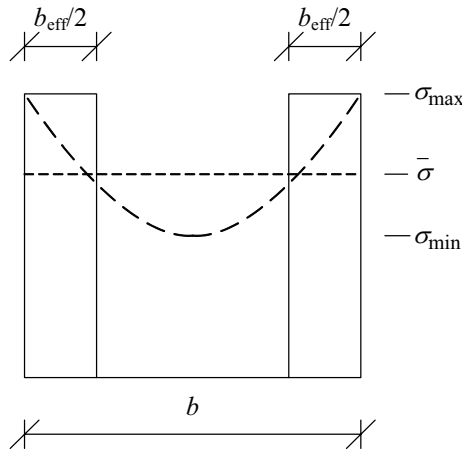


Figure 2.2 Effective width of plates. Stress distribution for a plate where the longitudinal edges are free to move in the plane of the plate.

The critical buckling stress for a complete plate is given by

$$\sigma_{cr} = k_{\sigma} \cdot \frac{\pi^2 \cdot E}{12 \cdot (1 - \nu^2)} \cdot \left(\frac{t}{b}\right)^2 \quad (2.6)$$

and we can by dividing Equation (2.6) with (2.5) write the effective width formula

$$\frac{b_{eff}}{b} = \sqrt{\frac{\sigma_{cr}}{f_y}} \quad (2.7)$$

which can be rewritten as

$$\chi = \frac{b_{eff}}{b} = \frac{1}{\lambda} \quad (2.8)$$

The method of von Kármán et al. (1932) was originally developed for aeronautical applications, i.e. very thin plates, and shows good agreement with results from tests with very slender plates. However, in the intermediate slenderness range the resistance is overestimated. In a thorough study by Winter (1947) on cold formed specimens, with b/t ratios in the same vicinity as normal structural applications, a modified version of the χ -function in Equation (2.8) was suggested according to

$$\chi = \frac{1}{\lambda} - \frac{0,22}{\lambda^2} \quad (2.9)$$

This equation is used today in e.g. EN 1993-1-5 (2006) for plate buckling, though in a rewritten form.

Müller (2003) made an attempt to formulate plate buckling curves in the same frame work as the curves in EN 1993-1-1 (2005) for column buckling. Müller started with the general curve for plate buckling by Maquoi and Rondal (1986)

$$(1 - \chi) \cdot (1 - \chi \cdot \bar{\lambda}^\gamma) = \eta \cdot \chi \quad (2.10)$$

in which the generalized imperfection factor $\eta = \alpha \cdot (\bar{\lambda} - \bar{\lambda}_0)$ and γ depends mainly on the boundary conditions of the plate. If $\gamma=2$ the curves for beam and column buckling in EN 1993-1-1 are obtained. According to Müller it is possible to interpolate between the plastic resistance for low slenderness and the von Kármán curve, Equation (2.8), for higher slenderness if $\gamma=1$. Hence, Equation (2.10) was rewritten as

$$(1 - \chi) \cdot (1 - \chi \cdot \bar{\lambda}) = \eta \cdot \chi \quad (2.11)$$

The solution of Equation (2.11) with respect to χ becomes

$$\chi = \frac{1}{\varphi + \sqrt{\varphi^2 - \bar{\lambda}}} \quad (2.12)$$

with

$$\varphi = \frac{1}{2} \cdot (1 + \alpha \cdot (\bar{\lambda} - \bar{\lambda}_0) + \bar{\lambda}) \quad (2.13)$$

Further, Müller proposed a curve that could be used for patch loading with $\alpha = 0,34$ and $\bar{\lambda}_0 = 0,8$. This curve was proposed to be used with the reduced stress method according to Section 10 in EN 1993-1-5 (2006). Moreover, Müller used 41 patch loading tests by Lagerqvist (1994) together with FE-analyses for definition of the load amplifiers, $\alpha_{ult,k}$ and α_{cr} , for verification of this curve.

2.2 Elastic critical buckling load

The critical load according to classical elastic theory of instability for a plate loaded with a partial in-plane edge load involves additional theoretical difficulties for obtaining rigorous solutions compared to a plate subjected to a distributed edge load. When only a part of the edge is loaded, the stress distribution throughout the plate varies considerably and this causes mathematical difficulties which have to be overcome.

The techniques used for establishing the solutions have been analytical methods, finite-difference methods and the finite element method (FEM). As in all buckling problems, according to classical elastic theory, the solution aims at establishment of a numerical value for the buckling coefficient, k_F , in Equation (2.14) which will depend on the geometrical and statical boundary conditions.

$$F_{cr} = k_F \cdot \frac{\pi^2 \cdot E}{12 \cdot (1 - \nu^2)} \cdot \frac{t_w^3}{h_w} \quad (2.14)$$

For the sake of consistency all values of k_F presented in this study will be on the form of Equation (2.14), even if the original solution found in a reference was on a different form.

Zetlin (1955) presented an analysis of the elastic stability of a plate subjected to a uniformly distributed load over a part of one edge according to Figure 2.3. The plate was simply supported with lateral movement prevented along all four edges and without restraint in the plane of the plate. The applied load was supported at the ends of the plate by parabolically distributed shear stresses. Nine values were presented on k_F for different panel aspect and load ratios. Zetlin concludes that eight of the values are accurate within 1% and the ninth within 10%. Five of the values are given in Table 2.1, all within 1% accuracy and with $a/h_w \geq 1$.

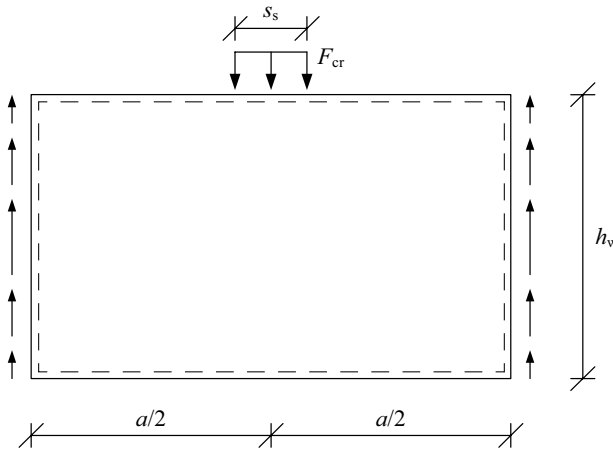


Figure 2.3 Plate model used by Zetlin (1955).

In a paper by Rockey and Bagchi (1970) a similar plate was studied, by means of the finite element method, except that the reactions to the load was assumed to be provided at the ends of the plate by uniformly distributed shear stresses. Further, the vertical edges were allowed to rotate as a rigid body about the neutral axis of the section. Rockey and Bagchi presented solutions for k_F for simply supported plates as well as plates where the flexural and torsional properties of the flanges were included in the analysis.

For the simply supported plates the solutions were presented in a diagram with k_F as a function of s_s/a for different values of a/h_w . The diagrams show that k_F increases with increasing s_s/a , i.e. for a given load the shorter load length the greater tendency for buckling.

For the case when the flexural and torsional stiffness of the flanges were included the results was given as a diagram showing k_F as a function of t_f/t_w . The girder had a web with $a/h_w = 1,0$ and t_f/t_w varying between 2,0 and 8,0 and the load length over web width was $s_s/a = 0,2$. The width of the flanges, b_f , was set to $h_w/4$. The results are shown in Table 2.2 and the influence of the flange thickness in distributing the applied load has importance, giving an increase in k_F of about 130 - 160% compared with a simply supported plate.

In a series of papers, Khan and Walker (1972), Khan and Johns (1975) and Khan et al. (1977), solutions for the problem studied by Rockey and Bagchi (1970) concerning simply supported plates, were presented. The investigation was based on an energy method approach and in Khan and Walker (1972), k_F was given as the solution of a rather complicated equation in terms of h_w , a , s_s and the wavelength of the buckle in the direction perpendicular to the applied load. By minimizing this equation with respect to the wavelength the solution which gave the smallest k_F could be determined. In Khan and Johns (1975) the solution was expanded to combined loading and in Khan et al. (1977) the solution was developed in a more computer-friendly direction. The results obtained by Khan et al. (1977) are in good agreement with the results presented by Rockey and Bagchi, see Table 2.1.

In his doctoral thesis, Lagerqvist (1994), the critical load for both simply supported plates and girder webs including flanges subjected to patch loading was studied by means of FEM. In the former case the same model as used by Rockey and Bagchi (1970) was used and the results can be found in Table 2.1. As can be seen the results are in good agreement with the other presented solutions for k_F . Further, Lagerqvist proposed the following equation for prediction of k_F for a simply supported plate based on the results in Table 2.1.

$$k_F = 2 + 2,12 \cdot \left(\frac{h_w}{a}\right)^2 + \left(\frac{s_s}{h_w}\right)^2 \cdot \left[0,5 + 2 \cdot \left(\frac{h_w}{a}\right)^2\right] \quad (2.15)$$

Table 2.1 k_F for partially loaded plates from Zetlin (1955), Rockey and Bagchi (1970), Khan et al. (1970), Lagerqvist (1994) and Ren et al. (2005).

a/h_w	s_s/h_w	k_F Zetlin (1955)	k_F Rockey (1970) ^{a)}	k_F Khan (1977)	k_F Lagerqvist (1994)	k_F Ren (2005)
1,0	0		3,25		3,20	3,22
	1/65	3,32				
	0,05	3,36	3,27			
	0,1		3,30		3,23	3,26
	0,2		3,45		3,32	3,36
	0,25			3,42	3,38	3,43
	0,3		3,60			3,51
	0,4		3,70			3,71
	0,5		3,95	3,90	3,87	3,97
	0,6		4,15			
	0,75		4,50	4,65		
	0,8		4,80			
	0,9		5,10			
1,0	6,20	5,55	5,57			
2,0	0		2,40		2,36	
	0,1		2,45		2,38	
	0,2		2,50		2,41	
	0,25			2,41	2,43	
	0,4		2,60			
	0,5			2,59	2,60	
	0,6		2,80			
	0,75			2,84	2,84	
	0,8		2,90			
	1,0		3,20	3,15	3,17	
3,0	0,25			2,32		
	0,5			2,43		
	0,75			2,66		
	1,0			2,95		
4,0	0				2,07	
	4/65	2,15				
	0,2	2,12			2,12	
	0,25			2,21	2,14	
	0,5			2,34	2,29	
	0,75			2,54	2,52	
	1,0			2,80	2,79	

^{a)} Obtained from diagram

For the case with the more realistic section, i.e. a girder including flanges, Lagerqvist (1994) performed FE-analyses on a model according to Figure 2.4. For this particular load situation, Lagerqvist assumed that the best description of the load introduction in a real girder was to apply the load in the centre line of the web and to have the vertical deformations of flange coupled along the same distance as the load was applied, i.e. equal to s_s . This prevents rotation of the flange along the longitudinal axis within the loading area. The flanges were also restrained against vertical deformation at the ends of the girders, symbolizing the support from a vertical stiffener.

The model in Figure 2.4, was used both to compare with the data from Rockey and Bagchi (1970) and to evaluate an equation for k_F for the case with flanges included. In the comparison with Rockey and Bagchi the above mentioned restraint that prevents the flanges from rotation within the loading area was excluded in the model. Further, a cross section with $a/h_w = 1$, $s_s/h_w = 0,2$, $b_f = h_w/4$, $h_w = 1,0$ m, $t_w = 0,004$ m and $t_f/t_w = 2, 4$ and 8 was used in the analyses. The results are shown together with those from Rockey and Bagchi in Table 2.2.

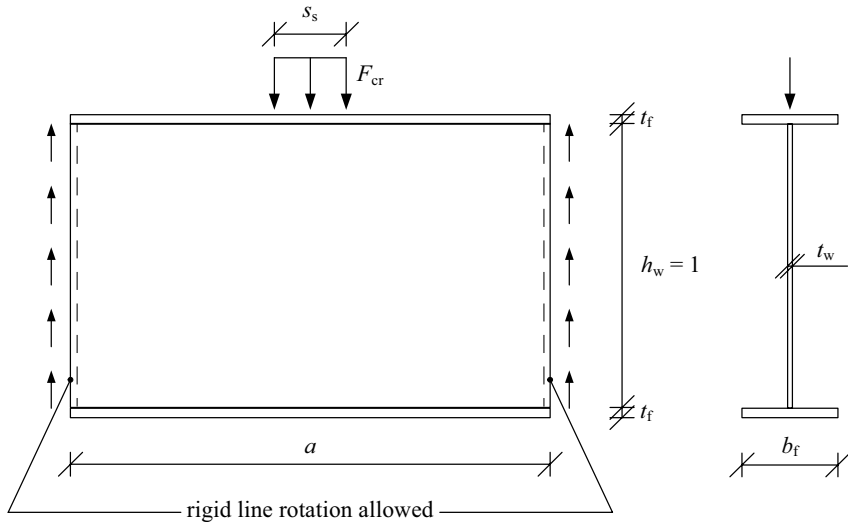


Figure 2.4 FE-model including web and flanges according to Lagerqvist (1994).

It can be noted that for the end points, i.e. $t_f/t_w = 2$ and 8 , there is a good agreement but the difference at $t_f/t_w = 4$ is more significant. If k_F from both references are put in a diagram it is noticed that the results of Lagerqvist seems to reach a horizontal asymptote while the curve running through k_F obtained by Rockey and Bagchi continues to increase for increasing t_f/t_w . Lagerqvist states that the latter behaviour is doubtful since one can assume that for a certain relation for t_f/t_w the support of the web, given by the flanges, can be replaced by with theoretically clamped longitudinal edges of the web. If that is the case, a continuing increase of

t_f/t_w have no effect and k_F reaches a horizontal asymptote. By this reason Lagerqvist considered the FE-model used reliable and continued to use it to find an expression for k_F .

Table 2.2 k_F including stiffness from flanges by Rockey and Bagchi (1970) and Lagerqvist (1994). $a/h_w = 1,0$, $s_s/h_w = 0,2$. Obtained from diagram.

t_f/t_w	2	3	4	5	6	7	8
k_F Rockey (1970)	7,75	7,85	7,95	8,10	8,30	8,55	8,80
k_F Lagerqvist (1994)	7,85		8,45				8,80

Lagerqvist believed that a good estimation of the contribution to k_F from the flanges could be obtained by describing k_F as a function of the relation between the torsional stiffness of the flange and the flexural stiffness of the web, defined by the ratio

$$\frac{G \cdot K}{D \cdot h_w} \quad (2.16)$$

with the torsional stiffness of the flange expressed as

$$G \cdot K = \frac{E}{2 \cdot (1 + \nu)} \cdot \frac{b_f \cdot t_f^3}{3} \quad (2.17)$$

and the stiffness of the web as

$$D \cdot h_w = \frac{E \cdot t_w^3}{12 \cdot (1 - \nu^2)} \cdot h_w \quad (2.18)$$

From Equations (2.16) - (2.18) a parameter, β , can be derived according to Equation (2.19) if the numerical constant 1,4 is neglected.

$$\beta = \frac{b_f \cdot t_f^3}{h_w \cdot t_w^3} \quad (2.19)$$

Lagerqvist wanted to give k_F as a function of β , s_s/h_w and a/h_w . To investigate the influence from β on k_F a series of FE-analyses was performed with seven different values on β for $a/h_w = 1, 2$ and 4 and with $s_s/h_w = 0,2$. Based on the results from the FE-analyses the following relatively simple equation for k_F was proposed.

$$k_F = 5,82 + 2,1 \cdot \left(\frac{h_w}{a}\right)^2 + 0,46 \cdot \sqrt[4]{\beta} \quad (2.20)$$

Finally, Lagerqvist did some additional FE-calculations to investigate the influence from s_s and an expression for k_F was proposed according to

$$k_F = \left(1 + \frac{s_s}{2 \cdot h_w}\right) \cdot \left(5,3 + 1,9 \cdot \left(\frac{h_w}{a}\right)^2 + 0,4 \cdot \sqrt[4]{\beta}\right) \quad (2.21)$$

However, Lagerqvist concluded from his experimental study that the term including s_s in Equation (2.21) has very small influence on k_F . Further, the final patch loading resistance still gives a good prediction of the ultimate load without the term in the first bracket for varying s_s , i.e. Lagerqvist proposed that only the last bracket in Equation (2.21) should be used for k_F for determination of the ultimate resistance.

Lagerqvist also proposed a simplified equation for k_F which was introduced into EN 1993-1-5 (2006) and where the term for the influence from the flanges was set to a reasonable fixed value and the influence from s_s was omitted.

$$k_F = 6 + 2 \cdot \left(\frac{h_w}{a}\right)^2 \quad (2.22)$$

Shahabian and Roberts (1999) presented a paper concerning the elastic critical buckling load of slender web plates subjected to combinations of in-plane loadings. The authors developed an approximate procedure for determining the critical load, i.e. k_F . It was found that the solution by Shahabian and Roberts did not correspond very well with more accurate solutions like the one by Khan et al. (1977). Though, by using a correction factor the results fall in the same region as for example the results by Khan et al.

In a paper by Ren and Tong (2005) a study regarding elastic buckling of web plates in I-girders under patch loading was presented. A similar type of model as the one used by e.g. Rockey and Bagchi (1970) and Khan et al. (1977) was studied by means of FEM and k_F was presented within the same range as others, see Table 2.1. A total of 66 FE-analyses were carried out on a simply supported rectangular plate, $a/h_w = 1,0 - 4,0$ and $s_s/h_w = 0 - 0,5$, with the upper and the lower edges restrained in the 1-direction and the vertical edges restrained in both the 1- and 2-directions, see Figure 2.5. In addition to this and unlike the other case also the rotation degree of freedom 6 of the vertical edges was constrained.

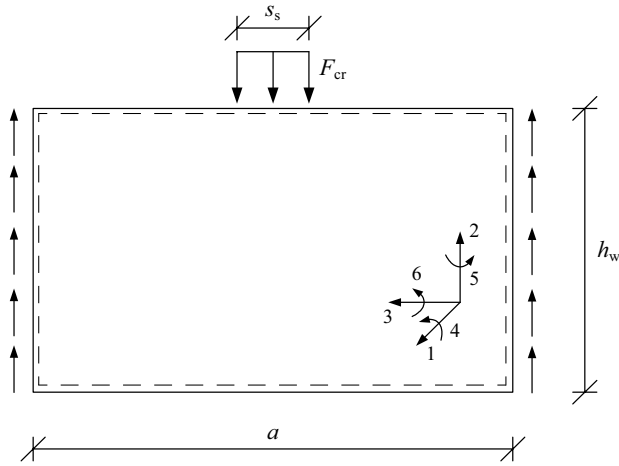


Figure 2.5 The model of simply supported plate by Ren and Tong (2005).

Ren and Tong proposed an equation for k_{F_s} of a simply supported rectangular plate according to

$$k_{F_s} = 2,05 + 1,2 \cdot \left(\frac{h_w}{a}\right)^2 + \left(\frac{s_s}{h_w}\right)^2 \cdot \left[0,5 + 2 \cdot \left(\frac{h_w}{a}\right)^2\right] \quad (2.23)$$

which was based on Equation (2.15) by Lagerqvist (1994).

Furthermore, Ren and Tong (2005) continued by analysing a similar plate as above except that degree of freedom 6, according to Figure 2.5, also was constrained for the upper and lower edges, i.e. the upper and lower edges were clamped. A total of 48 analyses with $a/h_w = 1,0 - 4,0$ and $s_s/h_w = 0 - 0,5$ was carried out for this type of model. An equation for k_{F_c} of a clamped plate was proposed as

$$k_{F_c} = \left(1 + 0,65 \cdot \left(\frac{s_s}{h_w}\right)^2\right) \cdot \left[6,3 - 0,05 \cdot \left(\frac{a}{h_w}\right)^2 + 0,6 \cdot \left(\frac{h_w}{a}\right)^2\right] \quad (2.24)$$

Now, Ren and Tong states that if the rotational restraint from the flanges of an I-girder is taken into account in the analyses it could be assumed that k_F should end up somewhere in between Equations (2.23) and (2.24). Considering Equation (2.20) it can easily be seen that for a girder with β , see Equation (2.19), approaching infinity would give a k_F approaching infinity. Therefore, the authors wanted to investigate the elastic buckling behaviour of webs in I-girders with the restraining effects of the flanges included.

In order to highlight the rotational restraint provided by the flanges, a slightly different model compared to Lagerqvist was used by Ren and Tong. The flanges and the web were established

separately in the model and only the degree of freedom 1 and 6 were coupled between the parts, i.e. the out of plane displacement and the rotation along the longitudinal direction according to Figure 2.5. Furthermore, the edges of the flange as well as the vertical edges of the web were constrained in degree of freedom 1, 2 and 5. The load was applied on the top edge of the web over the distance s_s . A total of 162 different FE-analyses were carried out with $a/h_w = 1, 2$ and 4 , $s_s/h_w = 0 - 0,5$ and $\beta = 0 - 128$. The authors states that β according to Equation (2.19) could be well used to evaluate k_F of I-girder webs. As the value of β increases from zero, k_F increases from k_{Fs} and when β becomes large k_F approaches the value of k_{Fc} . Based on this a basic expression for k_F was established according to

$$k_F = \frac{k_{Fs} + k_{Fc} \cdot \beta}{1 + \beta} \quad (2.25)$$

However, the influence of the aspect ratio of the web plate, a/h_w , must be considered as well, which was solved by introducing a factor λ

$$\lambda = 0,1 + 0,03 \cdot \frac{a}{h_w} + 1,63 \cdot \left(\frac{h_w}{a}\right)^2 \quad (2.26)$$

Finally, Ren and Tong proposed the following equation to determine k_F for I-girder webs

$$k_F = \frac{k_{Fs} + k_{Fc} \cdot \lambda \cdot \beta}{1 + \lambda \cdot \beta} \quad (2.27)$$

It is understood by the author of this thesis that Ren and Tong used the model described above in order to investigate the rotational restraint given by the flange. However, when a patch load is applied to a girder it is usually preventing the flange from rotating under the load plate and hence, the approach Lagerqvist used, i.e. preventing the rotation of the flange under the load plate, would give a more realistic value on k_F .

Galéa and Martin (2006) presented a newly developed software, *EBPlate*, for the determination of the elastic critical buckling stress of plates. The software is a very user friendly tool that can be used for rectangular plates, laterally supported along their four edges, and loaded with normal, transverse or shear stresses. It is possible to introduce the rotational and torsional stiffness of the flanges in the model and also both open and closed longitudinal stiffeners. Considering patch loading the only disadvantage with *EBPlate* is that it is not possible to clamp only a part of the edge that is loaded, i.e. the middle part where the transverse stress is applied.

2.3 Ultimate resistance

There are some things regarding patch loading that can be considered as generally accepted among the researchers. The response from a girder web subjected to a patch load can be described with one of three failure modes shown in Figure 2.6, i.e. yielding, buckling or crippling of the web. However, there is no clear distinction between crippling and buckling instead it could be seen as a gradual change of buckling shape. Normally, the buckling mode is first initiated and followed by a local crippling mode at loads in the vicinity of the ultimate load and according to Edlund (1988), tests on slender webs shows that the crippling mode and the buckling mode usually is combined. The actual failure mode that occurs depends mainly on the cross section geometry. Generally, high ratio of t_f/t_w usually imply a buckling or crippling failure, while a low ratio of t_f/t_w on the other hand usually means that a yielding failure will occur. Further, a stocky web normally implies yielding while slender webs implies buckling.

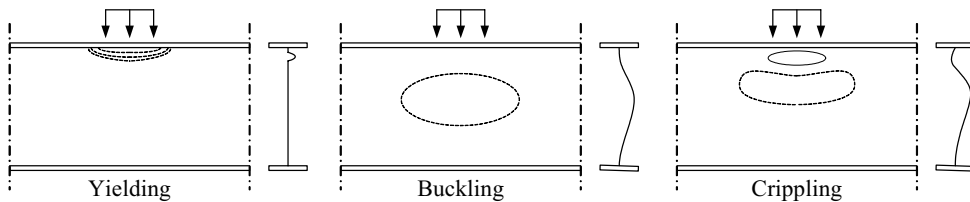


Figure 2.6 Schematic failure modes for girders subjected to patch loading.

All test results indicate that the ultimate resistance of a girder subjected to patch loading is almost independent of the web depth, h_w . However, the ultimate load is more or less directly proportional to the square of the web thickness and is influenced to a lesser extent by the loaded length, s_s , the flange stiffness and the yield strength of the web, f_{yw} .

The review of the ultimate resistance of girders subjected to patch loading is divided into two main sections. One section, Section 2.3.2, that deals with resistance models that is based on a mechanism solution, and one section, Section 2.3.1, that does not. Further, the interaction between patch loading and bending moment as well as patch loading and shear are treated in separate sections.

2.3.1 Empirical models and other non-mechanism models

The earliest contributions in the field considering ultimate resistance models were in general empirical models based on a small number of tests. As the years went by and the number of studies grew together with the knowledge the models became more advanced taking into account a wide variety of parameters. However, the use of a more advanced model will not automatically generate a better prediction of the failure load compared to a simpler model.

The first contribution, described herein, regarding an empirical model for the ultimate resistance were presented by Granholm (1960). A total of 11 patch loading tests with different geometries, h_w/t_w ranging from 126 to 264, and different loaded lengths as well as bending moments were conducted in the study. Granholm concluded that this is a local phenomenon and therefore the failure load is independent of the web depth, h_w . Further, a positive bending moment, i.e. when the part of the web closest to the loaded flange is in compression, could have a negative influence on the failure load while negative bending moment or shear stresses does not affect the failure load.

Based on the test results an expression for the failure load according to Equation (2.28), where F_R is in tons and t_w in mm, could be used with good accuracy, though somewhat on the safe side.

$$F_R = 0,85 \cdot t_w^2 \quad (2.28)$$

Approximately 10 years later Bergfelt (1971) stated that Equation (2.28) gives a fairly good estimation of the failure load for girders with thin flanges. Though, Equation (2.28) was modified to

$$F_R = 0,045 \cdot E \cdot t_w^2 \quad (2.29)$$

which is more or less the same equation as Equation (2.28) but expressed in a dimensionally correct way.

Further, Bergfelt presents a number of tests with fixed h_w/t_w and varying flange dimensions, t_f/t_w from 2 to 5, to investigate the influence of the flanges on the failure load. Based on the results a second expression for girders with thick flanges were proposed as

$$F_R = 0,045 \cdot E \cdot t_w^2 \cdot \left(0,55 + 0,22 \cdot \frac{t_f}{t_w} \right) \quad (2.30)$$

with Equation (2.29) as lower bound.

In a paper published by Skaloud and Drdacky (1975) another model was proposed for slender webs subjected to patch loading. The presented model, see Equation (2.31), includes several parameters and this was the first contribution that includes the web depth, h_w , and the yield strength, f_y , in the model.

$$F_R = 0,55 \cdot t_w \cdot \left(0,9 \cdot t_w + 1,5 \cdot s_s \cdot \frac{t_w}{h_w} \right) \cdot \sqrt{E \cdot f_{yw}} \cdot \sqrt{\frac{t_f}{t_w}} \quad (2.31)$$

Skaloud and Drdacky concludes that bending moment has a small effect on the failure load as long as the stresses, due to bending moment, do not approach the yield strength of the web. The tests used for calibration had a web slenderness, h_w/t_w , ranging from 200 to 400.

Two years later Drdacky and Novotny (1977) published another contribution with focus on thick girder webs, i.e. the study focused on a slenderness range below that by Skaloud and Drdacky (1975). A total of 16 test results on 8 girders are presented with h_w/t_w between 75 and 165. This means that all girders were loaded first on one flange and later the girder was turned upside down and loaded again on the other flange. Different loaded lengths, s_s , were used and for all tests the aspect ratio, $h_w/a = 1$. Further, b_f/t_f was 5 for 10 of the girders and approximately 3,1 for the other 6 girders. The test results were compared to Equation (2.31) with good agreement and the authors concluded that the resistance model could be used within the web slenderness range 75 to 400.

Bergfelt (1976) presented a semi-empirical design method for patch loading verified against more than 100 test results. The design model consists of two parts, one for yielding, Equation (2.32), and one for web crippling, Equation (2.33). The dominating failure mode depends on the ratio between stiffness of the loaded flange and the web thickness and on the loaded length. For weak flanges, i.e. $t_f/t_w < 1-2$, the influence of yielding dominates and for stiffer flanges and longer loaded lengths web buckling has greater influence. The parameter $f(s_s)$ in Equation (2.32) and Equation (2.33) depends on the loaded length and is between 1,0 and 1,3 according to Bergfelt.

$$F_{Ry} = 13 \cdot \eta \cdot t_i \cdot t_w \cdot f_{yw} \cdot f(s_s) \quad (2.32)$$

in which η depends on t_i/t_w according to

$t_i/t_w =$	0,5	1,0	1,0	2,0
$\eta =$	0,55	0,65	0,85	1,0

$$F_{Rc} = 0,6 \cdot t_w^2 \cdot \sqrt{E \cdot f_{yw}} \cdot \left(1 + 0,4 \cdot \frac{t_i}{t_w}\right) \cdot f(s_s) ; t_i/t_w > 1-2 \quad (2.33)$$

t_i is what Bergfelt call an idealized flange thickness that should be used if b_f/t_f differs from 25 and is determined according to

$$t_i = 4 \sqrt[4]{\frac{12 \cdot I_f}{25}} \quad (2.34)$$

In a paper by Elgaaly (1983) a thorough survey over the earlier contributions in the field is presented together with a new proposal for the patch load resistance. Elgaaly states that the local

membrane stresses in the web under the load can reach the yield strength of the web material. The localized membrane yielding may not necessarily constitute failure but will eventually induce web crippling, a local wrinkling or folding of the web. For tests of thick girder webs, higher loads than those causing membrane yielding, could be sustained and the girder failed in web crippling according to Elgaaly. Further, Elgaaly found that, during the tests the load-deflection curves indicated a change in slope around the yield load, which was due to significant membrane yielding of the web. Though, for thin girder webs, crippling can occur prior to yielding.

Elgaaly declared that all test results so far indicates that the failure load is almost independent of the web slenderness and the flange width to thickness ratio. However, the failure load is almost directly proportional to the square of the web thickness and also influenced to a lesser extent by the loaded length, the flange stiffness and the web material yield strength. It was proposed by Elgaaly that the ultimate resistance of a web under patch loading should be determined as

$$F_R = 0,5 \cdot t_w^2 \cdot \sqrt{E \cdot f_{yw} \cdot \frac{t_f}{t_w}} \quad (2.35)$$

Though, for girders that will fail due to yielding, i.e. girders with very stocky webs, the girder will be able to carry higher loads compared to Equation (2.35) but for all practical girder dimensions Equation (2.35) will give satisfactory estimations, according to Elgaaly. As the resistance model is semi-empirical and hence, partially based on test results and those results were limited to tests with a loaded length less than one third of the web depth, Elgaaly restricted the model according to Equation (2.35) to $s_s/h_w < 1/3$. For more distributed loadings, Elgaaly referred to Roberts and Chong (1981), see later in this review.

Drdacky (1986) presented a new tentative model for prediction of the ultimate resistance for girders subjected to patch loading. The model, according to Equation (2.36), was derived from the mechanism of the web collapse and the condition of a smooth transition from non-buckling to buckling of the web. It was calibrated against 170 tests both with and without longitudinal stiffeners.

$$F_R = 19,54 \cdot t_w^2 \cdot f_{yw} \cdot \left(1 + 0,004 \cdot \frac{s_s}{t_w}\right) \cdot \left(\frac{I_f}{t_w^4}\right)^{0,10} \quad (2.36)$$

In this new resistance model Drdacky excluded the web slenderness but states that for low values of h_w/t_w Equation (2.36) needs to be supplemented with a correction depending on the web slenderness. This was due to an observed conservatism, when the resistance model was compared to test results, in the range of web slenderness up to 75.

Spinassas et al. (1990) published a parametric study on girders subjected to patch loading by means of FE-analyses. The parameters varied were t_w , t_f , b_f , a/h_w , f_{yw} , s_s , the bending moment and the initial lateral imperfection. The authors found that an increase in t_f had a significantly positive influence on the ultimate load, especially in combination for lower h_w/t_w . Further, the authors found that t_w had a great influence on the resistance and also f_{yw} and s_s was found important, which is reflected by the proposed resistance formula

$$F_R = K \cdot E^{0,3} \cdot f_{yw}^{0,7} \cdot t_w^{1,53} \cdot \left(\frac{b_f \cdot t_f^3}{12} \right)^{0,06} \cdot s_s^{0,23} \quad (2.37)$$

The coefficient K was set to 1,3 in Spinassas et al. (1990) but in a later publication, Raoul et al. (1991) changed the coefficient K to 1,38 based on a comparison with 118 test results. This gave an average of 1,35 compared to the 118 tests.

2.3.2 Mechanism models

The mechanism models, or resistance models including plastic hinge mechanism in the loaded flange and/or in the web, were introduced by Roberts and co-workers in the late seventieth. At the same time also the Swedish researcher Bergfelt developed a model including a plastic hinge mechanism in the loaded flange. This part of the review will start with the contribution from Roberts and co-workers in chronological order and then continue with Bergfelt and others who have contributed in the field.

Roberts and Rockey (1978) and (1979) published two papers in which a resistance model was proposed for girders subjected to patch loading. The model is based on a plastic mechanism solution which involves plastic hinges in the loaded flange as well as yield lines that forms in the web plate. Certain approximations and empirical modifications were introduced to simplify the method in order to make it suitable for hand calculations. The model is still, despite of the approximations, capable of predicting the failure load and failure mode with satisfying results according to the authors. An alternative form of the mechanism model was also presented for girders in which failure is assumed to be initiated by direct yielding of the web.

Two years later Roberts (1981) presented a reduced form of the mechanism model together with some new tests with focus on the influence of the web depth and the web and flange thicknesses. The complete mechanism model presented in Roberts and Rockey (1979) will first be summarized here and then the modified solution reduced to a simple closed form will follow.

The resistance model for slender girder webs by Roberts and Rockey is based on a failure mechanism according to Figure 2.7. Dimensions β and α define the assumed position of the plastic hinges in the flange and the yield lines in the web respectively. The angle θ defines the

deformation of the web just before failure. Further, stretching of the web plate as deformation proceeds was neglected.

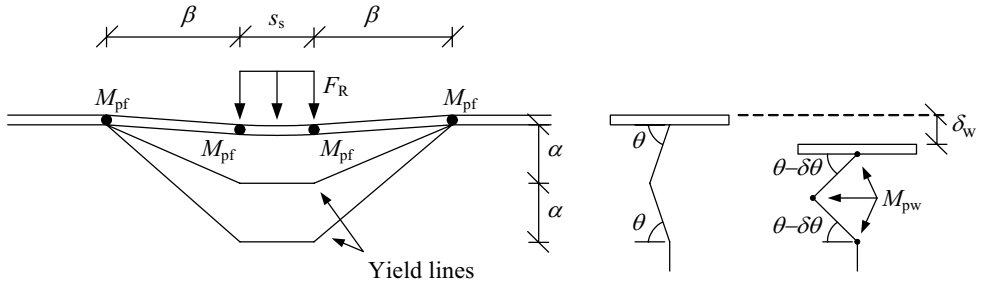


Figure 2.7 Assumed failure mechanism for slender webs according to Roberts and Rockey (1979).

When the applied load moves vertically through a small distance δ_w , the rotation of the plastic hinges in the flange is δ_w/β and of the yield lines in the web is $\delta_w/2\alpha\cos\theta$ since $\delta\theta$ equals $\delta_w/2\alpha\cos\theta$. The latter is obtained from

$$\delta_w = 2 \cdot \alpha \cdot \sin\theta - 2 \cdot \alpha \cdot \sin(\theta - \delta\theta) \quad (2.38)$$

which reduces to

$$\delta_w = 2 \cdot \alpha \cdot \cos\theta \cdot \delta\theta \quad (2.39)$$

for small values of $\delta\theta$.

The internal and external work for the failure mechanism is according to Equations (2.40) and (2.41).

$$W_i = 4 \cdot M_{pf} \cdot \frac{\delta_w}{\beta} + (8 \cdot \beta \cdot M_{pw} + 4 \cdot s_s \cdot M_{pw} - 4 \cdot \eta \cdot M_{pw}) \cdot \frac{\delta_w}{2 \cdot \alpha \cdot \cos\theta} \quad (2.40)$$

$$W_e = F_R \cdot \delta_w \quad (2.41)$$

where M_{pf} is the plastic moment resistance of the flange, i.e. $M_{pf} = f_{yf} \cdot b_f \cdot t_f^2/4$ and M_{pw} is the plastic moment resistance of the web per unit length, $M_{pw} = f_{yw} \cdot t_w^2/4$. η defines a length of the web plate beneath the load which is assumed to have yielded due to the presence of compressive membrane stresses and therefore offers no resistance to bending. Equating external and internal work gives

$$F_R = \frac{4 \cdot M_{pf}}{\beta} + \frac{4 \cdot \beta \cdot M_{pw}}{\alpha \cdot \cos\theta} + \frac{2 \cdot s_s \cdot M_{pw}}{\alpha \cdot \cos\theta} - \frac{2 \cdot \eta \cdot M_{pw}}{\alpha \cdot \cos\theta} \quad (2.42)$$

Minimizing F_R with respect to β gives

$$\beta^2 = \frac{M_{pf} \cdot \alpha \cdot \cos \theta}{M_{pw}} \quad (2.43)$$

The deformation of the flange before failure was estimated by means of elastic theory. It was assumed that the moment in the flange varied linearly from $+M_{pf}$ at one plastic hinge to $-M_{pf}$ at the next. Then the deflection of the flange is given by

$$\frac{M_{pf} \cdot \beta^2}{6 \cdot E \cdot I_f} \quad (2.44)$$

in which I_f is the second moment of area for the flange. The deflection of the flange must be compatible with the deformation of the web given by $2 \cdot \alpha \cdot (1 - \sin \theta)$, i.e.

$$\frac{M_{pf} \cdot \beta^2}{6 \cdot E \cdot I_f} = 2 \cdot \alpha \cdot (1 - \sin \theta) \quad (2.45)$$

Equations (2.43) and (2.45) gives

$$\frac{\cos \theta}{1 - \sin \theta} = \frac{4 \cdot E \cdot f_{yw} \cdot t_w^2}{f_{yf}^2 \cdot b_f \cdot t_f} \quad (2.46)$$

in which everything but θ is known. Now, by means of Equations (2.42), (2.43) and (2.46) together with an empirical choice of α , the resistance can be calculated. The experimental evidence suggests that the depth of the region of plastic deformation in the web, 2α for the assumed mechanism, is not too sensitive to the flange dimensions, according to Roberts and Rockey. A suitable choice for α is

$$\alpha = \frac{h_w \cdot t_w \cdot f^*}{16 \cdot t^* \cdot f_{yf}} \leq \frac{h_w}{6} \quad (2.47)$$

where t^* is a reference web thickness taken as 2,5 mm, which fit to the tests TG1-TG5 by Skaloud and Novak (1972), and f^* is a reference yield strength taken as 300 MPa. The term f^*/f_{yf} ensures that the solution is not too sensitive to small changes in M_{pf} resulting from variations in material yield strength and Equation (2.47) can be rewritten to

$$\alpha = \frac{h_w \cdot t_w}{40} \cdot \frac{300}{f_{yf}} \leq \frac{h_w}{6} \quad (2.48)$$

According to the authors the upper limit of α will prove satisfactory for most practical situations. Finally, to determine η it is assumed that the web contribution to the failure load is transmitted to a length η of the web in the vicinity of the patch load. Further, the authors assumed that the length η of the web plate yields in compression and hence, offers no resistance to bending deformations. Equating the web contribution to the failure load, i.e. the three last terms in Equation (2.42), to a force corresponding to the yielded length η of the web gives

$$(4 \cdot \beta + 2 \cdot s_s - 2 \cdot \eta) \cdot \frac{M_{pw}}{\alpha \cdot \cos \theta} = f_{yw} \cdot t_w \cdot \eta \quad (2.49)$$

from which η can be solved according to

$$\eta = \frac{(4 \cdot \beta + 2 \cdot s_s) \cdot M_{pw}}{2 \cdot M_{pw} + f_{yw} \cdot t_w \cdot \alpha \cdot \cos \theta} \quad (2.50)$$

The following limitations were also imposed on the work:

- The positions of the outer plastic hinges in the flange are limited to not exceed the distance between possible vertical stiffeners in the vicinity of the load, i.e. the value of β in Equation (2.43) is not allowed to exceed $0,5 \cdot (a - s_s)$.
- If β is assigned the value $0,5 \cdot (a - s_s)$, α should be determined according to Equation (2.48) with the term $300/f_{yf}$ omitted. This means that the angle θ should be determined directly through Equation (2.45).
- For larger loaded lengths, s_s , the predicted resistance overestimates the ultimate load from tests in some cases and therefore s_s should be limited to $0,2h_w$ or if $\beta = 0,5 \cdot (a - s_s)$ s_s should not exceed 2β . The lesser value should be used.

So far the rather complicated proposal in Roberts and Rockey (1979) have been described. However, that proposal was in Roberts (1981) modified to a simple closed form solution starting with the same mechanism, see Figure 2.7, and Equations (2.40) - (2.45). Equation (2.46) is rewritten as

$$\frac{\cos \theta}{1 - \sin \theta} = \frac{4 \cdot E \cdot f_{yw} \cdot t_w^2}{f_{yf}^2 \cdot b_f \cdot t_f} = H \quad (2.51)$$

Solving Equation (2.51) for $\cos \theta$ in terms of H gives

$$\cos \theta = \frac{2 \cdot H}{1 + H^2} \approx \frac{2}{H} \quad (2.52)$$

as H^2 is large compared with unity. Substituting Equations (2.43) and (2.52) into Equation (2.42) and omitting the terms containing s_s and η , gives a resistance according to

$$F_R = 2 \cdot \sqrt{2} \cdot t_w^2 \cdot \sqrt{\frac{E \cdot f_{yw}^2 \cdot t_f}{f_{yf} \cdot \alpha}} \quad (2.53)$$

Furthermore, Equation (2.53) indicates a slight anomaly in the mechanism solution because if f_{yf} is increased, F_R will decrease. Roberts solved this by assuming that f_{yf} is equal to f_{yw} . Moreover, in the original proposal α was taken as a function of both h_w and t_w , see Equation (2.48), but experimental evidence show that the failure load is independent of h_w according to Roberts. Hence, α was proposed to be taken as $25t_w$. The term containing s_s in Equation (2.42) is reintroduced and the solution for the resistance reduces to

$$F_R = 0,56 \cdot t_w^2 \cdot \sqrt{\frac{E \cdot f_{yw} \cdot t_f}{t_w}} \cdot \left[1 + \lambda \cdot s_s \cdot \left(\frac{t_w}{t_f} \right)^{3/2} \right] \quad (2.54)$$

in which λ is a function of the girder dimensions and material properties. To maintain the simplicity, Roberts sets $\lambda = 3/h_w$ and to have a lower bound solution for the available test data, the constant 0,56 is reduced to 0,5, i.e.

$$F_R = 0,5 \cdot t_w^2 \cdot \sqrt{\frac{E \cdot f_{yw} \cdot t_f}{t_w}} \cdot \left[1 + \frac{3 \cdot s_s}{h_w} \cdot \left(\frac{t_w}{t_f} \right)^{3/2} \right] \quad (2.55)$$

Equation (2.55) is the final formula for the ultimate resistance but Roberts assign two limitations to the resistance. First, when s_s/h_w becomes large, it is unrealistic to assume that the flange remains straight between the two inner plastic hinges and the geometrical considerations are suspect. Therefore, Roberts recommended that the value of s_s/h_w should be limited to 0,2. Second, for thin webs and flanges the model tends to underestimate the failure load and to avoid this a lower limit of three was imposed on the ratio t_f/t_w for comparison with test data. However, this limitation was not recommended for practical situations.

In addition to the resistance models described above, Roberts and Rockey (1979) and Roberts (1981) also proposed a solution for girders with thicker webs. It is stated that for stocky girders it is expected that the failure will be initiated by direct yielding of the web as thicker webs increases the ratio of the out of plane bending stiffness to the compressive membrane stiffness. This situation can be analysed by considering an alternative failure mechanism according to Figure 2.8.

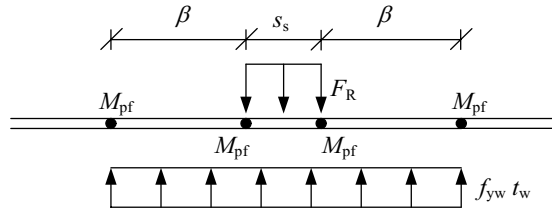


Figure 2.8 Assumed failure mechanism for web yielding according to Roberts and Rockey.

Roberts assumed that plastic hinges form in the flange and that the length of web between the outer plastic hinges yields in compression. The internal and external work for the mechanism in Figure 2.8 when the load moves vertically through a small distance δ_w are

$$W_i = 4 \cdot M_{pf} \cdot \frac{\delta_w}{\beta} \quad (2.56)$$

$$W_e = F_R \cdot \delta_w - f_{yw} \cdot t_w \cdot \left(s_s \cdot \delta_w + 2 \cdot \beta \cdot \frac{\delta_w}{2} \right) \quad (2.57)$$

Equating internal and external work for the mechanism gives

$$F_R = \frac{4 \cdot M_{pf}}{\beta} + f_{yw} \cdot t_w \cdot (s_s + \beta) \quad (2.58)$$

Minimizing Equation (2.58) with respect to β gives

$$\beta^2 = \frac{4 \cdot M_{pf}}{f_{yw} \cdot t_w} \quad (2.59)$$

Equation (2.58) together with Equation (2.59), introducing $M_{pf} = f_{yf} \cdot b_f \cdot t_f^2 / 4$, gives an expression for the resistance according to

$$F_R = f_{yw} \cdot t_w \cdot \left(s_s + 2 \cdot t_f \cdot \sqrt{\frac{f_{yf} \cdot b_f}{f_{yw} \cdot t_w}} \right) \quad (2.60)$$

In Roberts and Rockey (1979) it was stated that when using Equation (2.60), the limitation $s_s/h_w \leq 0,2$ is not needed.

In another paper by Roberts and Chong (1981) a similar mechanism model was derived for what is called distributed patch loading. This time the model contained a three hinge mechanism of the loaded flange and the model was compared to tests performed by Bossert and Ostapenko (1967). All ten tests were loaded over the entire distance between two vertical stiffeners. Also

for this case one resistance function was developed for web buckling and one for direct yielding of the web. It was assumed that one plastic hinge in the flange will develop over each stiffener and one at mid-span according to Figure 2.9.

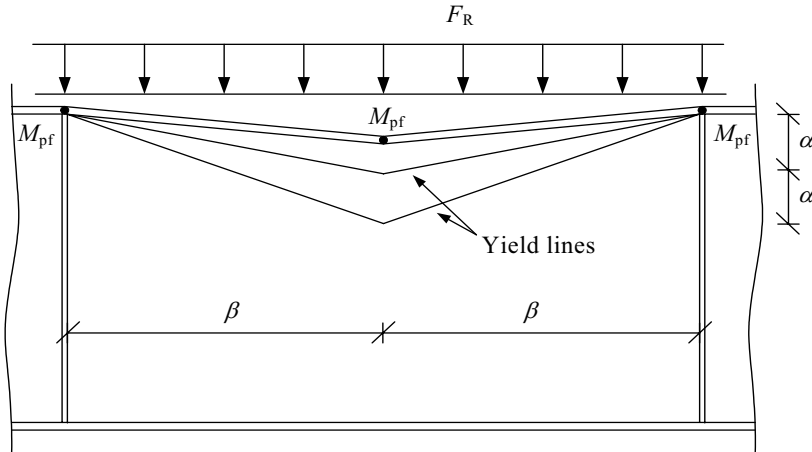


Figure 2.9 Assumed failure mechanism for distributed patch loading according to Roberts and Chong (1981).

Following the same analogy as for the four hinge model and equating external and internal work, a resistance equation was obtained according to

$$F_R = \frac{8 \cdot M_{pf}}{\beta} + \frac{8 \cdot \beta \cdot M_{pw}}{\alpha \cdot \cos \theta} \quad (2.61)$$

Once again, elastic theory was used for estimation of the deflection of the flange just prior to failure. This deflection must be compatible with the deflection of the web below the central plastic hinge, see Equations (2.44) and (2.45). Rearranging gives the following expression, from which the angle, θ , can be solved.

$$\sin \theta = 1 - \frac{M_{pf} \cdot \beta^2}{12 \cdot E \cdot I_f \cdot \alpha} \quad (2.62)$$

The uniformly distributed edge loading produces compressive membrane stresses, f_m , in the web, which reduce the plastic moment resistance of the web to $M_{pw} \cdot [1 - (f_m/f_{yw})^2]$. Assuming uniform distribution of f_m over the distance between the outer plastic hinges together with the second term on the right hand side of Equation (2.61) gives

$$f_m = \frac{4 \cdot M_{pw}}{\alpha \cdot \cos \theta \cdot t_w} \quad (2.63)$$

Introducing the reduced plastic moment resistance of the web into Equation (2.61) gives an approximation of the collapse load according to

$$F_R = \frac{8 \cdot M_{pf}}{\beta} + \frac{8 \cdot \beta \cdot M_{pw}}{\alpha \cdot \cos \theta} \cdot \left[1 - \left(\frac{4 \cdot M_{pw}}{\alpha \cdot \cos \theta \cdot t_w \cdot f_{yw}} \right)^2 \right] \quad (2.64)$$

α can empirically be chosen to $\alpha = 25t_w$ according to Roberts and Chong (1981) and by Equations (2.62) and (2.64) the resistance can be calculated. Now, for stockier girders it is possible that failure will be initiated by direct yielding of the web in the same manner as Roberts have shown before for his four hinge model. In this case, using the three hinge model and equating external and internal work, the resistance becomes

$$F_R = \frac{8 \cdot M_{pf}}{\beta} + 2 \cdot \beta \cdot t_w \cdot f_{yw} \quad (2.65)$$

The resistance should be taken as the lesser of Equations (2.64) and (2.65).

Two years later Roberts and Markovic (1983) presented another study on stocky girders, including tests with t_w from 3 mm to 10 mm and h_w/t_w between 50 and 166. The objective was to fill out the gap in the test data for thicker webs and to compare the resistance functions developed earlier by Roberts and co-workers with the test results. The authors studied the load-deflection curves, deflection was defined as the deflection of the loaded flange under the load, and concluded that at approximately one third of the ultimate load the slope of the curve changes without any significant out of plane deformations. This was due to membrane yielding of the web according to the authors. Close to ultimate load the curve flattens accompanied by a rapid increase of the out of plane deformations of the web, indicating that the failure was due to bending and not yielding of the web. Further, when comparing the ultimate loads from tests with Equations (2.55) and (2.60) it was found that Equation (2.55), i.e. the resistance function originally developed for slender webs, gave the best agreement irrespective of the web thickness.

Finally, Roberts and Newark (1997) presented a slightly modified design procedure for patch loading. The main equations are the same as described above but some modifications were made. Starting with the same equation as before but adding a safety factor called F by the authors

$$F_R = \left(\frac{4 \cdot M_{pf}}{\beta} + \frac{4 \cdot \beta \cdot M_{pw}}{\alpha \cdot \cos \theta} + \frac{2 \cdot s_{se} \cdot M_{pw}}{\alpha \cdot \cos \theta} - \frac{2 \cdot \eta \cdot M_{pw}}{\alpha \cdot \cos \theta} \right) \cdot \frac{1}{F} \quad (2.66)$$

where s_{se} is the loaded length now allowing for 45° distribution through the flange, i.e.

$$s_{se} = s_s + 2 \cdot t_f \quad (2.67)$$

A new approximation of α was proposed according to Equation (2.68) where f_{yw}/f_{yf} was incorporated to remove the anomaly, mentioned earlier, that the resistance decrease with increasing f_{yf} , see Equation (2.53).

$$\alpha = 20 \cdot t_w \cdot \frac{f_{yw}}{f_{yf}} \leq \frac{h_w}{8} \quad (2.68)$$

Further, for girders with thin flanges the value of β may be small compared with α and the geometry of the assumed mechanism becomes unrealistic. Therefore, if $\alpha > \beta/2$ the value of α should be reduced to $\beta/2$. The other limitations mentioned earlier in other papers are not mentioned in this paper and hence, it is assumed that they no longer are relevant.

Substituting Equations (2.43), (2.52) and (2.68) into Equation (2.66) gives

$$F_R = \left(K \cdot t_w^2 \cdot \sqrt{E \cdot f_{yw} \cdot \frac{t_f}{t_w} \cdot (1 + \lambda)} \right) \cdot \frac{1}{F} \quad (2.69)$$

in which K is a numerical constant and λ is a complex function of the system geometry and material yield strengths. By comparison with a wide range of test data Equation (2.69) was modified empirically according to

$$F_R = \left(1,1 \cdot t_w^2 \cdot \sqrt{E \cdot f_{yw}} \cdot \left(\frac{t_f}{t_w} \right)^{1/4} \cdot \left(1 + \frac{s_{se} \cdot t_w}{h_w \cdot t_f} \right) \right) \cdot \frac{1}{F} \quad (2.70)$$

where the safety factor $F = 1,45$. By using $F = 1,45$ a lower bound 95% confidence limit above unity is obtained. In the paper, also the mechanism solution for direct yielding of the web as shown in Equations (2.56) - (2.60) was described and the authors states that the lesser of Equation (2.60) and Equation (2.70) should be used for design. The only difference between the resistance equation for direct yielding in this paper and Equation (2.60) is that s_{se} should be used instead of s_s , i.e. no safety factor is needed for the case with direct yielding.

According to Roberts and Newark (1997) the predictions by Equations (2.60) and (2.70) compared with 142 test results gave a mean of 1,45 and a coefficient of variation of 0,24. The authors state that for routine design Equations (2.60) and (2.70) should be used but for girders with relatively strong flanges and closely spaced vertical stiffeners the full mechanism solution for web buckling should be used instead of Equation (2.70).

As can be noticed, Roberts and co-workers have produced an extremely large amount of both test data and knowledge in the field. Good agreement are shown between the proposed

resistance functions and test results. However, there are still a lot of restrictions concerning the model and several empirical parameters are included. The fact that there are two separate equations for the resistance although the test results does not show any clear distinction between direct yielding or buckling of the web is a weakness. Further, the approach to use the full mechanism solution, which is rather complicated, for relatively strong flanges and closely spaced vertical stiffeners makes the approach even more complex. For example, what is a relatively strong flange and what is closely spaced vertical stiffeners?

Bergfelt (1979) presented another mechanism solution based on a three hinge model, see Figure 2.10, not too different from the model proposed by Roberts and Chong (1981). In Bergfelt (1979) it is referred to Bergfelt (1971) for the origin of the mechanism. The three hinge theory is explained as follows. At a small load the flange behaves as a beam on an elastic foundation, consisting of the web. When the load increases a plastic hinge forms in the flange under the load and the web stresses reach f_{yw} below the hinge. The yielding region in the web extends and the negative bending moment in the flange increases. Finally, failure starts when a plastic hinge forms on each side of the load. If the load is transferred through a very stiff bar or plate, there might be a hinge on each side of the plate instead of one hinge centrally under the load according to Bergfelt.

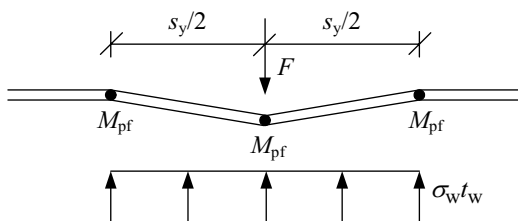


Figure 2.10 Ultimate failure model according to Bergfelt.

For girders with common ratios of t_f/t_w , between 2 and 5 according to Bergfelt, web crippling starts as buckling of the web region under the load and not because the yield stress was reached, which is a bit contradictive to the previous paragraph. In order to find an adequate value on σ_w in Figure 2.10, Bergfelt used the von Karman approximation of the average failure stress

$$\sigma_w = \sqrt{\sigma_{cr} \cdot f_{yw}} \tag{2.71}$$

After some mathematical work Bergfelt finally arrives at the following expression for the failure load

$$F_R = 0,8 \cdot t_w^2 \cdot \sqrt{E \cdot f_{yw}} \cdot \sqrt{\frac{t_i}{t_w}} \cdot f(s_s, h_w, etc); t_i/t_w > \approx 2 \tag{2.72}$$

where t_i is according to Equation (2.34) if the flange dimensions differs from $b_f/t_f = 25$, if not t_i equals t_f . The term $f(s_s, h_w, etc)$ in Equation (2.72) contains a number of functions according to

$$f(s_s, h_w, etc) = f(s_s) \cdot f(h_w) \cdot f(f_{yw}) \cdot f(M_E) \cdot f(\delta) \cdot f(s_v) \cdot f(s_h) \quad (2.73)$$

in which $f(s_v)$ and $f(s_h)$ gives the influence of vertical and horizontal stiffeners respectively. The other factors are correction functions, generally close to 1,0 according to Bergfelt.

$f(s_s)$ relates the influence of the loaded length s_s . Bergfelt suggested a simple formula, roughly covering many test results, according to

$$f(s_s) = 1 + 40 \cdot \frac{s_s}{s_y} \cdot \frac{t_w}{h_w} \leq 1,4 \quad (2.74)$$

where

$$s_y = 5,2 \cdot \frac{b_f}{\eta} \cdot \left(\frac{t_f}{t_w}\right)^2 \cdot \sqrt{\frac{t_w}{t_i}} \cdot \frac{f_{yf}}{\sqrt{f_{yw} \cdot E}} \quad (2.75)$$

in which η is a correction factor for flange bending moment.

The next factor $f(h_w)$ is a correction factor for the influence of the web depth, h_w . Bergfelt did not find any significant influence for slender webs but mentioned that the web depth can have influence for stocky webs, $h_w/t_w \leq 60$.

$f(f_{yw})$ is a correction factor for the influence from the yield strength of the web to the post-buckling strength according to Bergfelt. However, there are not many test results on girders with “extremely” high or low strengths which makes the formula uncertain. Bergfelt proposed a correction factor according to

$$f(f_{yw}) = \sqrt[6]{700 \cdot \frac{f_{yw}}{E}} \quad (2.76)$$

$f(M_E)$ is a correction factor taking into account the compression stress in the flange from a bending moment. Finally, the correction factor for initial imperfections of the web $f(\delta)$ should according to Bergfelt be calculated as

$$f(\delta) = 1 - 15 \cdot \left(\delta - 0,001 \cdot t_f \cdot \frac{h_w}{t_w} \right) / t_w ; 0,8 < f(\delta) \leq 1 \quad (2.77)$$

which holds for $t_f/t_w > 2$. If no special regard is taken to the initial imperfections of the web the constant in Equation (2.72) is 0,77 instead of 0,8 $f(\delta)$ according to Bergfelt.

In another study by Bergfelt (1983) a total of 26 tests were presented which confirms the rather small influence of the web depth, for slender webs down to $h_w/t_w = 150$, on the failure load. Further, the new test results supports the resistance function according to Equation (2.72).

In Shimizu et al. (1989) a modified version of the mechanism solution originally by Roberts and Rockey (1979) was presented. Seven test results were presented with s_s/a equal to 0,3 or 0,5 and $h_w/t_w = 167$. The authors reports that two yield lines form in the web for all girders, in contradiction to the three yield lines that Roberts and Rockey, observed. Further, Shimizu et al. explained the difference in collapse behaviour by the fact that their s_s/a is greater in comparison to the ratio s_s/a from tests that Roberts and Rockey used for deriving their mechanism. On basis of the new findings for longer loading lengths, Shimizu et al. proposed a modified mechanism model shown in Figure 2.11.

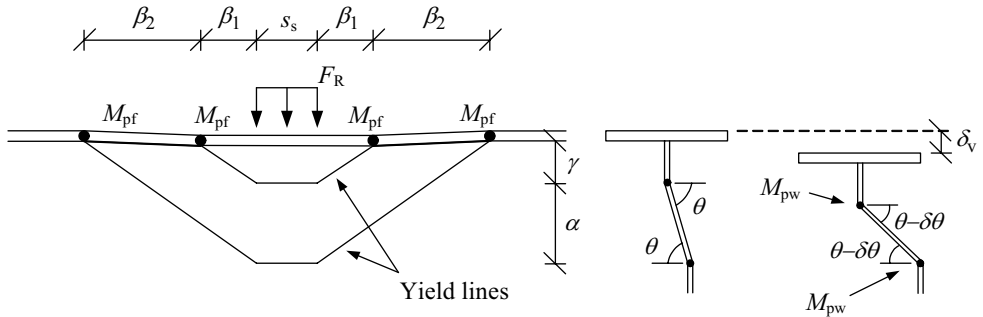


Figure 2.11 Modified mechanism according to Shimizu et al. (1989).

Following the same analogy as Roberts and Rockey, the external and internal virtual work for the mechanism are as follows.

$$W_i = 4 \cdot M_{pf} \cdot \frac{\delta_v}{\beta_2} + 2 \cdot M_{pw} \cdot (s_s + 2 \cdot \beta_1 + 2 \cdot \beta_2) \cdot \frac{\delta_v}{\alpha \cdot \cos \theta} \quad (2.78)$$

$$W_e = F_R \cdot \delta_v \quad (2.79)$$

Equating internal and external work gives

$$F_R = 4 \cdot \frac{M_{pf}}{\beta_2} + 2 \cdot \frac{M_{pw} \cdot (s_s + 2 \cdot \beta_1 + 2 \cdot \beta_2)}{\alpha \cdot \cos \theta} \quad (2.80)$$

and minimizing with respect to β_2

$$\beta_2 = \sqrt{\frac{M_{pf} \cdot \alpha \cdot \cos \theta}{M_{pw}}} \quad (2.81)$$

β_1 can then be derived from the relation

$$\frac{\beta_1}{\beta_2} = \frac{\gamma}{\alpha} \quad (2.82)$$

which is obtained through Figure 2.11. Using the same assumption as Roberts and Rockey, i.e. that the flange deflection should be compatible with the web deformation and that the moment is linear between the plastic hinges in the flange, gives

$$\frac{M_{pf}}{6 \cdot E \cdot I_f} = \alpha \cdot (1 - \sin \theta) \quad (2.83)$$

Also Shimizu et al. defines the length, η , of the web under the load that yields and can not develop plastic hinges. Adding η to the resistance function gives

$$F_R = 4 \cdot \frac{M_{pf}}{\beta_2} + 2 \cdot \frac{M_{pw} \cdot (s_s + 2 \cdot \beta_1 + 2 \cdot \beta_2 - \eta)}{\alpha \cdot \cos \theta} \quad (2.84)$$

Putting the web part of the right hand side of Equation (2.84) equal to $\eta \cdot f_{yw} \cdot t_w$ gives an expression for η according to

$$\eta = 2 \cdot M_{pw} \cdot \frac{s_s + 2 \cdot \beta_1 + 2 \cdot \beta_2}{2 \cdot M_{pw} + f_{yw} \cdot t_w \cdot \alpha \cdot \cos \theta} \quad (2.85)$$

Now, the authors state that by using Equations (2.81) - (2.85) the resistance can be determined. Though, the values of α and γ needs to be determined through tests, which is not that suitable for design.

Ungermann (1990) suggests, together with other design models, a design model for patch loading. The model included the buckling load, F_{cr} , the yield resistance, F_y , and the slenderness parameter, λ . The yield resistance is evaluated from a three hinge model according to Figure 2.12 and is calculated as

$$F_y = 2 \cdot c_u \cdot t_w \cdot f_{yw} \quad (2.86)$$

where

$$2 \cdot c_u = \frac{s_s}{2} + \sqrt{\left(\frac{s_s}{2}\right)^2 + \frac{4 \cdot b_f \cdot t_f^2 \cdot f_{yf}}{t_w \cdot f_{yw}}} \quad (2.87)$$

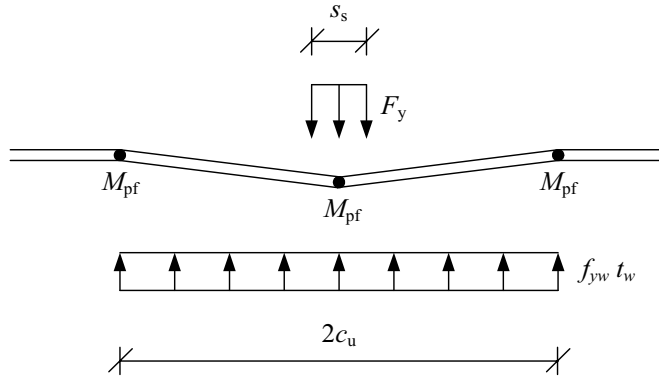


Figure 2.12 Mechanical model according to Ungermann (1990).

According to Ungermann, results from tests show that the resistance for patch loading is independent of h_w and instead Ungermann used the small buckle that appears close to the loaded flange just before the ultimate load is reached. Ungermann showed that the height of this small buckle could be represented by $60t_w$. Further, Ungermann used $k_F = 2,31$ and together with $h_w = 60t_w$ Equation (2.14) can then be rewritten as

$$F_{cr} = 0,0348 \cdot E \cdot t_w^2 \quad (2.88)$$

Now, the slenderness parameter can be determined as

$$\lambda = \sqrt{\frac{F_y}{F_{cr}}} \quad (2.89)$$

and the resistance is given by

$$\begin{cases} F_R = 2 \cdot c_u \cdot t_w \cdot f_{yw} \cdot \left(\frac{0,525}{\lambda} + \frac{0,375}{\lambda^2} \right) & \text{if } \lambda > 0,80 \\ F_R = 22 \cdot \sqrt[7]{\varepsilon^4} \cdot t_w^2 \cdot f_{yw} & \text{if } \lambda \leq 0,80 \end{cases} \quad (2.90)$$

where $\varepsilon = \sqrt{235/f_{yw}}$.

In 1994, as mentioned earlier, Lagerqvist (1994) presented his doctoral thesis on the subject. Except for a number of tests also a new design model was developed. A paper by Johansson and Lagerqvist (1995) was published based on the same concept but in an earlier stage due to the large time span from submission to publication. Though, the work by Lagerqvist and Johansson described herein will focus on the latest findings, i.e. Lagerqvist (1994) and a later paper by Lagerqvist and Johansson (1996).

The actual design model proposed by Lagerqvist is harmonized with other models normally used for describing other buckling problems. This means that the model has three significant parts. First, a prediction of the yield resistance, F_y , based on the mechanical model shown in Figure 2.13 and second, the theoretical critical load, F_{cr} , which is used only for the definition of the slenderness parameter λ . The third part is the reduction factor, $\chi(\lambda)$, that relates the resistance to the slenderness. The approach by Lagerqvist covers all failure modes, see Figure 2.6, in one verification and the transition from yielding to buckling is continuous and smooth.

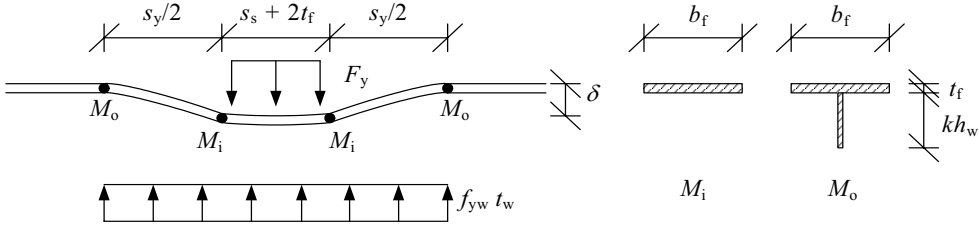


Figure 2.13 Mechanical model for the yield resistance according to Lagerqvist.

Starting with the mechanical model shown in Figure 2.13, which is almost similar to the mechanism proposed by Roberts and Rockey for direct yielding of the web. The difference is that the outer plastic hinges in the flange also contains a part of the web, forming a T-section. This was incorporated in the model because Lagerqvist noticed from tests that for increased web slenderness the effective loaded length, $l_y = s_s + 2 \cdot t_f + s_y$, also increased. By incorporating a part of the web in M_o , l_y will increase with increasing h_w . The yield resistance was derived by equating external and internal virtual work for the system in Figure 2.13 in the same manner as Roberts and Rockey did, which gives

$$F_y = 4 \cdot \frac{M_i + M_o}{s_y} + f_{yw} \cdot t_w \cdot \left(s_s + 2 \cdot t_f + \frac{s_y}{2} \right) \quad (2.91)$$

Minimizing Equation (2.91) with respect to s_y gives

$$s_y = \sqrt{\frac{8 \cdot (M_i + M_o)}{f_{yw} \cdot t_w}} \quad (2.92)$$

The plastic moment resistance for the outer plastic hinges, M_o , was determined under the assumption that the neutral axis is located in the flange and reads according to Lagerqvist

$$M_o = \frac{f_{yf} \cdot b_f \cdot t_f^2}{4} + \frac{f_{yw} \cdot t_w \cdot k^2 \cdot h_w^2}{2} \cdot \left(1 + \frac{t_f}{k \cdot h_w} - \frac{f_{yw} \cdot t_w}{2 \cdot f_{yf} \cdot b_f} \right) \quad (2.93)$$

Further, if k is not too small, which it has to be in order to give contribution to the resistance, Lagerqvist states that the first term in the bracket is the dominating contributor and it is a safe simplification to neglect the second and third terms. Then

$$M_o = \frac{f_{yf} \cdot b_f \cdot t_f^2}{4} + \frac{f_{yw} \cdot t_w \cdot k^2 \cdot h_w^2}{2} \quad (2.94)$$

Inserting Equations (2.92) and (2.94) into Equation (2.91) and rearranging gives

$$F_y = f_{yw} \cdot t_w \cdot \left(s_s + 2 \cdot t_f + 2 \cdot t_f \cdot \sqrt{\frac{f_{yf} \cdot b_f}{f_{yw} \cdot t_w} + k^2 \cdot \left(\frac{h_w}{t_f}\right)^2} \right) \quad (2.95)$$

Now, the only unknown in Equation (2.95) is the factor k . By comparison with test results it was found that $k^2 = 0,02$ gave a reasonably good prediction of the patch loading resistance. Hence, the yield resistance can be written as

$$F_y = f_{yw} \cdot t_w \cdot \left(s_s + 2 \cdot t_f + 2 \cdot t_f \cdot \sqrt{\frac{f_{yf} \cdot b_f}{f_{yw} \cdot t_w} + 0,02 \cdot \left(\frac{h_w}{t_f}\right)^2} \right) \quad (2.96)$$

In Section 2.2, the buckling coefficient developed by Lagerqvist was described and therefore only the final equations are given here to make the procedure complete. The elastic critical load is determined as

$$F_{cr} = k_F \cdot \frac{\pi^2 \cdot E}{12 \cdot (1 - \nu^2)} \cdot \frac{t_w^3}{h_w} \quad (2.97)$$

where

$$k_F = 5,3 + 1,9 \cdot \left(\frac{h_w}{a}\right)^2 + 0,4 \cdot \sqrt[4]{\frac{b_f \cdot t_f^3}{h_w \cdot t_w^3}} \quad (2.98)$$

The slenderness parameter is given by

$$\lambda = \sqrt{\frac{F_y}{F_{cr}}} \quad (2.99)$$

Next, Lagerqvist proposed a reduction factor calibrated against 190 tests with $M_E/M_R \leq 0,4$. The reduction factor gives a lower 5-percent fractile equal to 1,0 for F_u/F_R for the 190 tests and is determined as

$$\chi(\lambda) = 0,06 + \frac{0,47}{\lambda} \leq 1,0 \quad (2.100)$$

This gives a patch loading resistance according to

$$F_R = F_y \cdot \chi(\lambda) \quad (2.101)$$

Lagerqvist (1994) also proposed a simplified model suited for design purposes. In this model the buckling coefficient, Equation (2.98), was simplified by omitting the term for the influence of the flanges, which gives a k_F according to

$$k_F = 6 + 2 \cdot \left(\frac{h_w}{a}\right)^2 \quad (2.102)$$

Johansson et al. (2001) presents the new design rules that was introduced in Eurocode 3 for plated structures. The design rules for patch loading follows the procedure by Lagerqvist (1994) and Lagerqvist and Johansson (1996) with one exception. The reduction factor in Equation (2.100) was simplified to

$$\chi(\lambda) = \frac{0,5}{\lambda} \leq 1,0 \quad (2.103)$$

The design model for patch loading was also calibrated versus test results by a statistical evaluation according to Annex Z¹ of Eurocode 3 part 1-1 by Johansson et al. It was found that the partial safety factor, γ_M^* , should be set to 1,1 and the design resistance become

$$F_{Rd} = F_y \cdot \chi(\lambda) / \gamma_M^* \quad (2.104)$$

Finally, the equations for patch loading resistance in EN 1992-1-5 (2006) will be shown. It is basically the same equations as above but with slightly different notation and one limitation compared to the procedure by Lagerqvist (1994) and Johansson et al. (2001). The design resistance is obtained from

$$F_{Rd} = \frac{f_{yw} \cdot L_{eff} \cdot t_w}{\gamma_{M1}} \quad (2.105)$$

where

$$L_{eff} = \chi_F \cdot l_y \quad (2.106)$$

in which

1. Annex Z of Eurocode 3 part 1-1 is with minor changes today Annex D of EN 1990 (2002).

$$l_y = s_s + 2 \cdot t_f \cdot (1 + \sqrt{m_1 + m_2}) \leq a \quad (2.107)$$

and

$$m_1 = \frac{f_{yf} \cdot b_f}{f_{yw} \cdot t_w} \quad (2.108)$$

$$m_2 = 0,02 \cdot \left(\frac{h_w}{t_f}\right)^2 \quad \bar{\lambda}_F > 0,5 \quad (2.109)$$

$$m_2 = 0 \quad \bar{\lambda}_F \leq 0,5$$

The fact that m_2 depends on $\bar{\lambda}_F$ is somewhat impractical since a value of $\bar{\lambda}_F$ has to be assumed first and later might have to be recalculated if wrong assumption was made, e.g. if m_2 should be zero but assumed not.

The critical load is calculated according to

$$F_{cr} = 0,9 \cdot k_F \cdot E \cdot \frac{t_w^3}{h_w} \quad (2.110)$$

with k_F according to Equation (2.102). The slenderness is determined as

$$\bar{\lambda}_F = \sqrt{\frac{l_y \cdot t_w \cdot f_{yw}}{F_{cr}}} \quad (2.111)$$

and the reduction factor can be calculated with Equation (2.103).

2.3.3 Interaction with bending moment

In almost every case when a girder is subjected to a concentrated load it is together with a co-existing bending moment. Therefore, many researchers and design codes have proposed different models to take this into account. It should be noted though that most of the interaction equations are connected to a resistance model and will depend on that model.

Bergfelt (1971) proposed that the interaction between patch loading and bending moment should be taken care of by means of the interaction equation

$$\left(\frac{F_E}{F_R}\right)^8 + \left(\frac{M_E}{M_R}\right)^2 = 1 \quad (2.112)$$

In Bergfelt (1976), the author states that there only seems to be an influence from the bending moment on the patch load resistance if $M_E/M_R > 0,6$.

In Elgaaly (1983) another proposal for the interaction was presented according to

$$\left(\frac{F_E}{F_R}\right)^3 + \left(\frac{M_E}{M_R}\right)^3 = 1 \quad (2.113)$$

In 1992 yet another interaction equation was proposed by Herzog (1992). Herzog states that if the applied patch load is related to the pure web crippling load according to Equation (2.114) and the acting bending moment, M_E , to the one for fully plastic flanges without web contribution an interaction formula according to Equation (2.115) will give a safe prediction. Equation (2.114) originally comes from Herzog (1986) and was developed with regression analyses and was compared to the ultimate load from 136 tests. It was defined as the 50% fractile of the web crippling load.

$$F_R = 25 \cdot f_{yw} \cdot t_w \cdot \sqrt[3]{\frac{t_f}{t_w}} \cdot \sqrt{0,4 + \frac{h_w}{a}} \quad (2.114)$$

$$\left(\frac{F_E}{F_R}\right)^2 + \frac{M_E}{M_{Rf}} = 0,9 \quad (2.115)$$

with $M_{Rf} = f_{yf} \cdot b_f \cdot t_f \cdot (h_w + t_f)$

The interaction formula was compared to 42 tests with most of the tests on the safe side. However, the agreement was not that good and it is somewhat strange to put 0,9 as the maximum level. This means that even if the moment is very small the full patch load resistance cannot be utilized.

Ungermann (1990) suggests an interaction formula according to

$$\frac{F_E}{F_R} + \frac{M_E}{M_R} = 1,4 \quad (2.116)$$

In the paper Johansson and Lagerqvist (1995) an interaction formula was proposed which was coupled to an earlier proposal for the patch loading resistance, slightly different from that proposed by Lagerqvist (1994). The interaction equation was given as

$$\frac{F_E}{F_R} + 1,25 \cdot \frac{M_E}{M_R} = 1,75 \quad (2.117)$$

Due to some modifications in the resistance model for patch loading in Lagerqvist (1994), compared to the proposal in Johansson and Lagerqvist (1995)¹, new interaction equations were presented. Equation (2.118) was proposed for welded girders and Equation (2.119) for rolled beams.

$$\frac{F_E}{F_R} + 0,8 \cdot \frac{M_E}{M_R} = 1,4 \tag{2.118}$$

$$\left(\frac{F_E}{F_R}\right)^2 + \left(\frac{M_E}{M_R}\right)^2 = 1 \tag{2.119}$$

The proposal by Lagerqvist (1994), i.e. Equation (2.118), is the same equation as the one in EN 1993-1-5 (2006).

In general, the conditions $F_E/F_R \leq 1$ and $M_E/M_R \leq 1$ should be fulfilled for the interaction equations mentioned in this Section.

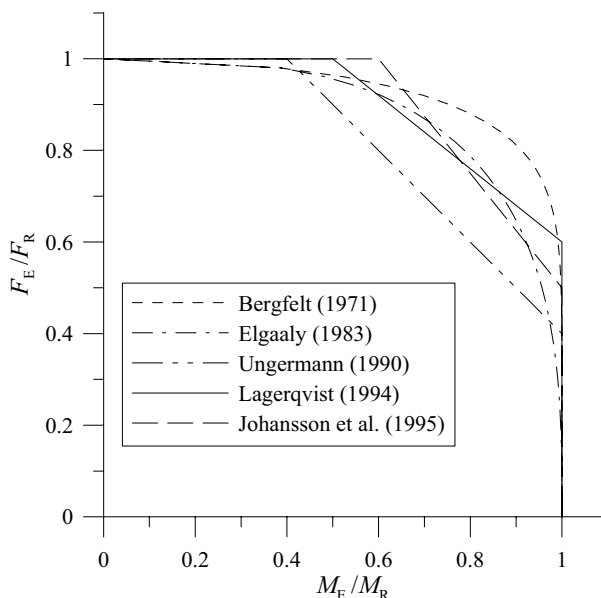


Figure 2.14 Interaction formulas proposed in the literature.

As can be seen in Figure 2.14 the proposal by Ungermann (1990) gives the strongest interaction with a reduction of the patch load resistance when $M_E/M_R > 0,4$. However, as mentioned before, the interaction formula depends on the actual prediction of the patch loading resistance used.

1. Johansson and Lagerqvist (1995) was submitted in 1993, accepted in March 1994 and published in 1995, which explains why it contains an earlier version of the resistance model for patch loading compared to Lagerqvist (1994).

2.3.4 Interaction with shear

Considering interaction between patch loading and shear, the shear force caused by the patch load is always present. Hence, it is impossible to exclude the influence from shear when comparing a design model with test results. Zoetemeijer (1980) concluded that the shear force caused by the patch loading itself have no influence on the patch loading resistance. However, from his study on rolled sections Zoetemeijer did propose a interaction equation, where only the shear force given by loads other than the transverse load should be included, according to

$$\left(\frac{F_E}{F_R}\right)^2 + \left(\frac{V_E}{V_R}\right)^2 \leq 1 \quad (2.120)$$

where V_E is the shear force without the contribution from the patch load.

In a study performed by Shahabian and Roberts (2000) on plated girders it was found that Equation (2.120) did not fit very well to the results. A total of 24 plated girders was included in the experimental work with h_w/t_w ranging from 146 to 290 and s_s/h_w from 0,05 to 0,1. Based on the test results Shahabian and Roberts proposed an interaction expression according to

$$\frac{F_E}{F_R} + \left(\frac{V_E}{V_R}\right)^2 \leq 1 \quad (2.121)$$

again with V_E as the shear force without the contribution from the patch load.

Further, within the research project ComBri “*Competitive Steel and Composite Bridges by Improved Steel Plated Structures*” further investigations by Kuhlmann and Braun (2007) considering shear and patch load was conducted. By means of two own tests, tests from the literature and a large amount of numerical simulations a new interaction expression was proposed as

$$\frac{F_E}{F_R} + \left(\frac{V_E}{V_R}\right)^{1,6} \leq 1 \quad (2.122)$$

where V_E is the shear force without the contribution from the patch load. The equation was examined in combination with the in Section 5.3 proposed patch loading resistance with good results, according to Kuhlmann and Braun.

2.3.5 Review of experimental investigations

As mentioned earlier, a large amount of test data is available from many researchers, Lagerqvist collected the ones performed before 1994 and those have been used here and are only referred to through Lagerqvist (1994) and the test data can be found in Appendix C. However, there are a few other test series performed not added to the test data base by Lagerqvist or carried out after 1994, which also can be found in Appendix C. One is presented later in this thesis and deals with varying loaded lengths.

One small test serie found was presented by Raoul et al. (1990) including three tests on plated girders. One of the tests was a regular patch loading test while the other two was performed in order to investigate the influence considering load eccentricity and an imposed rotation on the loaded flange. Only the first test with $a/h_w = 1,4$, $h_w/t_w = 212$ and $s_s/h_w = 0,18$, is included in the test data base.

Another test serie found in the literature was carried out by Shahabian and Roberts (2000). The study was mainly focused upon the interaction between shear and patch loading. A total of 24 tests, two on each girder, were performed. Four of the tests was pure patch loading tests with $a/h_w = 1, 1,5$ and 2 , $h_w/t_w = 146 - 290$ and $s_s/h_w = 0,05 - 0,1$.

A test serie containing stainless steel girders and was presented by Unosson (2003). A total of five tests with $a/h_w \approx 4$, $h_w/t_w = 50-110$ and $s_s/h_w = 0,09-0,38$. The ultimate loads from tests was compared to the predicted resistance according to Lagerqvist (1994) with a mean of 1,28 and a coefficient of variation of 0,073 as well as with EN 1993-1-5 (2006) with a mean of 1,34 and a coefficient of variation of 0,074.

The last test found in the literature was carried out by Kuhlmann and Seitz (2004). The main objective with the research presented by Kuhlmann and Seitz was patch loading of longitudinally stiffened girder webs but one reference test without longitudinal stiffeners was conducted with $a/h_w = 2$, $h_w/t_w = 200$ and $s_s/h_w = 0,58$.

The tests described above are added to the data base collected by Lagerqvist, see Appendix C, and will be used for further evaluations of a new design model.

2.4 Serviceability limit state

The serviceability limit state in general and for girders subjected to patch loading in particular is a subject less studied compared to the ultimate limit state. This is probably due to the subjectivity of the problem, i.e. it is not as straight forward as the ultimate resistance.

One difficulty with serviceability is to define the limit state. This may vary depending on type of structure and how the owner weight different factors. Possible serviceability requirements for

patch loading are e.g. requirements that limit residual deformations and that limits web breathing. In this thesis it is the serviceability limit state during bridge launching that is of most interest and how to determine a reasonable criteria. For steel bridges EN 1993-2 (2003) requires no membrane yielding in the serviceability limit state. Behind this is a more basic requirement of reversible behaviour, which is less strict. Some yielding may occur as long as shake down is possible.

During launching, a girder section can be subjected to over 10 repeated support reactions from launching shoes if the girder is long, and subsequently it is important to limit the residual deformations to make sure that the attended girder can withstand the loads that it was designed for. Further, for bridge launching it is not a stationary patch load that is applied but a travelling load. Research in this area is very limited but there are some work done that will be briefly described here together with some general work on repeated patch loads.

In Skaloud and Novak (1972) a total of 22 patch loading tests were presented. 11 of the tests were performed under static conditions but the remaining 11 was loaded with a cyclic load that was stepwise increased. For each load step, 1000 loading cycles were applied. The aim with the cyclic load tests was to investigate; if the web deflection increase during a certain number of loading cycles in the plastic range, if the web deflection increase, does it cease after a limited number load applications and finally does the increase in deflection during cyclic loading affect the ultimate load. Both a static as well as a cyclic loading test was conducted on identical girders to enable a comparison in ultimate load. The girders had the dimensions $a/h_w = 1$, $h_w/t_w = 250$ and 400 and the ratio $s_s/h_w = 0,1$ and 0,2. An increase in the web deflection was observed but the increase stopped at a constant level after a few, 3-5, load cycles according to the authors. The same behaviour was observed when the load was increased in the next load step. Further, the ultimate load from the cyclic loading tests were in all cases with $h_w/t_w = 400$ higher than the ultimate load from the static loading tests. For the cases with $h_w/t_w = 250$ the ultimate load was higher in some and lower in some cases if the ultimate load from the cyclic loading tests and static loading tests were compared.

As a complement to Skaloud and Novak (1972), Novak and Skaloud (1973) presented an extended test serie including 29 new tests. The test serie included both static and cyclic patch loading where $a/h_w = 1$ and 2, $h_w/t_w = 400$ and $s_s/h_w = 0,1$ or 0,2 (for the girders with $a/h_w = 2$). 12 of the cyclic loading tests were conducted with a slower loading rate, approximately 100 times slower than the other cyclic tests. The velocity of the movement of the loading jack was 6 mm/min and 50 loading cycles were applied in each successive loading step. The conclusions, drawn by the authors, from the work were that for the faster cyclic loading tests the ultimate load were not lower compared with the static tests. For the slow cyclic loading tests the ultimate load was lower in some cases and higher in some. The trend was that for higher flange stiffness the ultimate load in the cyclic loading tests were higher compared to the static

loading case. However, the difference in ultimate load between the cyclic and static loading, irrespective of speed, was less than 10%.

Drdacky (1986) presented some results regarding the plastification of girder webs subjected to patch loading. The beginning of plastification was determined by means of an acoustic emission method and checked by strain gauges placed in discrete points. Drdacky found that a part of the web can be in plastic state (membrane yielding) already at 25% of the ultimate load for stocky webs. From the results presented on girders with h_w/t_w from 25 to 400, which is not very thoroughly reported, it can be seen that when h_w/t_w increase this level also increase. However, it is also shown that the loaded length, s_s , plays an important role. Longer s_s but otherwise equal girder dimensions gives higher level of load before membrane yielding occur. Drdacky proposed a design rule for girders subjected to dynamic patch loads, which was that the ultimate resistance from the static case should be reduced by 50%.

In Kutmanová and Skaloud (1992) another study on repeated partial edge loading was presented. Most of the tested girders were longitudinally stiffened but 16 girders had no longitudinal stiffeners. Some of girders were subjected to constant loading for the sake of comparison. However, information on how many girders that were subjected to constant or repeated loadings were not given. The girders without longitudinal stiffeners had $h_w = 500$ mm, $a/h_w = 1$, $t_w = 4$ mm and $s_s/h_w = 0,1 - 0,3$. Further, the flange size was varied between what was called “thin” and “thick” flanges.

The load in the repeated loading tests by Kutmanová and Skaloud cycled between zero and a value P_{max} . P_{max} was varied between the constant loading ultimate load and the onset of yielding load also from the constant loading tests. Thus, the webs of the tested girders were in the elasto-plastic range and consequently their performance was expected to be governed by low-cycle fatigue according to the authors. The results from the repeated patch load tests were given as the onset of surface yielding loads and the low-cycle fatigue load, determined as the maximum load values under which no appearance of cracks or other kind of failures were detected after 5×10^4 load cycles. These loads were given as a fraction of the ultimate load, F_u , from the constant loading tests for both “thin” and “thick” flanges. The onset of surface yielding was for both kind of flanges $0,39F_u$ and the low-cycle fatigue load was $0,75F_u$ and $0,9F_u$ for “thin” and “thick” flanges, respectively. The information regarding the tests and the results are limited and only one web slenderness, h_w/t_w , was tested.

Lagerqvist (1994) presented a rough estimation of a load level for avoiding residual deformations. Based on the load-deformation curves from his tests, Lagerqvist noticed that with a few exceptions the behaviour was linear at least up to 70% of the ultimate load. If this is assumed to be the upper limit of the elastic range, a resistance of $0,7F_R$ in the serviceability limit state could be a criterion.

Granath et al. (2000) presented a numerical study similar to the one presented later in this thesis, where different girders were subjected to a travelling load together with a bending moment. Unfortunately, some information regarding how the load was applied and whether the loaded flange was constrained from rotation or not are missing. The girders were divided into a *Normal girder*, $h_w/t_w = 100$ and $b_f/t_f = 14$, a *Slender girder*, $h_w/t_w = 167$ and $b_f/t_f = 28$, and a *Stocky girder*, $h_w/t_w = 50$ and $b_f/t_f = 14$. The amplitude of the initial imperfections used were $h_w/160$, $h_w/96$ and $h_w/200$ respectively.

The results showed that for the *Normal girder* loaded with $0,5F_{u,FE}$ and $0,69M_R$ no increase of the remaining buckle amplitude took place after three load passages. However, when the load level was increased to $0,72F_{u,FE}$ and $0,73M_R$ the remaining buckle amplitude was increasing for each passage and after three passages the increase was approximately 5 mm and after twelve passages approximately 8 mm. The above mentioned load levels, i.e. $0,5F_{u,FE}$ and $0,72F_{u,FE}$, have been recalculated to fulfil the interaction between patch loading and bending moment, see Equation (2.118), since there should be a significant affect from bending moments at these levels.

For the *Slender girder* two load levels were used, $0,46F_{u,FE}$ and $0,52M_R$ as well as $0,68F_{u,FE}$ and $0,50M_R$. The former load level gave a remaining buckle amplitude growth of approximately 2 mm, though almost constant. For the latter load level the remaining buckle amplitude was first growing with approximately 3 mm and then gradually changing shape after six load passages from a sinusoidal shape to an S-shape with a smaller local buckle close to the loaded flange.

The *Stocky girder* was also subjected to two different load levels namely $0,49F_{u,FE}$ and $0,46M_R$ as well as $0,68F_{u,FE}$ together with $0,61M_R$. As expected the former load level gave almost no increase of the remaining buckle amplitude. However, for the latter load level the growth was clear and also for this case the buckle changed shape as for the slender web.

The general conclusion that was drawn in Granath et al. (2000) was that for a travelling load, a load level of approximately $0,50F_{u,FE}$ gave reversible behaviour, i.e. 70% of the ultimate load as proposed by Lagerqvist (1994) for stationary loads are too high for travelling loads. It should be noted though that the amplitude of the initial imperfection used for the *Slender girder* was large, compared to the in EN 1993-1-5 recommended $h_w/200$.

Granath (2000) presented a serviceability limit state criterion for patch loading based on a large number of non-linear FE-analyses. The limit state was defined such that the effective stress at the web surface should not exceed the yield strength of the web. Granath performed non-linear FE-analyses on 155 tests collected earlier by Lagerqvist to determine at what load level, F_{FEM} , the effective stress at the web surface reach the yield strength of the web material. Those analyses showed that for low $\bar{\lambda}_F$, according to Equation (2.111), the difference between F_{FEM} and F_u was large but for high $\bar{\lambda}_F$ the difference was very small. This behaviour is expected as

for a slender girder the yielding, if any, will occur late as the web will fail due to instability meanwhile a stocky girder web will yield earlier, in relation to the ultimate load, during loading. In addition to the analyses of the tested girders Granath carried out a total of 486 other analyses to cover more cases, e.g. girders made of high strength steel and girders subjected to large global bending moments.

Granath (2000) proposed a design criterion for patch loading in the serviceability limit state developed through regression analysis based on all FE-analyses performed. The resistance for a girder is calculated as

$$F_{R, sls} = \min \begin{cases} F_{stocky} \\ F_{slender} \end{cases} \quad (2.123)$$

with

$$F_{stocky} = 0,885 \cdot f_{yw} \cdot t_w \cdot (s_s + 5 \cdot t_f) \cdot 8 \sqrt{\frac{b_f}{h_w}} \quad (2.124)$$

and

$$F_{slender} = 3,93 \cdot f_{yw} \cdot t_w^2 \cdot \sqrt{(s_s + 5 \cdot t_f) \cdot \sqrt{\frac{E}{h_w \cdot t_w \cdot f_{yw}}} \cdot \sqrt{\frac{t_f}{a}}} \quad (2.125)$$

According to Granath 95% of both the stocky and slender girders have a F_{FEM} that is higher than $F_{R,sls}$.

Finally, an interaction formula for patch loading together with bending moment in the serviceability limit state was proposed by Granath according to

$$\begin{cases} \text{If } \frac{M_E}{W_{eff} \cdot f_{yw}} \leq 0,43 \rightarrow \frac{F_E}{F_{R, sls}} \leq 1 \\ \text{If } \frac{M_E}{W_{eff} \cdot f_{yw}} > 0,43 \rightarrow \frac{F_E}{F_{R, sls}} + 1,75 \cdot \frac{M_E}{W_{eff} \cdot f_{yw}} \leq 1,75 \end{cases} \quad (2.126)$$

The work presented in Granath (2000) is very extensive but all analyses that form the basis for the serviceability limit state criterion is based on stationary loading, which is not of primary interest here.

2.5 Summary of the review

Considering the elastic critical buckling load for simply supported plates, Zetlin (1955), Rockey and Bagchi (1970), Khan et al. (1977), Lagerqvist (1994) and Ren and Tong (2005) have all presented values on k_F with reasonable good agreement with each other. The models used were almost identical, though the boundary conditions for the vertical edges were slightly different. Rockey et al. and Lagerqvist used models that allowed for rotation of the vertical edges as rigid lines around the neutral axis of the section, which was not allowed by the others.

Rockey and Bagchi (1970) also presented results on k_F for a section including the flexural and torsional properties of the flanges. This is believed more relevant for patch loading and it was shown that when the flanges were included the critical load was increased significantly. Lagerqvist (1994) did a thorough study of the critical load on cross sections including web and flanges by means of FE-analyses in order to find approximate solutions for k_F where the dominating parameters were included. Recently, Ren and Tong (2005) performed a study aiming for an expression that gives a k_F for a section with flanges in between the solution for a simply supported plate and a plate clamped at the horizontal edges. For weak flanges the solution of k_F should end up close to the solution for a simply supported plate and for strong flanges close to the solution for clamped edges. However, the model including flanges used for the investigation of the rotational restraint did not prevent any rotation under the load, which makes the approach a bit doubtful to recommend for design purposes. From the author of this thesis point of view, the expression for k_F proposed by Lagerqvist was derived with the most realistic model and therefore the proposal by Lagerqvist will be further used later in this thesis. In addition, critical loads obtained through the software *EBPlate*, Gal ea and Martin (2006), will also be included in the further studies in this thesis.

Regarding ultimate limit state there are an abundance of studies and expressions for the resistance. From fully empirical models to models based on some kind of mechanism, with and without yield lines in the web. The general opinion that the web thickness are the parameter that contributes mostly to the resistance was confirmed by the results presented by Raoul et al. (1991), see Equation (2.37). Further, Roberts and co-workers proposed a model with four plastic hinges in the loaded flange together with three yield lines in the web for predicting the failure load regarding web crippling. In addition Roberts proposed a model for direct yielding of the web and the recommendation was to use the lesser of the resistance from the two models. Bergfelt on the other hand proposed a three-hinge mechanism using the von K arm an approach to describe the resistance of the web. The solution by Bergfelt contains a number of correction factors which makes the method rather complicated.

Following the concept by Roberts and Bergfelt using mechanism solutions, Ungermann (1990) and Lagerqvist (1994) developed their own resistance models. Those models included a plastic resistance, based on a plastic hinge mechanism in the loaded flange, the critical buckling load

and a reduction factor to relate the slenderness to the resistance. The model by Ungermann used a three-hinge mechanism and a simplified expression for the critical buckling load, while Lagerqvist used a four-hinge mechanism and a more sophisticated expression for k_F mentioned above. Furthermore, Lagerqvist's approach has another advantage, that is that the same equations are used irrespective of the type of structural member considered. Ungermann on the other hand proposed two different equations, one for $\lambda \leq 0,80$ formulated for rolled beams and one for $\lambda > 0,80$ derived for welded girders.

The author of this thesis considers the approach by Ungermann and Lagerqvist as very interesting since it follows the same analogy as other buckling problems in the design codes. Moreover, a four-hinge mechanism is more likely to develop in reality and for instance Lagerqvist found proofs for this in his experimental investigation. The last advantage, compared to most of the other developed models, is that the resistance model by Lagerqvist considers only one verification covering all failure modes and the transition from yielding to crippling and buckling is smooth and continuous.

Considering the influence on the patch loading resistance from a co-existing bending moment there exists a number of suggestions in the literature. Some of them were considered in the review and the general conclusion found was that for small ratios for M_E/M_R the influence is negligible. Further, the influence from an external shear force on the patch loading resistance was investigated by some researchers where the latest contribution from Kuhlmann and Braun (2007), which is examined together with the in this thesis proposed patch loading resistance with good results, is assumed to be a good criterion for this.

When it comes to the patch loading resistance in the serviceability limit state, e.g. launching of bridge girders, the amount of papers found in the literature was very limited. The only actual design criterion was proposed by Granath (2000) where the limit state was defined such that the effective stress at the web surface should not exceed the yield strength of the web material. The final criterion was developed through regression analysis based on a large number of FE-analyses in which the serviceability load level, F_{FEM} , was determined for different geometries and load conditions. The disadvantage with the model by Granath is that it was developed for stationary loads, which is not the load situation when launching a bridge girder.

Lagerqvist proposed a rough estimation, based on his test results, that no residual deformations would appear if $0,7F_R$ was used as the serviceability limit state criterion. Drdacky (1986) found, not surprisingly, that membrane yielding of the web starts at a lower load level in relation with the ultimate load for low ratio of h_w/t_w compared to a higher ratio of h_w/t_w .

The primarily interest considering serviceability limit state in this thesis is to find a serviceability criterion for bridge girders that is launched into position. This means that the girder is subjected to a number of travelling concentrated forces, when travelling over several

supports, during launching and also that the subsequent load situation when acting in the actual bridge is shear and bending moment. Hence, the actual resistance to patch loading after several repeated loads are not of primary interest. The only study at all considering travelling loads was presented in Granath et al. (2000) where FE-analyses of three different geometries were carried out subjected to up to 12 load passages. It was concluded by Granath et al. that even at low load levels significant residual deformations were found.

3 EXPERIMENTAL WORK

3.1 General

The experimental investigation carried out was focused on the influence from the loaded length on the ultimate resistance for patch loading of I-girders. When studying the literature, one can immediately see that the main tests performed was conducted with short loaded lengths. It is generally known that the resistance of a girder subjected to patch loading increase with increasing loaded length. Further, to avoid problems during launching it is common to increase the length of the launching shoe and then the question arise how well this is covered by the design rules.

Three patch load tests on identical girders were conducted with varying loaded lengths. In addition, a total of 12 uniaxial tests were conducted in order to determine the mechanical properties in terms of stress-strain curves for the plates used for manufacturing of the girder specimens used for the patch loading tests. The material used in all tests was S355 delivered from Dillinger Hütte, Germany. The complete set of test results are displayed in Appendix A and B.

3.2 Uniaxial coupon tests

The uniaxial tests were conducted to determine the mechanical material properties of the plates used for the specimens. In a later stage of this work the stress-strain curves from the tests will be used in further numerical investigations, i.e. by means of the finite element method.

The tested I-girders had 20 mm thick flanges and stiffeners and a 6 mm thick web of steel grade S355. It is common that different thicknesses have a somewhat different mechanical behaviour due to the rolling. This was investigated by means of six tensile tests on each thickness and these six tests were divided into three tests along and three tests transverse the rolling direction. In Figure 3.1, four stress-strain curves are shown, one for each thickness and direction.

As can be seen, a slight anisotropy, i.e. difference in behaviour between the rolling and transverse directions, is present for the thinner material. A summary of the tests can be found in Table 1 below, whereas individual test results from the uniaxial tests are displayed in Appendix A.

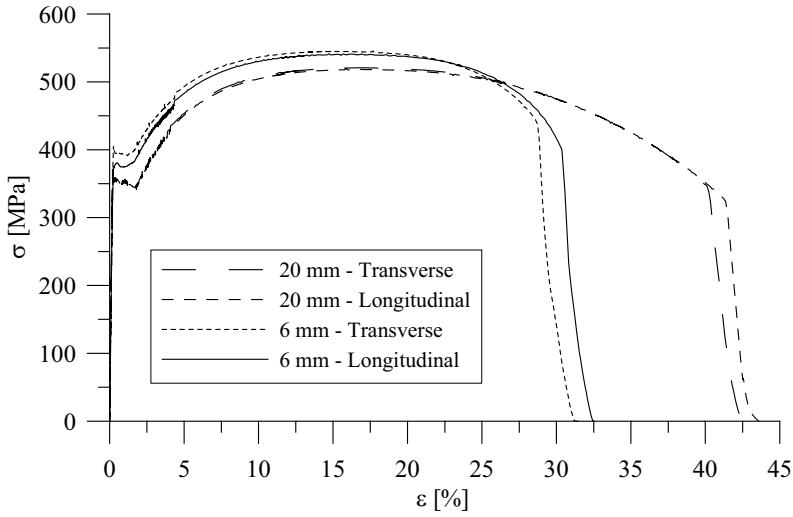


Figure 3.1 Stress-strain relation from uniaxial tests along and transverse to the rolling direction for both thicknesses. Only one curve from each thickness and direction is shown.

Table 3.1 Average values from the uniaxial coupon tests.

Section	Direction	Number of tests	f_y [MPa]	f_u [MPa]
Web	Longitudinal	3	371	542
Web	Transverse	3	394	543
Flange/Stiffener	Longitudinal	3	354	519
Flange/Stiffener	Transverse	3	354	521

The flanges of the tested girders had the rolling direction along the girder while the webs were oriented with the rolling direction perpendicular to the girder.

3.3 Patch loading tests

3.3.1 Geometry and test set-up

All three girders were doubly symmetric with the same flange and web dimensions. The vertical stiffeners at the supports had the same dimensions as the flanges. The only parameter that differed between the tests was the loaded length, s_g . The test girders were simply supported and at one of the supports a Teflon-plate together with a stainless steel plate worked as a support without any restraint in the horizontal direction, i.e. avoiding normal forces in the girder. The dimensions of the test girders are shown in Figure 3.2. Further, the fillet welds between the web

and flanges had a throat thickness of 5 mm. The exact dimensions for each girder are displayed in Appendix B.

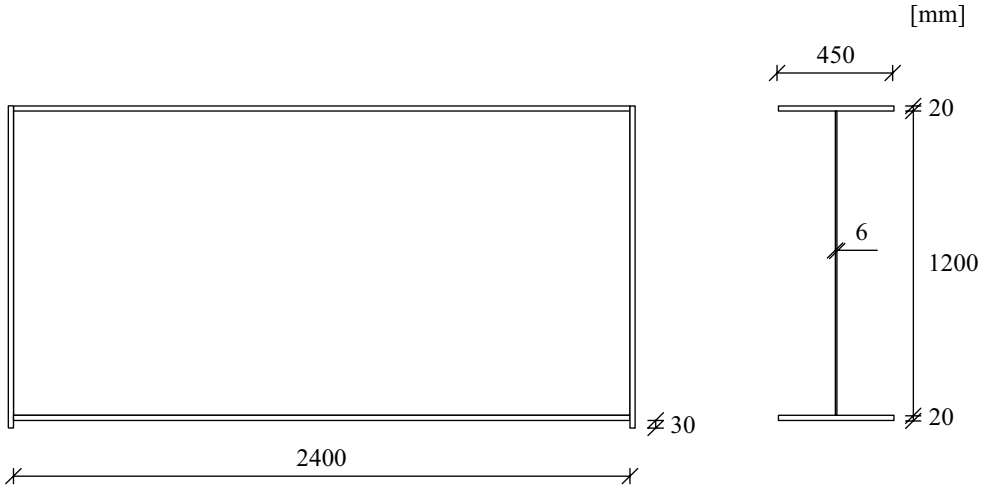


Figure 3.2 Geometry of the test girders.

The loaded length, s_s , depends on how it is defined. The aim was to investigate the influence from long loading lengths, in this case 200 mm, 700 mm and 1440 mm was chosen. For a girder loaded through one loading plate like most of the girders tested by others it is easy to define s_s , i.e. s_s equals the length of the loading plate. However, in this case two different set-ups were used since it is very difficult to find a stiff enough loading plate with the width of 1440 mm. For the test with 200 mm loading plate a plate of thickness 40 mm and length 200 mm was used. For the two other cases it was decided to use two or four plates with load distributing beams on top, see Figure 3.3. In the latter cases, i.e. where more than one plate were used, the plates had a thickness of 40 mm and a length of 330 mm. In here, the tests are called P200, P700 and P1440 and the figures comes from the distance between the outer edges of the outer loading plates, if more than one, or the width of the plate for the 200 mm case, see Table 3.2 and Figure 3.3. If this should be treated as s_s or not can be discussed and will depend on the mechanical model used when defining the yield resistance. According to EN 1993-1-5 (2006) the recommendation, if the load is distributed through several concentrated forces, is that the resistance should be checked for each individual force as well as for the total load where s_s should be taken as the centre-to-centre distance between the outer loads and adding the load spread through the loading plate. There is also a limitation that s_s should not be taken as larger than h_w . In Table 3.2 the loaded length according to EN 1993-1-5 is shown as well.

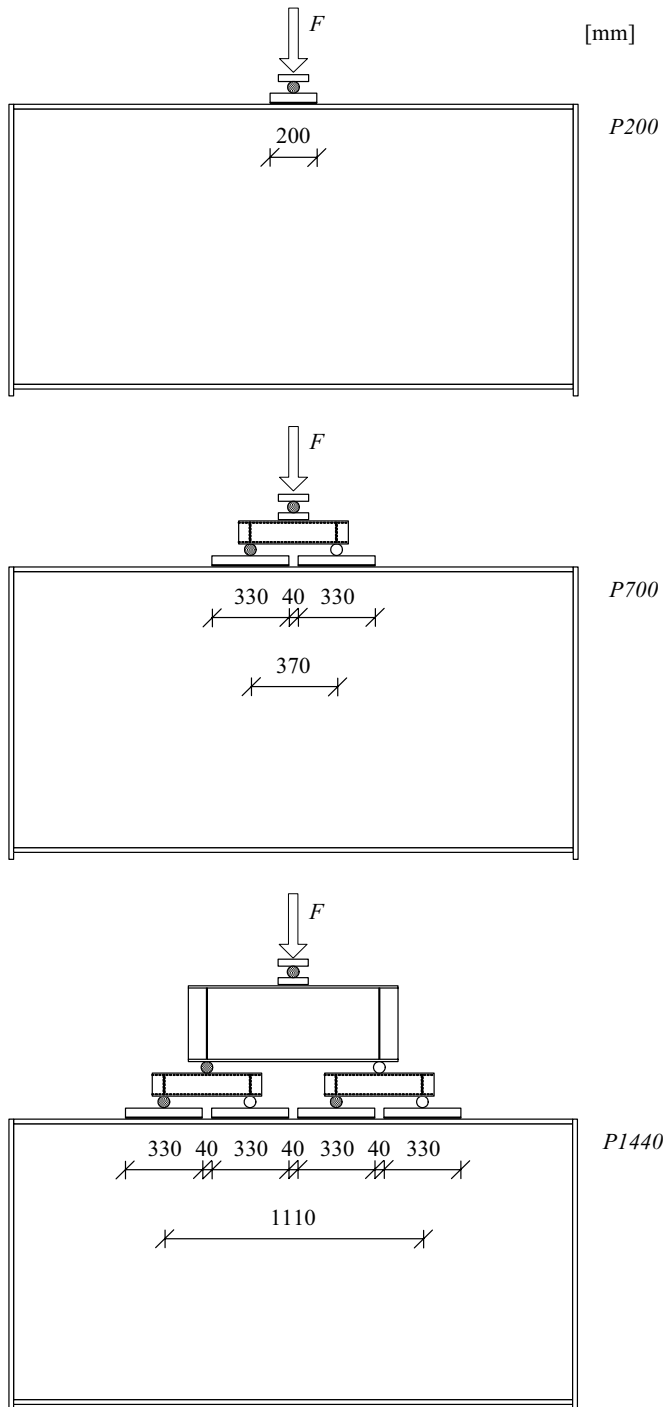


Figure 3.3 Test set-up for the three different tests. The grey bars are locked in the longitudinal direction.

Table 3.2 Test label, loaded length depending on definition and s_s/h_w for the different definitions.

Test	Loaded length outer dist [mm]	s_s/h_w	Loaded length EN 1993-1-5 [mm]	s_s/h_w
P200	200	0,17	80	0,067
P700	700	0,58	450	0,38
P1440	1440	1,2	1190	0,99

In Figure 3.4 a photo of the P1440 test set-up is shown.



Figure 3.4 Photo of the P1440 test with the load distributing beams on top of the girder.

The tests were performed in a test rig with a hydraulic INSTRON actuator with a capacity of 1000 kN controlled by an INSTRON control unit. A constant vertical displacement rate of 0,005 mm/s was used until the ultimate load was passed whereafter the rate was increased to 0,025 mm/s.

3.3.2 Measurements

Before testing, the initial imperfections, i.e. the out of plane imperfections, of the web were measured. This was done by means of a device and a LVDT (Linear Variable Displacement Transducer), measuring perpendicular to the web using the flanges as reference. The device consisted of a steel bar guiding the LVDT along a vertical path specified by a grid applied to the web indicating the points that should be measured. The grid on one specimen is shown in Figure 3.5.

During the tests, the data from the different measurements, i.e. the load and stroke from the actuator, strains from a number of strain gauges and displacements, was recorded and stored on a computer.

Vertical displacements were measured on the loading plate/plates and in the middle of the girder on the bottom flange. This means three LVDT's (one on each side of the loading plate) for the P200 girder, three on the P700 girder, one on each loading plate and one on the bottom flange, and five on the P1440 girder, as shown in Figure 3.5.

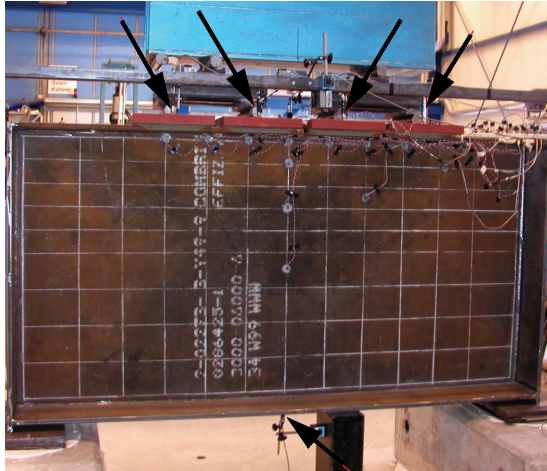


Figure 3.5 The P1440 test where the arrows indicate the LVDT's measuring vertical displacement. On the web a grid was applied for measurement of initial imperfections and lateral deformations during the test.

Strains were measured during the tests by a number of uniaxial and triaxial rosette strain gauges. The strain gauges were attached in the same position on both sides of the web in order to enable evaluation of membrane strains. A total of 14 monoaxial strain gauges were used for the P200 and P700 girders and 22 for the P1440 girder, i.e. 7 or 11 on each side of the web respectively. Four triaxial strain gauges were used in all tests. An example of the layout of the strain gauges is shown in Figure 3.6 for the P1440 girder. The same analogy was used for the other tests as well. The strain gauge layout for the P200 and P700 can be found in Appendix B.

Further, during the tests also the out of plane deformation of the web were measured at certain load steps. When these loads were reached the deformation of the specimen was halted and the measurement was conducted. The buckling measurements on the web were only performed along a vertical line centrally below the applied load. The same equipment was used as used for the initial imperfection measurements.

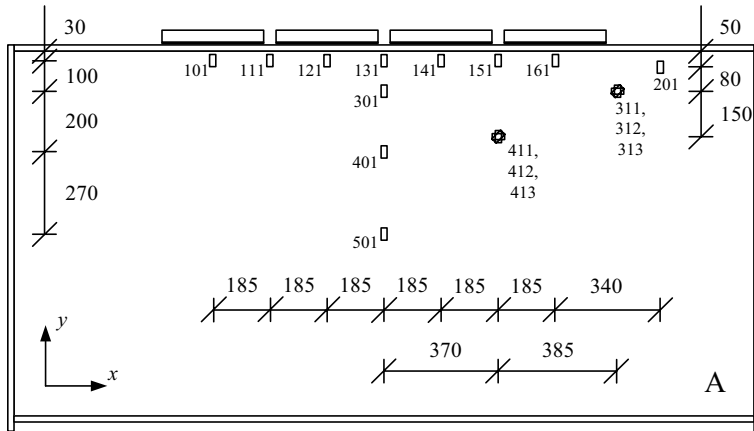


Figure 3.6 Strain gauge layout on one side of the web of the P1440 test girder.

Moreover, during the tests of the specimens P700 and P1440 a photogrammetric measuring method was tried. One side of the web was given a pattern that was photographed at every 100 kN. The aim was to obtain strain fields on the web, at least before severe buckling of the web had started, to investigate how the strains were distributed in the web due to the patch loading. The method has been shown to work well on concrete beams, see e.g. Carolin et al. (2004), but unfortunately the quality of the pattern was not good enough in this case. Hence, no results from this method were obtained within this study.

Furthermore, to make it possible to take pictures of one side of the web the nearby area on that side of the girder had to be clear, i.e. no equipment could stand on that side of the girder during the tests. This led to, for the P700 and P1440 tests, some problems when measuring the displacements of the loading plates. Since no equipment could be placed on one side of the girder only the vertical displacements on one side of the loading plate could be measured. A not fully flat upper flange or a loading plate not perfectly positioned, may lead to a tilting loading plate under deformation of the specimen (loading). This combined with a single side measurement of the vertical displacement on the loading plate may lead to an awkwardly graphical interpretation of the load-displacement behaviour. Regarding the load-displacement curve of P1440, this may be the cause of the somewhat unexpected correlation between the vertical deformation and the load.

Considering the P200 test, no photogrammetric measurements were conducted, hence the displacements of the loading plates were measured on both sides of the girder.

3.4 Test results

In this section the main results from the tests are shown graphically as load-deformation curves as well as lateral web deformation and vertical strains along the centre line of the web at certain load steps. The full strain curves from all strain gauges are shown in Appendix B.

3.4.1 P200

Figure 3.7 shows the applied force vs. the vertical web deformation, i.e. the vertical displacement of the loading plate subtracted with the vertical deformation of the lower flange, for the P200 test. The ultimate load for the P200 test was $F_u = 544$ kN.

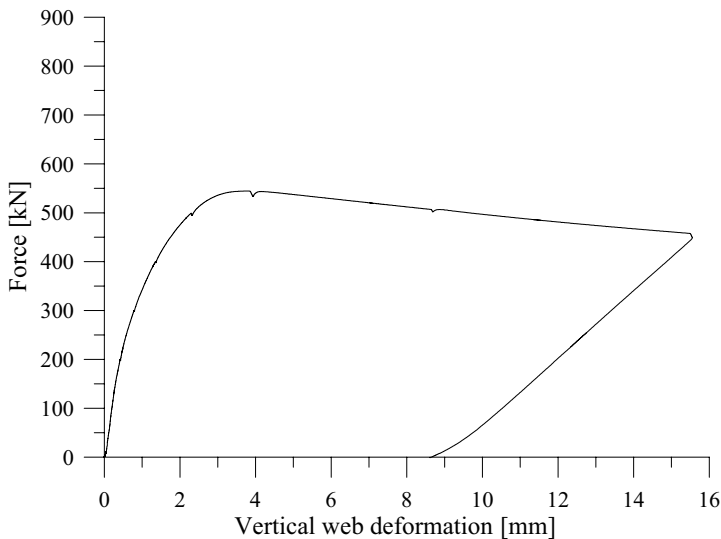


Figure 3.7 P200. Force vs. vertical web deformation.

The initial lateral imperfections of the web were measured before testing as described earlier. In Figure 3.8, the initial imperfections along the centre line of the web, directly below the applied load, are shown. As can be seen the maximum imperfection is approximately 0,27 times the web thickness, i.e. 1,6 mm, and the web imperfection had a bow-shape. In the following figures the points are measured values and the lines connecting the points are only a fit to the measured results.

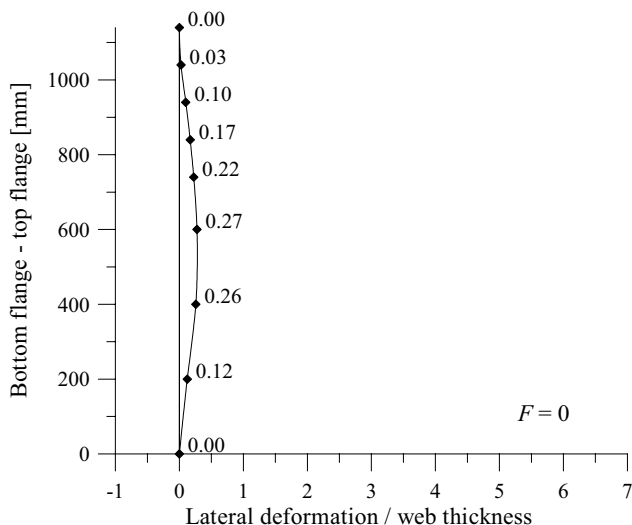


Figure 3.8 P200. Initial lateral imperfections along the centre line of the web, i.e. below the applied load.

In order to obtain information concerning how the failure occurs for the different girders the lateral deformations of the web along a vertical line under the load and the measured strains recalculated to membrane stresses along the same vertical line were monitored during the tests. In Figure 3.9 - Figure 3.13, the lateral deformation and the membrane stresses are shown for different loads regarding the P200 test. The stress value at zero height was assumed to be zero, since it was not measured. It might have been another value though very small. In a similar measurement by Lagerqvist (1994) the membrane stress 20 mm from the lower flange was constantly 0,02 times the yield stress at all displayed loads up to the ultimate load. The stresses are displayed in relation to the yield strength of the web material and were determined through the uniaxial stress-strain curve. This means that the strains on each web surface was translated to stresses and then the average of the stresses are used here, assuming a linear variation through the thickness.

Figure 3.9 - Figure 3.11 shows how the buckle increases with increasing load and how the compressive membrane stresses pattern develops. The membrane stresses increase significantly in the upper part of the web and the pattern follows the expected with a stress level that decreases with the distance to the loaded flange.

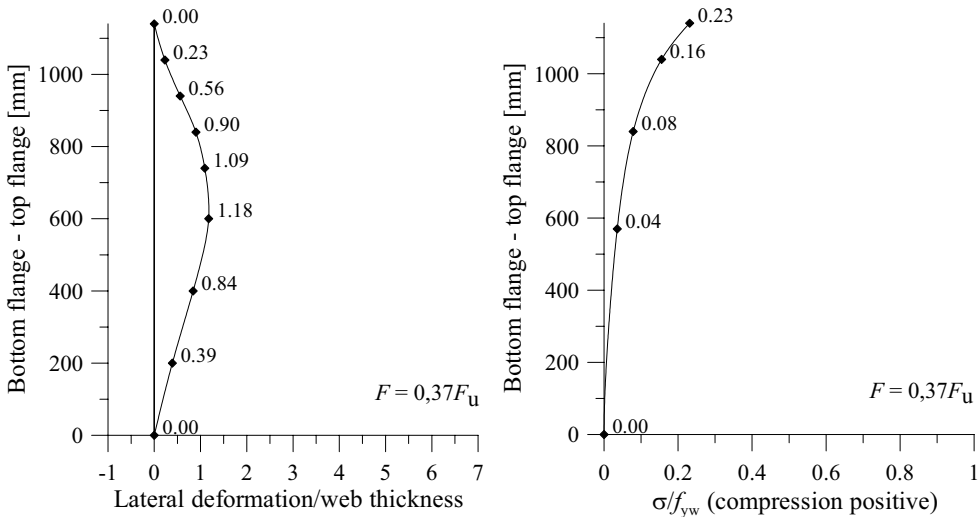


Figure 3.9 P200. Out of plane deformations and vertical membrane stresses along a vertical line at mid-span, $F = 200$ kN.

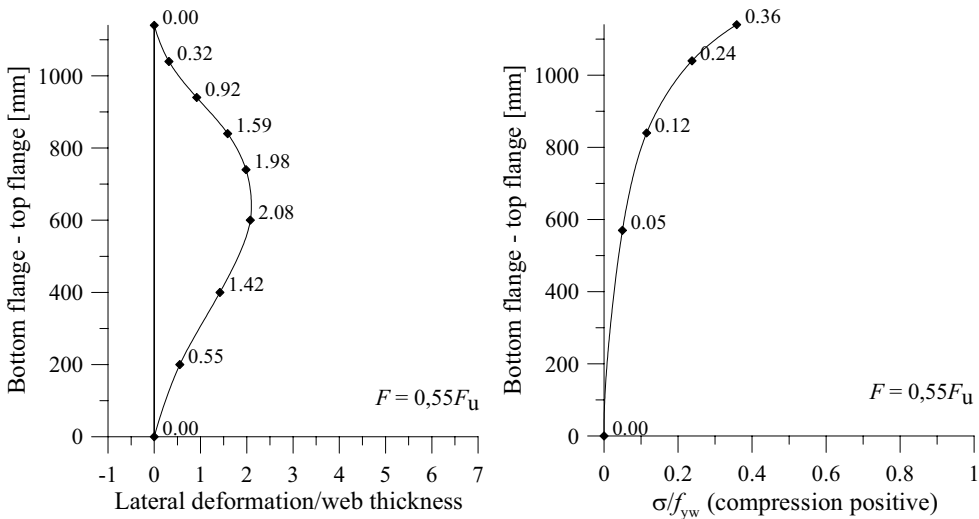


Figure 3.10 P200. Out of plane deformations and vertical membrane stresses along a vertical line at mid-span, $F = 300$ kN.

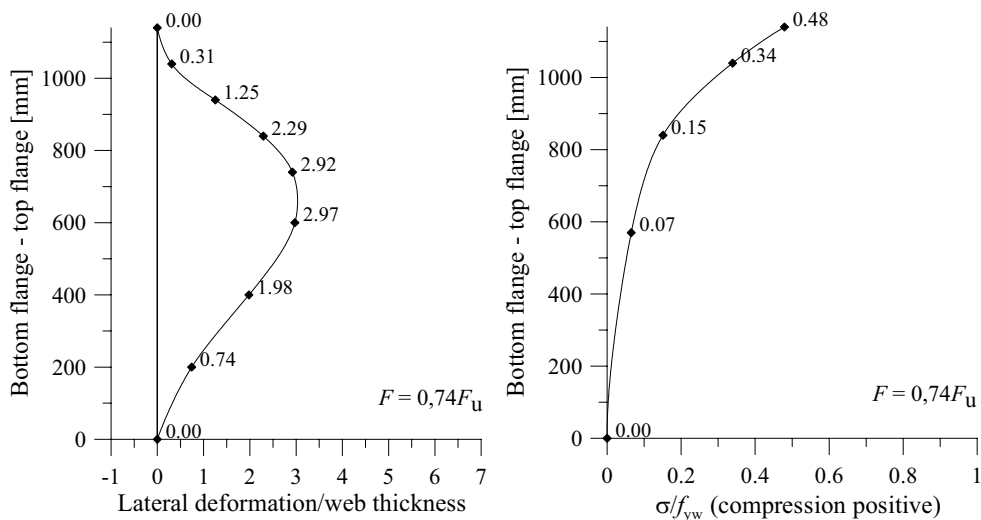


Figure 3.11 P200. Out of plane deformations and vertical membrane stresses along a vertical line at mid-span, $F = 400$ kN.

When the load is approximately 90% of the ultimate load, Figure 3.12, the following is noticed. First, the buckling shape of the web starts to change and secondly, the membrane stress at the second strain gauge position from the top are decreasing significantly due to bending of the web. The compressive stress at this position on one side have passed the yield strength and are situated on the yield plateau and the tension stresses on the other side of the web have almost reached the yield strength. The stresses at the uppermost position are still compressive on both sides of the web but on one side they are decreasing compared to the stress at the former load level, shown in Figure 3.11, indicating bending of the web at this position as well.

At ultimate load, Figure 3.13, the buckling shape has changed to the characteristic S-shape and the membrane stresses are very much influenced by bending at the upper positions. The membrane stresses are very low at the measured positions but at the web surfaces the stresses has past the yield strength on the compressed side of the web at the three uppermost positions and on the tension side they have reached or have almost reached the yield strength. At the lowest position situated at mid-depth of the web the stresses are significantly lower compared to the others but also here there are one compression side and one tension side of the web.

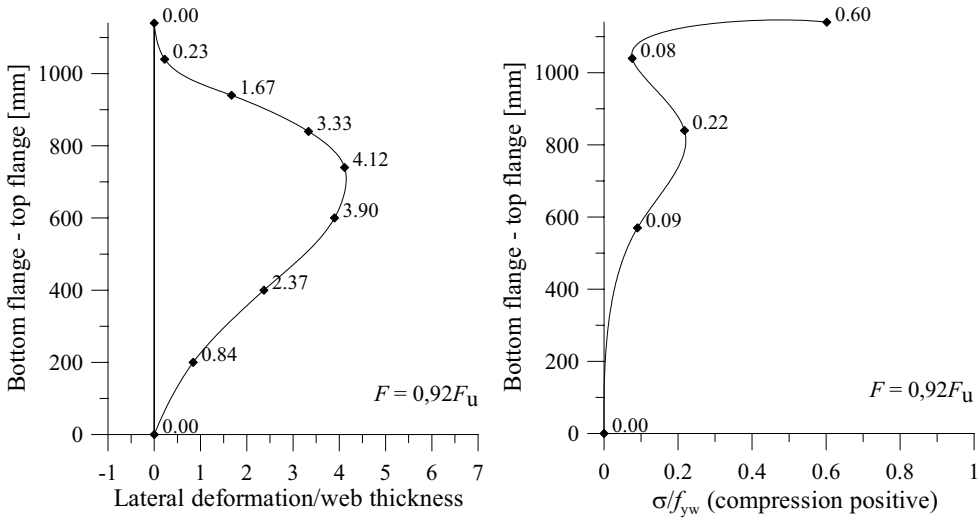


Figure 3.12 P200. Out of plane deformations and vertical membrane stresses along a vertical line at mid-span, $F = 500$ kN.

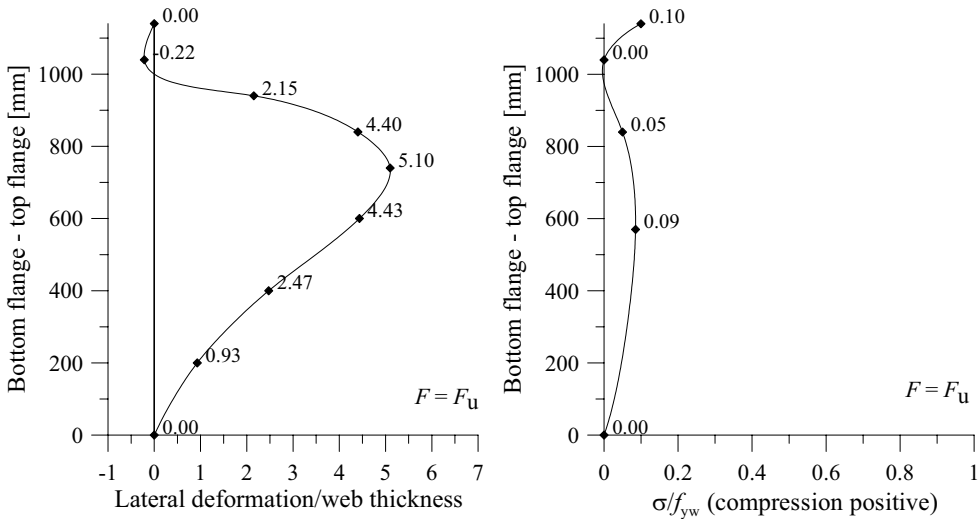


Figure 3.13 P200. Out of plane deformations and vertical membrane stresses along a vertical line at mid-span, $F = 544$ kN.

Figure 3.14 shows the vertical membrane stresses determined from the strain gauges placed on the web along the loaded flange. The diamonds corresponds to the strain gauge positions 101, 111 and 121 attached 30 mm below the loaded flange, see Figure B.1 in Appendix B, and the dots corresponds to the 201 and 211 strain gauges situated 50 mm below the flange. Now, if the stresses from the filled diamonds and dots shown in Figure 3.14 are translated to a web

resistance it should approximately correspond to the applied load. However, for the P200 this was not the case at ultimate load. This is explained by the bending of the web that took place close to the ultimate load close to the flange. If instead the web resistance at the stage when the applied load is 500 kN corresponding to the unfilled diamonds and dots in Figure 3.14 the agreement is much better, in fact very good.

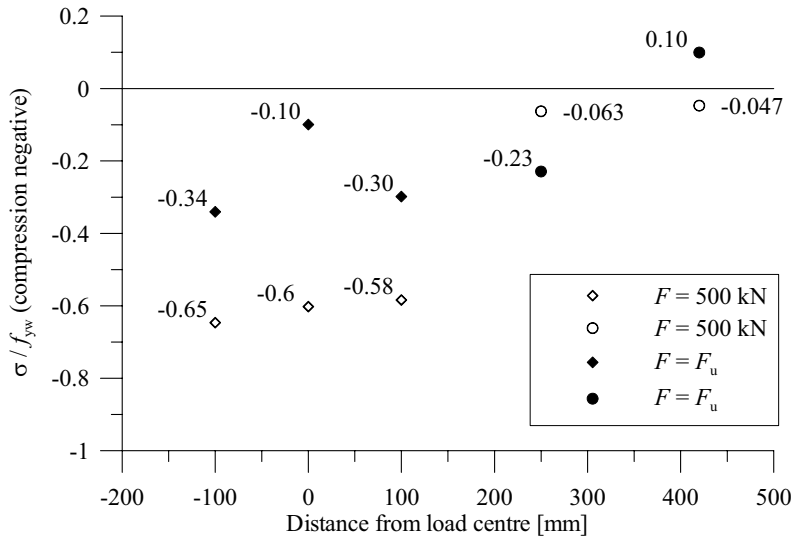


Figure 3.14 P200. Vertical membrane stresses along the loaded flange at 500 kN (unfilled) and at ultimate load (filled). Diamonds represents the strain gauges located 30 mm below the loaded flange and bullets represents strain gauges 50 mm from the loaded flange.

In Figure 3.15, the failure mode for the P200 test is shown and it is possible to see that the strain gauges at the upper part of the web are attached more or less directly on the buckles.

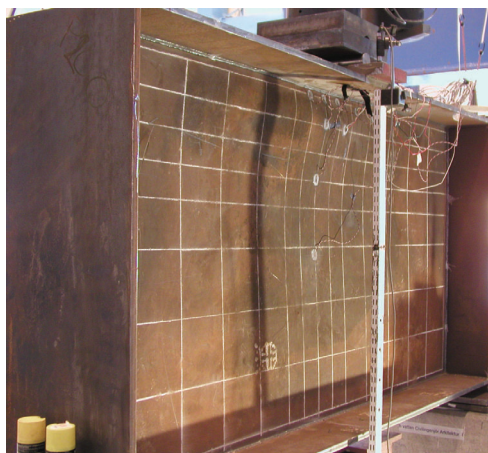


Figure 3.15 Failure mode of the P200 test.

3.4.2 P700

Figure 3.16 show the applied force vs. the vertical web deformation, i.e. the mean vertical displacement of the two loading plates subtracted with the vertical displacement of the lower flange, for the test P700. The initial less stiff part of the curve could be explained by either initial settlements of the test set-up or small rotations of the loading plates, as mentioned in Section 3.3.2, or a combination of both. The ultimate load for the P700 test was $F_u = 660$ kN.

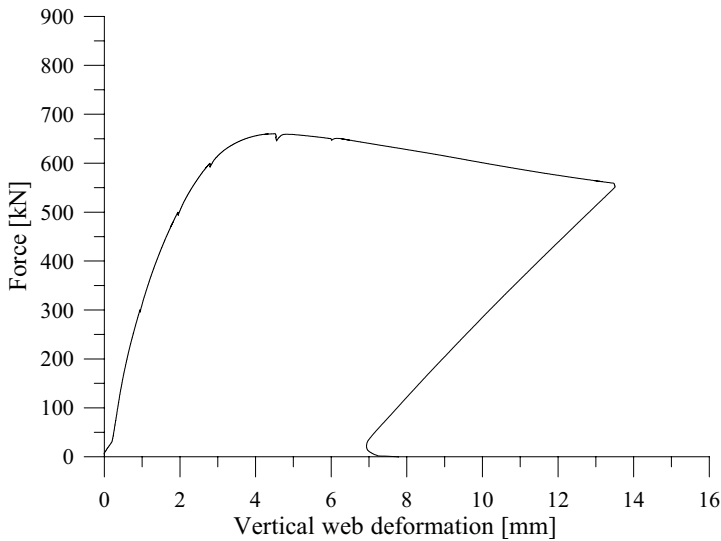


Figure 3.16 P700. Force vs. vertical web deformation.

In Figure 3.17, the initial imperfections along the centre line of the web are shown. As can be seen the maximum imperfection is approximately 1,07 times the web thickness, i.e. 6,4 mm, and the web imperfection has a bow-shape. This is a significantly larger initial imperfection compared to the P200 girder. However, the imperfection of the P700 is approximately $h_w/200$ which is considered to be an allowed panel imperfection.

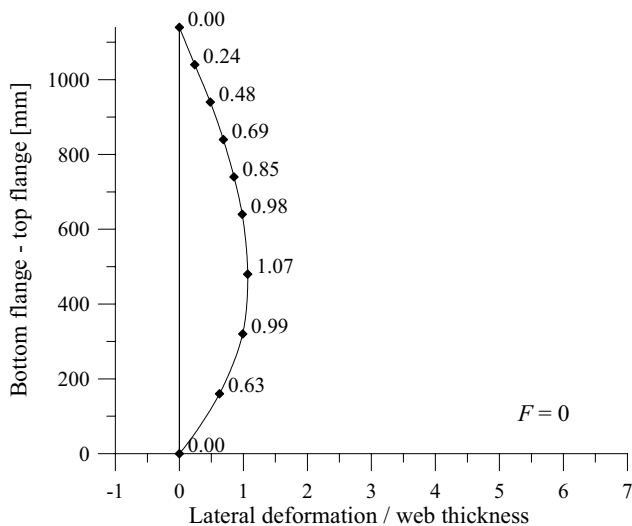


Figure 3.17 P700. Initial lateral imperfection along the centre line of the web.

Figure 3.18 - Figure 3.21 shows the lateral deformations of the web and the membrane stresses from 45% of the ultimate load up to the ultimate load. For the P700 test it was observed that the shape of the web buckle never turned into an S-shape and that the membrane stresses were clearly lower compared to the P200 test. If Figure 3.18 and Figure 3.19 are considered it can be seen that the membrane stresses at the uppermost position are not increasing as fast as at the second uppermost position. This is believed to be due to that the strain gauge closest to the flange is in between the two loading plates in the longitudinal direction and considering Figure 3.22 it can be seen that the membrane stresses under the middle of the loading plates are higher, i.e. the membrane stresses are a little lower at mid-span. Apart from that the pattern are similar to that for the P200 test at lower load levels.

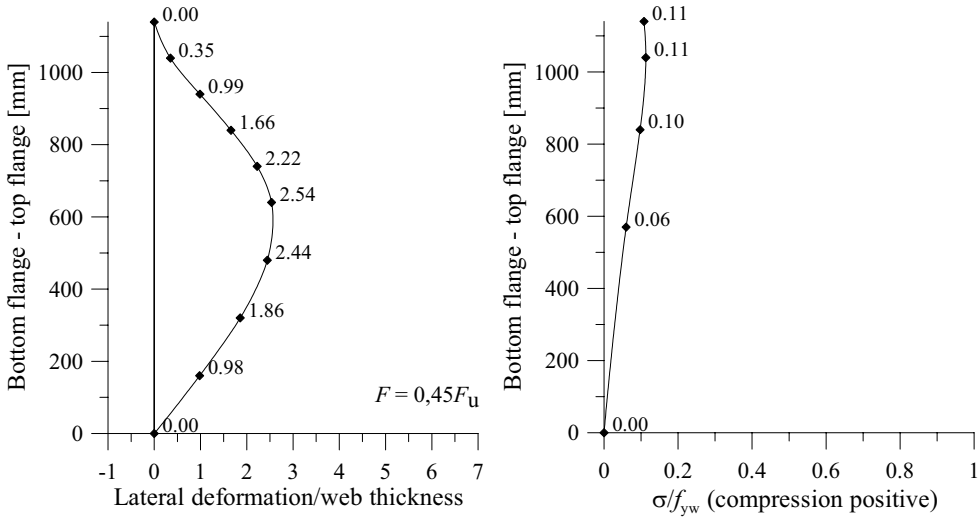


Figure 3.18 P700. Out of plane deformations and vertical membrane stresses along a vertical line at mid-span, $F = 300$ kN.

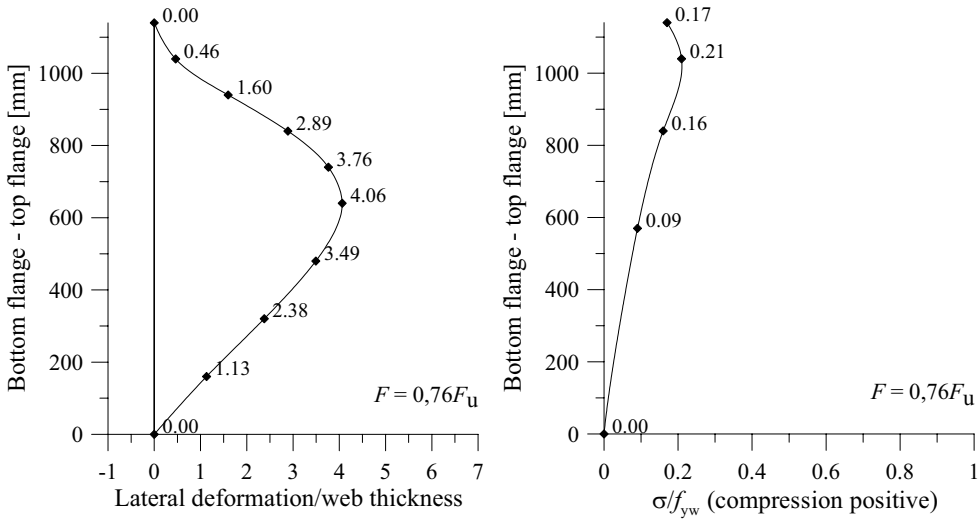


Figure 3.19 P700. Out of plane deformations and vertical membrane stresses along a vertical line at mid-span, $F = 500$ kN.

When the load have reached $0,91F_u$, Figure 3.20, the second position from the loaded flange show clear signs of bending of the web and the membrane stresses were decreasing at this point. Also the third position from the loaded flange show of increasing bending effects, with surface stresses on the yield plateau on the compression side and not far from yielding on the tension

side of the web. Only the uppermost position have compression stresses on both sides of the web.

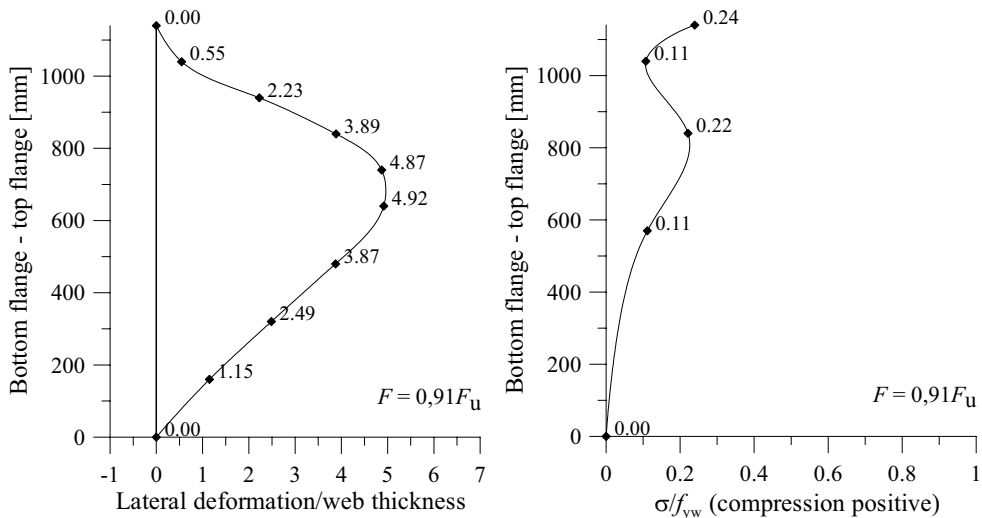


Figure 3.20 P700. Out of plane deformations and vertical membrane stresses along a vertical line at mid-span, $F = 600$ kN.

At ultimate load, the second and third positions show of clear bending effects and the membrane stresses are almost zero. Both positions have stresses close to or above the yield strength on both the compression and tension sides of the web. The stresses at the position closest to the flange are still compressive on both sides of the web.

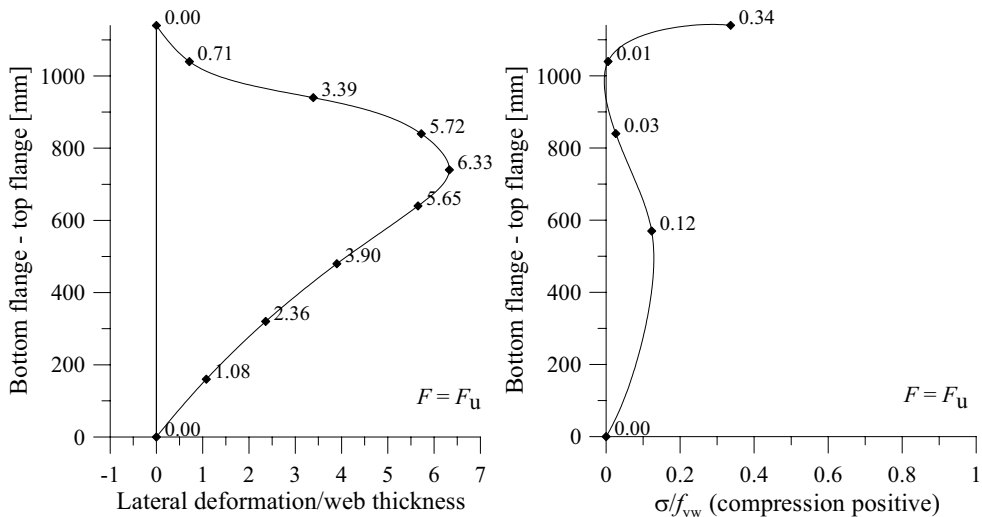


Figure 3.21 P700. Out of plane deformations and vertical membrane stresses along a vertical line at mid-span, $F = 660$ kN.

Figure 3.22 shows the vertical membrane stresses determined from the strain gauges placed on the web along the loaded flange. The diamonds corresponds to the strain gauge positions 101, 111 and 121, 30 mm below the loaded flange, see Figure B.2 in Appendix B, and the dots corresponds to the 201 strain gauge situated 50 mm below the flange. If the membrane stress pattern in the web is translated to a web resistance it correspond well to the applied load. Hence, it can be assumed that Figure 3.22 gives a reasonable picture of the membrane stress distribution in the web at ultimate load.

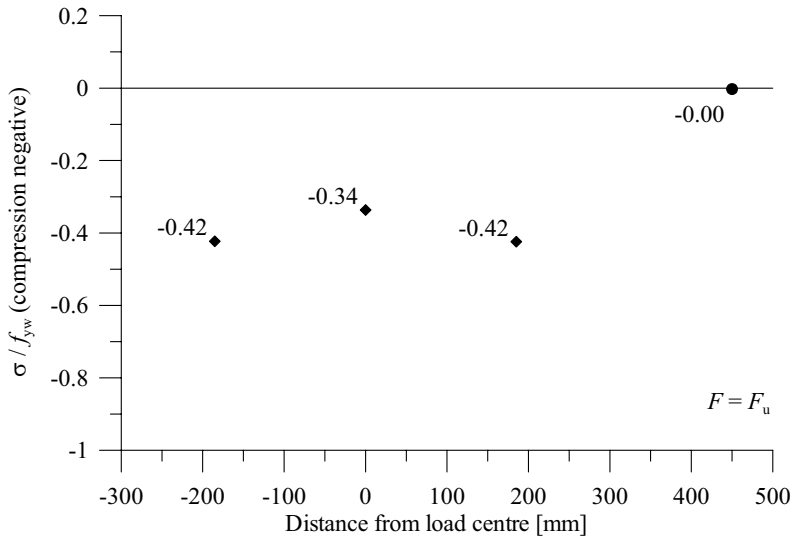


Figure 3.22 P700. Vertical membrane stresses at ultimate load from strain gauges placed along the loaded flange. Diamonds represents the strain gauges located 30 mm below the loaded flange and the bullet represents a position 50 mm from the flange.

The failure mode of the P700 girder is shown in Figure 3.23, where it can be seen that the typical reversed folding under the loaded flange did not appear in this case.



Figure 3.23 Failure mode of the P700 girder.

3.4.3 P1440

Figure 3.24 shows the applied force vs. the vertical web deformation, i.e. the mean vertical displacement of the two inner loading plates subtracted with the vertical displacement of the lower flange, for the test P1440. The initial strange part of the curve can be explained by small rotations of the loading plates causing an initial lift of the loading plates on the side where the measurements took place as mentioned in Section 3.3.2. The ultimate load for the P1440 test was $F_u = 808$ kN.

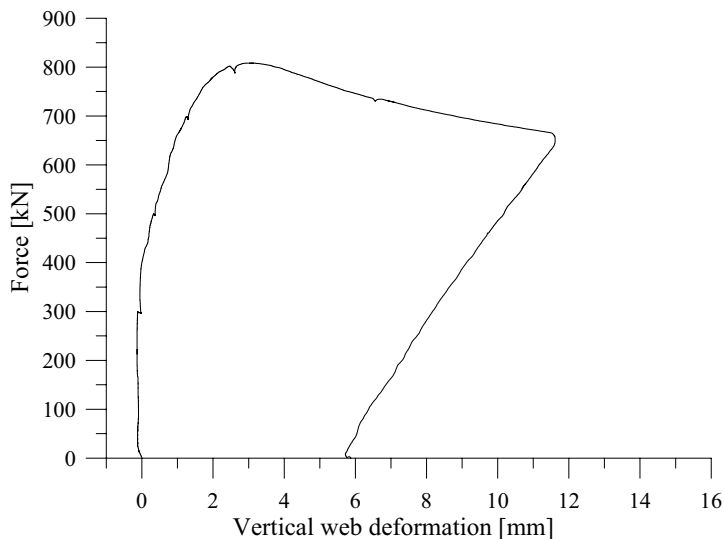


Figure 3.24 P1440. Force vs. vertical web deformation.

In Figure 3.25, the initial imperfections of the web centrally below the applied load are shown. As can be seen the maximum imperfection is approximately 0,62 times the web thickness, i.e. 3,7 mm, and the web imperfection has a bow-shape. For this test specimen the largest amplitude of the buckle is somewhat moved downwards the web.

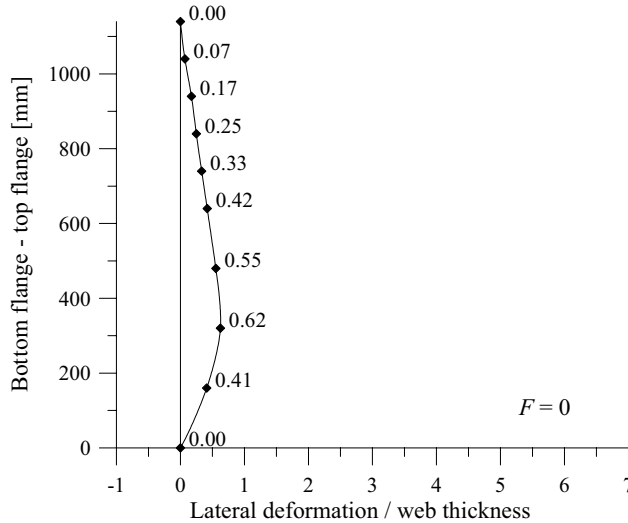


Figure 3.25 P1440. Initial lateral imperfections of the web centrally below the applied load.

Figure 3.26 - Figure 3.29 shows the lateral deformations of the web and the membrane stresses determined from the strains from 37% of the ultimate load up to the ultimate load. For the P1440 test it was also observed that the shape of the web buckle never turned into an S-shape and that the membrane stresses were even lower compared to the P700 test. Further, just like the P700 test the uppermost strain gauge were positioned in between two loading plates in the longitudinal direction which could explain why the membrane stress are lower at this position compared to the position below in the early stage of the test.

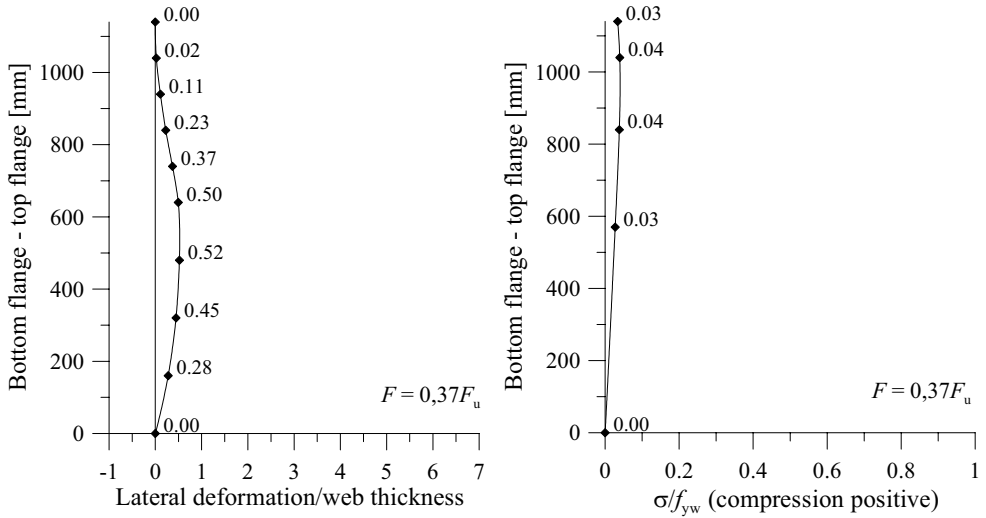


Figure 3.26 P1440. Out of plane deformations and vertical membrane stresses along a vertical line at mid-span, $F = 300$ kN.

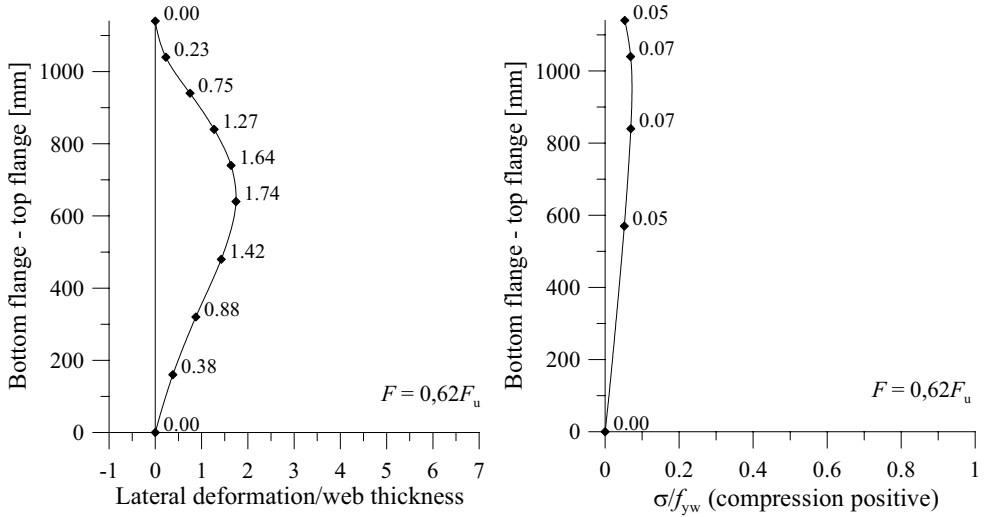


Figure 3.27 P1440. Out of plane deformations and vertical membrane stresses along a vertical line at mid-span, $F = 500$ kN.

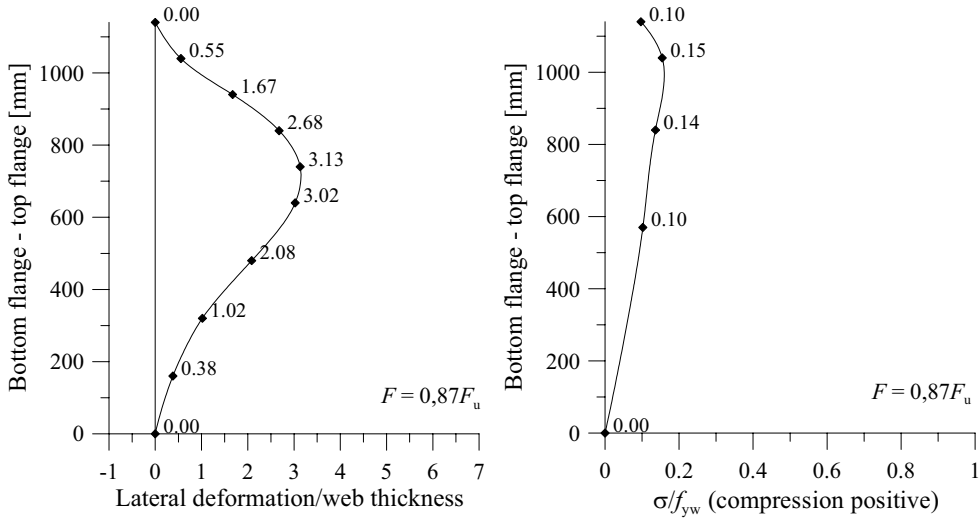


Figure 3.28 P1440. Out of plane deformations and vertical membrane stresses along a vertical line at mid-span, $F = 700$ kN.

In Figure 3.29 the lateral deformation and the membrane stresses at mid-span are shown. It is noted that the membrane stresses at the second and third position are affected by bending and the stresses on the compression side of the web have passed the yield point. The stresses on the tension side at these positions were close to but below the yield strength.

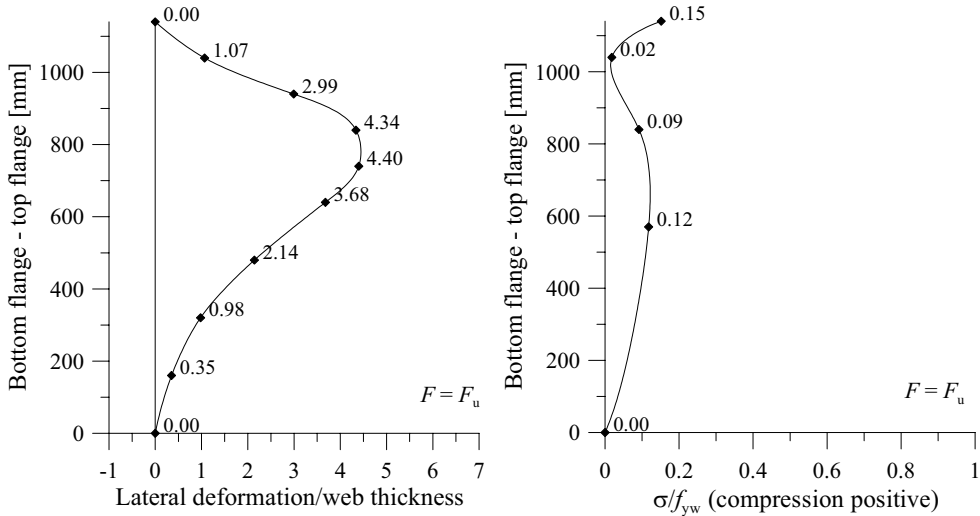


Figure 3.29 P1440. Out of plane deformations and vertical membrane stresses along a vertical line at mid-span, $F = 808$ kN.

Figure 3.30 shows the vertical membrane stresses from the strain gauges placed on the web along the loaded flange. The diamonds corresponds to the strain gauge positions 101, 111, 121, 131, 141, 151 and 161 attached 30 mm below the loaded flange, see Figure B.3 in Appendix B, and the dots corresponds to the 201 strain gauge situated 50 mm below the flange. If the membrane stresses are translated to a web resistance it is approximately 80% of the applied load. However, if the stresses at the surface of the web are investigated for the outer diamonds corresponding to -0,12 and -0,05, respectively it is obvious that the membrane stress at those positions are affected by bending. The stresses on the compression side of the web has clearly passed the yield point and on the tension side they are just below or on the yield plateau. This can explain why the web resistance obtained from the membrane stresses and the applied load does not correspond perfectly.

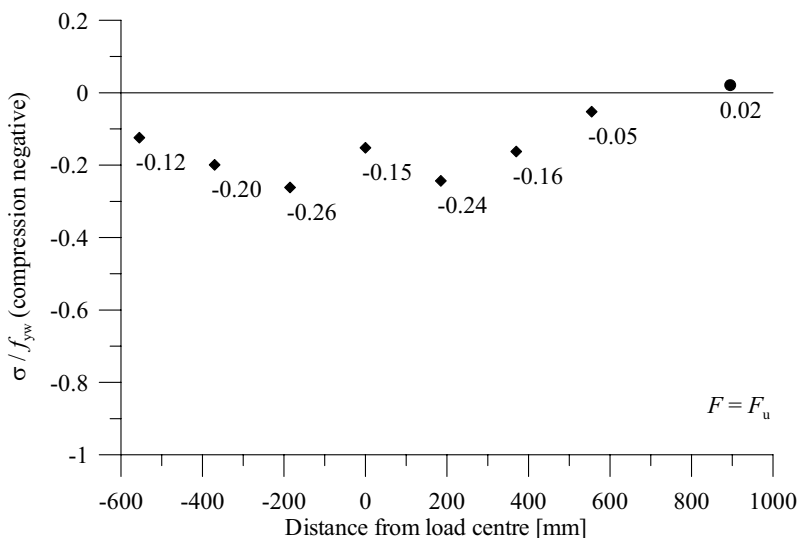


Figure 3.30 P1440. Vertical membrane stresses along the loaded flange at ultimate load. Diamonds represents the stresses from strain gauges located 30 mm below the loaded flange and the bullet represent a membrane stress at a position 50 mm from the flange.

Finally, the failure mode for the P1440 test is shown in Figure 3.31. It should be noted that the buckle in the web was more spread in the longitudinal direction compared to the other tests.

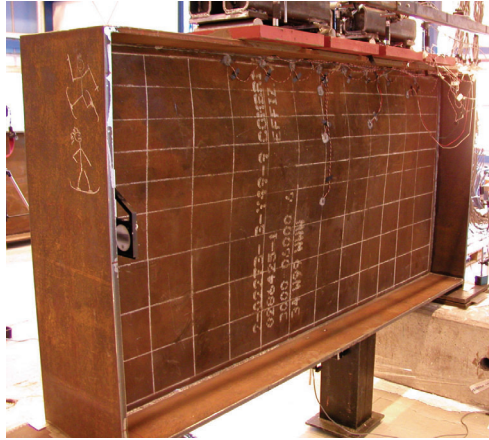


Figure 3.31 Failure mode of the P1440 girder.

3.5 Concluding remarks from the experimental work

For comparison, the characteristic resistance according to EN 1993-1-5 (2006), was calculated with measured geometry and material properties and with $\gamma_{M1} = 1$, and compared with the results from the three tests. The equations for the resistance can be found in the literature review in Section 2.3.2. The yield strength of the web was taken as the mean between the transverse and the rolling direction. Depending on how to define s_s two different values on the resistance is shown together with the ultimate load from the tests in Table 3.3 and Table 3.4. As can be seen in Table 3.3, where the distance between the outer edges was used as s_s , the calculated resistance is clearly lower compared to the ultimate load from tests.

Table 3.3 Comparison between test results and characteristic resistance according to EN 1993-1-5 (2006).

Test	Loaded length s_s [mm]	Ultimate load F_u [kN]	Resistance F_R [kN]	F_u/F_R
P200	200	544	301	1,81
P700	700	660	393	1,68
P1440	1440	808	498	1,62

As s_s was decreased according to the recommendations in EN 1993-1-5 the resistance decrease, see Table 3.4, and the safety margin was of course even higher in this case.

Table 3.4 Comparison between test results and characteristic resistance according to EN 1993-1-5 (2006).

Test	Loaded length s_s [mm]	Ultimate load F_u [kN]	Resistance F_R [kN]	F_u/F_R
P200	80	544	275	1,98
P700	450	660	350	1,89
P1440	1190	808	465	1,74

For the P200 case where one plate of width 200 mm was used it seems a bit conservative to recalculate s_s to 80 mm, i.e. two times the thickness of the plate, as the elastic moment resistance of the plate is

$$M_R = W_{el} \cdot f_y = \frac{b \cdot t^3}{12} \cdot \frac{2}{t} \cdot f_y = \frac{0,6 \cdot 0,04^3}{12} \cdot \frac{2}{0,04} \cdot 235 \cdot 10^3 = 37,6 \text{ kNm} \quad (3.1)$$

and the applied moment was

$$M_E = \frac{F_u \cdot l}{4} = \frac{544 \cdot 0,2}{4} = 27,2 \text{ kNm} \quad (3.2)$$

under the assumption that the loading plate only rests on the edges, i.e. acting as simply supported along the edges. If instead, the loading plate is assumed to have an evenly distributed load from the flange the applied moment should be calculated as

$$M_E = \frac{F_u \cdot l}{8} = \frac{544 \cdot 0,2}{8} = 13,6 \text{ kNm} \quad (3.3)$$

Hence, it could be assumed that the plate in this case can transfer the load through its length of 200 mm.

The main focus with this experimental investigation was the influence from the loaded length on the ultimate resistance. Not surprisingly, the ultimate load increased with increasing loaded length.

The failure mode of the P200 test included two buckles in the web, one small reversed buckle directly under the loaded flange and one larger buckle over the rest of the web, i.e. the web changed shape from an initial bow-shape to an S-shape. Regarding the P700 and the P1440 tests, only one large buckle formed in the web, i.e. the lateral deformations of the web at failure was bow-shaped. Further, when the loaded length increased, the buckle also increased in the longitudinal direction of the girder.

The highest membrane stresses were found in the P200 girder and were decreasing with increasing loaded length. It is shown that the membrane stresses in general were affected by

bending of the web and at failure all tests had surface stresses above the yield strength a several positions.

According to the rules in EN 1993-1-5, an s_s equal to h_w is allowed and that is confirmed by the test results herein. However, it might be possible to allow an even higher ratio of s_s/h_w . This matter will be further discussed later in this thesis.

4 NUMERICAL STUDY

4.1 General

In addition to the in tests presented in Section 3 also a numerical study was performed. It covers calibration against the tests followed by a parametric study. All pre- and post-processing were performed with the finite element package ABAQUS CAE versions 6.5 and 6.6. For the calculations ABAQUS/Standard, versions 6.5 and 6.6, was used. Element types and procedures refer to ABAQUS and more extensive descriptions can be found in the ABAQUS manuals (2006). All finite element (FE) analyses were performed with an implicit solver, i.e. ABAQUS/Standard. The parametric study was, like the experimental work, focused on the loaded length and its influence on the ultimate load.

4.2 Finite element model

Initially, a sensitivity analysis regarding element size resulted in the use of a mesh containing approximately 9500 elements with an element side length of ~ 25 mm, was performed. Elements of type S4R was used as it has shown to work well earlier in several similar cases, see e.g. Gozzi et al. (2004) and Olsson (2001). The S4R is a general-purpose shell element that allow for change in thickness with reduced integration. Tryland et al. (1999) performed similar numerical simulations also using a similar element type with four nodes and reduced integration, though in LSDyna. In Figure 4.1 the mesh used for calibration of the P700 test is depicted. More or less the same mesh was used for all FE-analyses in this section.

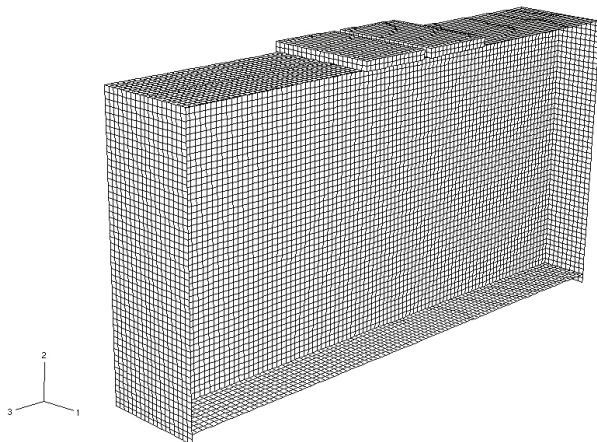


Figure 4.1 Finite element model for the P700 test.

At the lower edge of the stiffeners, boundary conditions in the vertical direction, the 2-direction in Figure 4.1, were applied as well as in the longitudinal direction, the 3-direction, on one side of the girder. Moreover, also the midpoints of the lower edges of the stiffeners were constrained in the 1-direction. The loading plates were constrained from moving in the 1-direction as well.

To model the load transfer into the girder in the most realistic way the loading plates were included in the model, see Figure 4.1. The loading plates were modelled as separate parts with solid elements, C3D8R, and the load was applied as prescribed vertical displacement of the mid-line of the loading plates as shown in Figure 4.2. However, the P1440 test could not be modelled using equal displacement of the mid-line of the loading plates, instead equal line loads were applied along the mid-line of each loading plate.

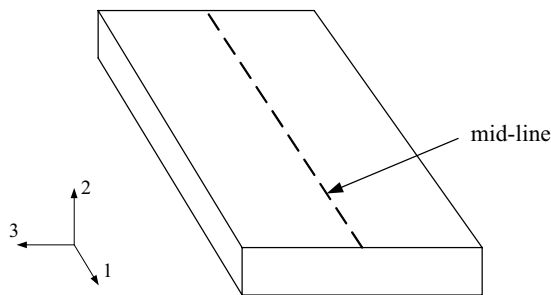


Figure 4.2 Explanation of the mid-line for the loading plates. Coordinate system as in Figure 4.1.

To model the contact between the loading plate and the upper surface of the loaded flange in ABAQUS a tie constraint was defined between the flange surface and the lower surface of the loading plate. The definition of the tie constraint was in this case that the surface of the flange directly under the loading plate should move equally as the loading plate during the analysis. This is not the best way to do this, instead one could define contact surfaces between the flange and the plates, which would allow partly separation of the two surfaces. Though, the approach using tie constraints is more economic and much easier to obtain convergence with. For stiff loading plates and less stiff flanges partly separation is likely to happen around the ultimate load, i.e. that only the edges of the loading plate rests on the flange. This behaviour could be seen in the P200 test after ultimate load and the P200 test was also modelled with contact surfaces in order to see the difference between the approaches. The difference was found to be negligible. However, this behaviour was not observed in the other two tests, which could partly depend on the fact that the loading plates was allowed to rotate and follow the flange deformation during the test.

If the strains recorded in the tests are considered no strain reversals occur during the tests. Hence, the loading is assumed to be monotonic and the material could be modelled as a von Mises material with an isotropic hardening rule. The material properties, in terms of stress-

strain relation, used in the FE-model were taken from tensile coupon tests of the plate material used for manufacturing the girders, see Section 3.2. The web plate material showed of a small anisotropy and due to that a mean curve from the behaviour along and transverse the rolling direction was used for the web plate material properties. Elastic properties used was a Young's modulus for the web plate of 185 GPa and for the flange material 200 GPa, found from the stress-strain curves, and a Poisson's ratio of 0,3. A Young's modulus of 185 GPa is a rather low value but it was decided to be used since this was the value obtained from the stress-strain curves.

Initial imperfections were introduced as the first eigenmode obtained from a buckling analysis. The magnitude of the initial imperfections were taken as the measured values before testing, according to Section 3.4. Longitudinal residual stresses were introduced in the model according to simplified pattern shown to the right in Figure 4.3.

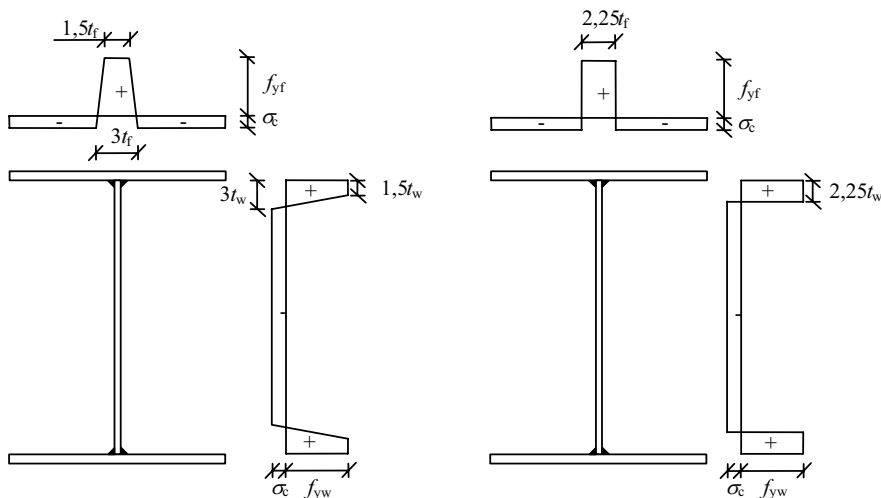


Figure 4.3 Schematic residual stress pattern according to BSK 99 (1999) (left) and the simplified pattern used in the FE-model herein (right). The compression stress, σ_c , was chosen to fulfil the stress equilibrium over the cross section.

The buckling analysis used to obtain the eigenmode for the initial imperfection was followed by a non-linear analysis.

4.3 Calibration

The reason for the calibration study of the tests was to verify that the model, element type and size, material properties and so on, were suitable for this kind of analysis and that the model was reliable for further studies. In this case the results from the FE-analyses were in close agreement with the test results by means of ultimate load and load-displacement relation, see Table 4.1 and

Figure 4.4. Further, the lateral deformations of the web, i.e. the web buckle, from the tests also corresponds well to the FE results as can be seen in Figure 4.5.

Table 4.1 Comparison between the test and the FE results.

Test	Tests ultimate load F_u [kN]	FE ultimate load $F_{u,FE}$ [kN]	$F_u/F_{u,FE}$
P200	544	540	1,01
P700	660	678	0,97
P1440	808	833	0,97

The global behaviour in terms of the load-displacement relation is shown for the P200 and the P700 girder in Figure 4.4. The displacement is defined as the vertical web deformation, i.e. the displacement of the loading plate/plates subtracted with the displacement of the lower flange, at mid-span. The agreement is as can be seen very good both regarding ultimate load and stiffness.

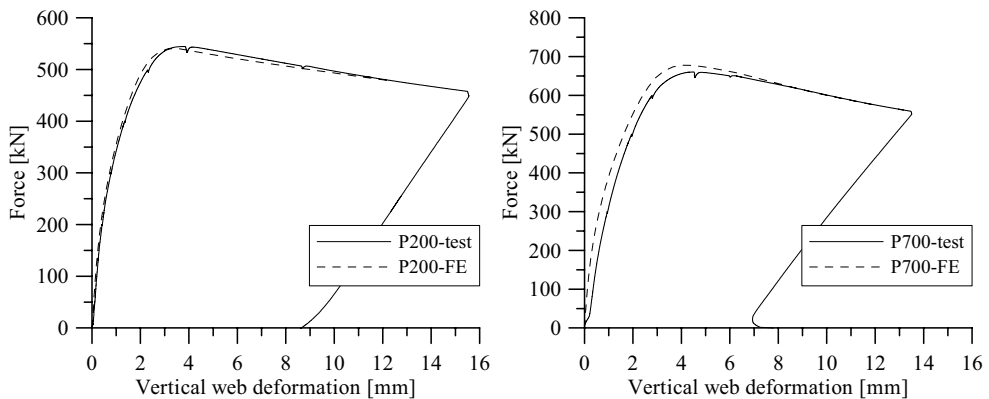


Figure 4.4 Comparison of the load-web deformation relation between tests and FE-analyses for the P200 and the P700 girders.

In Figure 4.5 the lateral deformation of the P700 test is shown together with the results from the corresponding FE-analysis. The lateral deformations were taken along a vertical line at mid-span and are shown at five different loads. As can be seen the initial imperfection is not perfectly captured with the first eigenmode and that sort of influences the rest of the curves. However, the overall agreement is reasonable and considered as good enough.

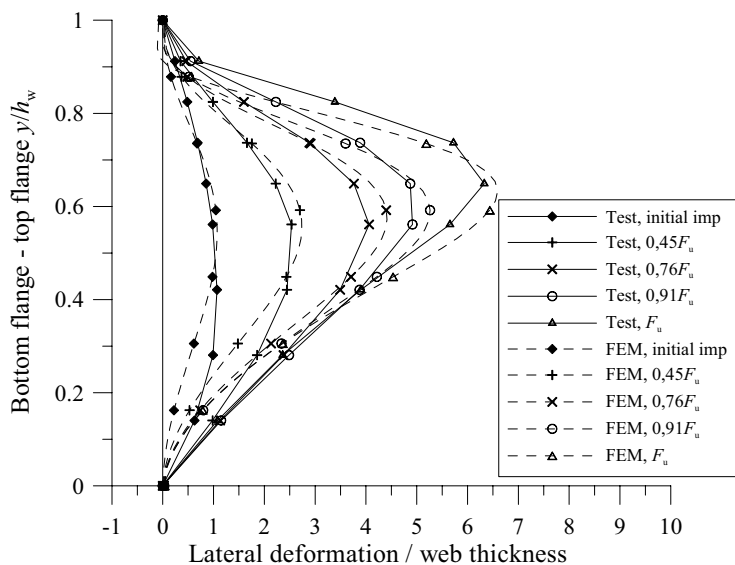


Figure 4.5 Comparison of lateral deformations of the web plate, along the mid-line of the web, between the P700 test and FE-analysis.

Finally, the failure modes for the P1440 test and FE-analysis are shown in Figure 4.6.

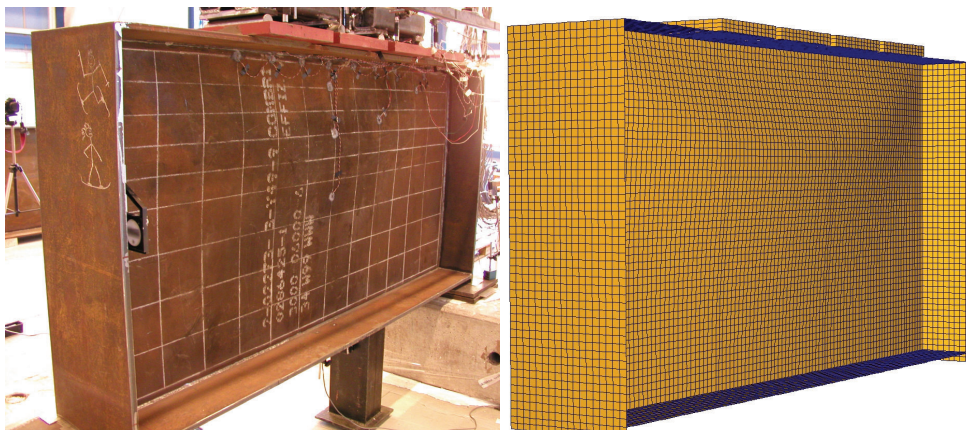


Figure 4.6 Failure mode for the P1440 test and FE-analysis after ultimate load.

Based on the results from the comparison between the FE results and the test results it was concluded that the model can provide reliable results and hence, it is suitable for further studies.

4.4 Parametric study

In order to get more input to the study regarding the influence of the loaded length on the ultimate patch loading resistance a parametric study was carried out by means of FE-analyses. The modelling was performed according to the same principles used in the simulations of the tests, since those models had good agreement with the tests and it was assumed to be able to produce reliable results for other cases as well. Exceptions from the principles used to simulate the tests are:

- No load plates were used, instead the load was applied as a prescribed displacement of the flange corresponding to a loading plate with width s_s .
- Initial imperfections were taken into account as the first eigenmode with a maximum amplitude of $h_w/200$.

Table 4.2 shows s_s , s_s/h_w and ultimate load from the eight different analyses. The values on s_s were partly chosen to fit the definition of s_s in EN 1993-1-5 (2006), i.e. for the P200, P700 and P1440 tests the corresponding s_s according to EN 1993-1-5 are 80, 450 and 1190 respectively.

As mentioned before, the value that should be used for s_s is not obvious. According to the underlying mechanical model used for the derivation of the equations in EN 1993-1-5, which originally comes from Lagerqvist (1994), s_s is the distance between the assumed plastic hinges in the flange, see Figure 2.13. For the P700 and P1440 tests where the load is more distributed through several loading plates, the assumed plastic hinges in the loaded flange is not likely to appear at the outer edges of the outer loading plates.

Table 4.2 *Loaded lengths and ultimate load from the parametric study together with results from the three tests using s_s according to the recommendation in EN 1993-1-5.*

Label	Loaded length s_s [mm]	s_s/h_w	s_s/a	$F_{u,FE}$ [kN]
P0-bc	0	0	0	448
P80-bc	80	0,067	0,033	476
P200-bc	200	0,17	0,083	537
P450-bc	450	0,38	0,19	640
P700-bc	700	0,58	0,29	701
P900-bc	900	0,75	0,38	750
P1190-bc	1190	0,99	0,50	818
P1440-bc	1440	1,2	0,60	885

If the ultimate loads shown in Table 4.2 are compared with the results from the tests, Table 4.1, it can be seen that for the P200 test an s_s of 200 from the parametric study corresponds well to the test ultimate load. However, for the two other tests an s_s of 450 and 1190 show the best agreement with the test results. In Figure 4.7 the ultimate loads from the tests and the parametric study are shown as a function of s_s/h_w . The points form an almost horizontal line with very small variations, which indicates that the model used in EN 1993-1-5 can catch the variation in loaded length. Though, Figure 4.7 indicates that the model in EN 1993-1-5 is rather conservative with an average for $F_{u,FE}/F_R$ of 1,78.

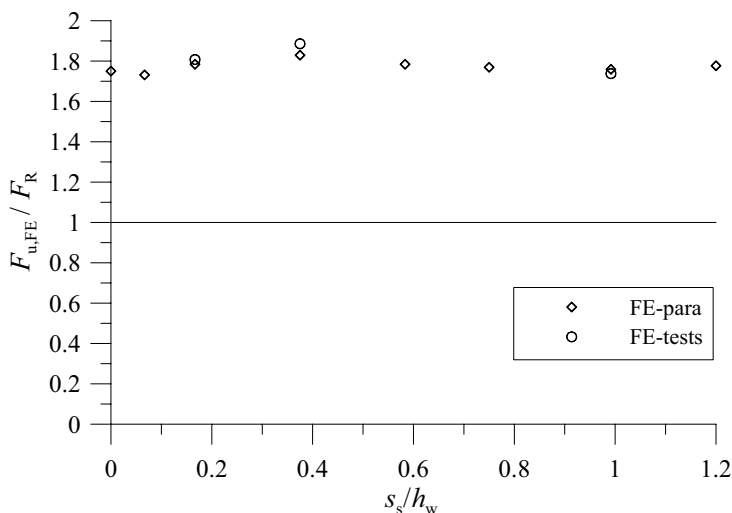


Figure 4.7 Ultimate load from tests and parametric study over resistance according to EN 1993-1-5 as a function of loaded length over web depth.

4.5 Concluding remarks from the numerical study

The numerical analyses of the experimental tests showed of good agreement both with respect to ultimate load and load-deformation curves. Also the lateral deformation of the web was modelled with reasonable good agreement.

From the parametric study with focus on the loaded length it was concluded that s_s should follow the recommendations in EN 1993-1-5 (2006), i.e. for several loading plates the centre-to-centre distance between the outer most plates plus the load spread through the plates should be used. Further, it was observed that the rules in EN 1993-1-5 could well describe the variation in loaded length even though it uses the simplified buckling coefficient, k_F , according to Equation (2.102). However, the resistance is rather conservative and could definitely be improved.

The need of the requirement in EN 1993-1-5 that s_s should not be taken as larger than h_w can be discussed. The results presented in the parametric study do not show of any signs that the

resistance model for patch loading would not be applicable for longer s_s . However, it could strongly be questioned if the design resistance for patch loading is the correct choice for $s_s > h_w$. It would be wrong to call a load with $s_s > h_w$ for concentrated and further, neither the mechanism model used to derive the yield resistance nor the elastic buckling load was developed with such long loaded lengths.

5 PATCH LOADING RESISTANCE

5.1 General

Patch loading resistance of girders without stiffeners in the ultimate limit state is a well-studied subject as can be seen in the literature review in Section 2. There exists almost as many design models as researchers but from the author of this thesis point of view it is the model by Lagerqvist (1994), also in a slightly modified version implemented in EN 1993-1-5 (2006), that is of most interest. Hence, the model by Lagerqvist will serve as basis for the design model proposed herein. The advantages with the model by Lagerqvist are;

- that it is harmonized with the models for other buckling problems,
- that the model relies on a mechanical model,
- that all three different cases, i.e. patch loading, end patch loading and opposite patch loading, can be treated with the model and
- that the model show of good agreement with test results.

However, there is a disadvantage too, namely the by some questioned parameter m_2 in the yield resistance that comes from the fictitious T-section at the outer plastic hinges, see Figure 2.13. Following the questions regarding the T-section a study of the yield resistance by means of numerical analyses was performed herein. The study on the yield resistance can be found in Section 5.2.

The yield resistance was modified due to the study mentioned above, which resulted in a new calibration of the reduction factor, see Section 5.3, against the test data base. Finally, the proposed design procedure was calibrated against test results according to the procedure in Annex D of EN 1990 (2002) and compared to other design models.

In this thesis, only patch loading will be considered, i.e. not end patch loading or opposite patch loading.

5.2 Yield resistance

The yield resistance is usually defined as an upper limit resistance that a member can carry if no instability is present. If the slenderness of the member is high it is susceptible to buckling and the yield resistance is reduced by a reduction factor to an actual resistance. Roberts and Rockey (1979) presented the first resistance function for direct yielding as shown in Figure 2.8. Furthermore, Roberts approach was to use the lower of the resistance to buckling and the

resistance to direct yielding. Lagerqvist on the other hand, used a slightly modified version of the model by Roberts and Rockey but combined it with a reduction factor to handle possible buckling. The common feature of those two models is the use of a four-hinge mechanism model. Bergfelt (1979) and Ungermann (1990), Figure 2.10 and Figure 2.12, proposed models that were based on a three-hinge model, though Bergfelt mentioned that for longer loaded lengths the concentrated force at the middle hinge should be replaced by two point loads, representing the edges of the loading plate, on top of two plastic hinges instead.

In his tests, Lagerqvist observed indentations in the flange at the outer edges of the loading plate close to ultimate load. Further, during the tests Lagerqvist measured the displacement of the loaded flange at three positions; one under the middle of the load plate and one at each edge of the load plate. The difference between those displacements was very small and therefore one can assume that one hinge form at each side of the load plate. With this in mind, it was decided to use the four-hinge mechanism for the yield resistance.

The yield resistance for patch loading is not well defined because the contributing length from the web increases with deformation. In addition, strain hardening sets in at small deformations which complicates the definition further. The definition of the yield resistance will unavoidably include a subjective choice of a deformation limit. If strain hardening is neglected, the yield resistance given by the web can be approximated as a function of the web yield strength and the contributing web area according to

$$F_y = l_y \cdot t_w \cdot f_{yw} \quad (5.1)$$

where l_y is the length of the web that responds to the applied load. l_y also corresponds to the distance between the two outer plastic hinges in the flange according to Figure 5.1.

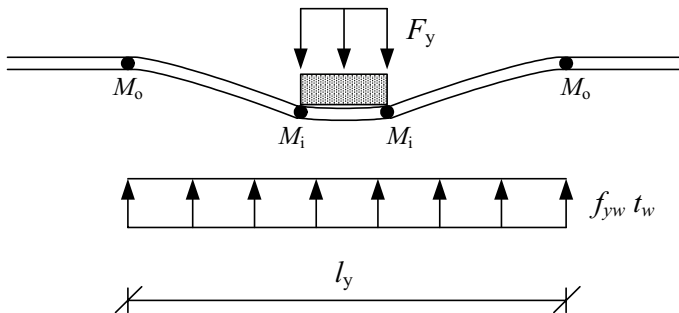


Figure 5.1 Four-hinge mechanism model for the yield resistance for patch loading.

In the model by Roberts and Rockey (1979), only the flanges are assumed to contribute to the moment resistance in the plastic hinges and the yield resistance can be written as

$$F_y = f_{yw} \cdot t_w \cdot \left(s_s + 2 \cdot t_f \cdot \sqrt{\frac{f_{yf} \cdot b_f}{f_{yw} \cdot t_w}} \right) \quad (5.2)$$

where the term within brackets is the length of the web, l_y , responding to the applied load. This was in Roberts and Newark (1997) adjusted, to take into account the load spread through the flange, according to

$$F_y = f_{yw} \cdot t_w \cdot \left(s_s + 2 \cdot t_f \cdot \left(1 + \sqrt{\frac{f_{yf} \cdot b_f}{f_{yw} \cdot t_w}} \right) \right) \quad (5.3)$$

In the proposal by Lagerqvist (1994) a part of the web was included in the moment resistance of the outer plastic hinges to increase the yield resistance with increasing web depth. This was included in the model because Lagerqvist observed that for increasing web slenderness the length of the deformed part of the flange increased. The proposal by Lagerqvist was to include $0,14h_w$ in the T-section and this gives a yield resistance according to

$$F_y = f_{yw} \cdot t_w \cdot \left(s_s + 2 \cdot t_f \cdot \left(1 + \sqrt{\frac{f_{yf} \cdot b_f}{f_{yw} \cdot t_w} + 0,02 \cdot \left(\frac{h_w}{t_f} \right)^2} \right) \right) \quad (5.4)$$

in which $0,02 \cdot (h_w/t_f)^2$ comes from the web part of the T-section and this is also what is referred to as m_2 in EN 1993-1-5 (2006).

Now, the parameter m_2 has been questioned by e.g. Davaine et al. (2004) and therefore an investigation regarding its relevance was carried out. The investigation was conducted by means of FE-analyses with a model as shown in Figure 5.2. A total of 18 non-linear FE-analyses with material properties according to the stress-strain curves used in Section 4, i.e. S355 steel, were performed complemented by one analysis with material properties corresponding to a Weldox 700 (S690 QT) with nominal $f_y = 700$ MPa. In order to avoid buckling of the web and make it possible to define the plastic resistance the web was constrained against lateral deformations.

The boundary conditions applied were; vertical restraints along the vertical ends of the web, a horizontal restraint in the neutral axis at the ends of the web allowing the web to rotate around this point and vertical restraints at the ends of the loaded flange, symbolizing the support from a vertical stiffener. The load was applied as a prescribed vertical displacement of the area under a fictitious loading plate, i.e. s_s multiplied with b_f .

The following parameters were varied in the investigation;

- flange thickness, t_f

- flange width, b_f ,
- web thickness, t_w ,
- aspect ratio, a/h_w , and
- loaded length, s_s .

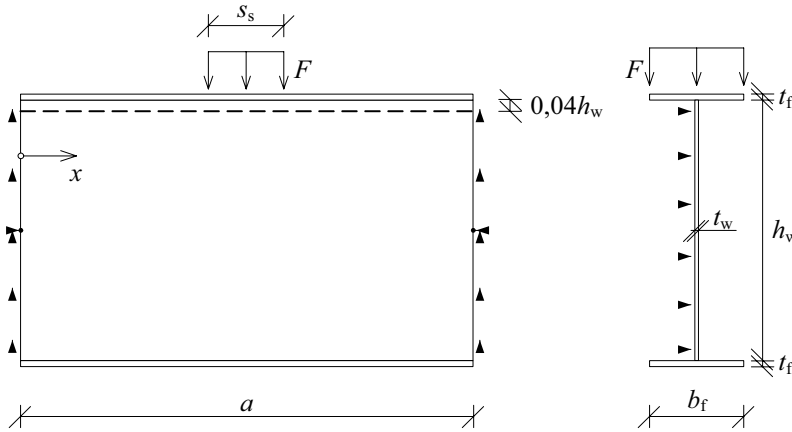


Figure 5.2 FE-model used in the numerical investigation of the yield resistance.

The results are shown as both a load-vertical web deformation curve and the vertical stress distribution in the web below the upper flange, along the dashed line in Figure 5.2. The latter are displayed at a stage when the girder was assumed to have reached the plastic stage, also indicated with a diamond in the load-deformation plot. The displacements used in the load-vertical web deformation curves were the displacement of the loaded flange under the load relative to the displacement of the lower flange at mid-span. For comparison the simplified stress distribution according to Lagerqvist (1994) and Roberts and Rockey (1997), i.e. according to EN 1993-1-5 (2006) with and without m_2 , are shown together with the numerical results. Further, the vertical stresses shown were normalized with f_{yw} .

The effective loaded length from the numerical analyses, $l_{y,FE}$, was determined as the web that was in compression according to

$$l_{y,FE} = \int_{l_1}^{l_2} \frac{\sigma_w}{f_{yw}} dx \quad (5.5)$$

where l_1 and l_2 defines the area under the stress curve that was in compression, i.e. between l_1 and l_2 there are compression stresses in the web. The l_y -values with and without m_2 as well as $l_{y,FE}$ were normalized with $l_{y,FE}$ to simplify comparison, i.e.

$$l_{y,FE, \text{norm}} = \bar{l}_{y,FE} = 1 \quad (5.6)$$

$$l_{y,m_1+m_2, \text{norm}} = \bar{l}_{y,m_1+m_2} = \frac{s_s + t_f \cdot (1 + \sqrt{m_1 + m_2})}{l_{y,FE}} \quad (5.7)$$

$$l_{y,m_1, \text{norm}} = \bar{l}_{y,m_1} = \frac{s_s + t_f \cdot (1 + \sqrt{m_1})}{l_{y,FE}} \quad (5.8)$$

with $m_1 = \frac{f_{yf} \cdot b_f}{f_{yw} \cdot t_w}$ and $m_2 = 0,02 \cdot \left(\frac{h_w}{t_f}\right)^2$

In Table 5.1 all different geometries used in this numerical study are displayed together with the normalized effective loaded lengths according to Equations (5.7) and (5.8).

Table 5.1 Geometry and effective loaded length for the different models used in the study.

Label	h_w [mm]	t_w [mm]	t_f [mm]	b_f [mm]	a [mm]	s_s [mm]	\bar{l}_{y,m_1+m_2}	\bar{l}_{y,m_1}
YR1a	1000	8	8	125	1000	200	1,72	0,95
YR1b	1000	8	8	250	1000	200	1,71	1,02
YR1c	1000	4	8	125	1000	200	1,68	1,00
YR1d	1000	4	8	250	1000	200	1,62	1,06
YR1e	992	4	16	125	1000	200	1,48	1,07
YR1f	992	4	16	250	1000	200	1,35	1,08
YR1g	976	4	32	250	1000	200	1,26	1,09
YR1h	1000	2	8	250	1000	200	1,53	1,09
YR1i	976	4	32	400	1000	200	1,16	1,09
YR1j	992	4	16	250	1000	100	1,47	1,11
YR1k	976	4	32	250	1000	100	1,23	1,11
YR1f-W7	992	4	16	250	1000	200	1,44	1,14
YR2a	1000	8	8	125	2000	200	1,69	0,93
YR2b	1000	8	8	250	2000	200	1,72	1,05
YR2c	1000	4	8	125	2000	200	1,55	0,94
YR2d	1000	4	8	250	2000	200	1,59	1,04
YR2e	992	4	16	125	2000	200	1,43	1,04
YR2f	992	4	16	250	2000	200	1,33	1,06
YR2g	976	4	32	250	2000	200	1,21	1,05

It is obvious that l_y including m_2 , second column from the right in Table 5.1, overestimates the actual length meanwhile l_y without m_2 show of good agreement with the results from the numerical study. Figure 5.3 shows how the vertical stress distribution in the web plate appears in the FE-analysis of *YRIf* when the girder is assumed to have reached the plastic state at the same increment as shown in Figure 5.4.

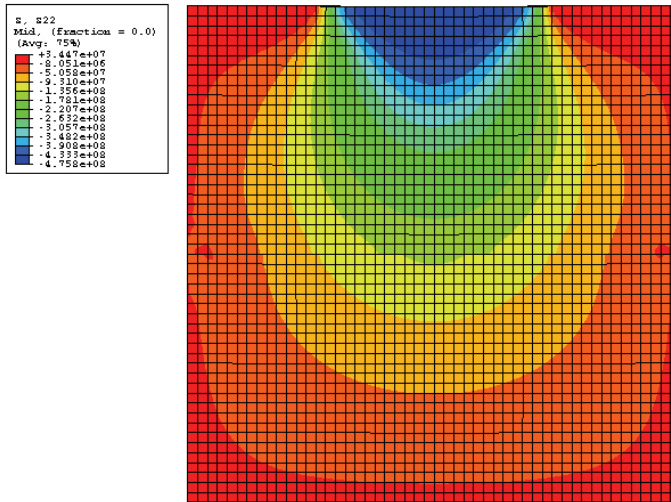


Figure 5.3 Vertical stress distribution in the web plate for girder *YRIf*.

The results considering *YRIf* are shown in Figure 5.4 and as can be seen the effective loaded length, l_y , can be better estimated without m_2 . In the left part of Figure 5.4 the vertical stress distribution from FE represents the solid line and the stress distribution according to Equations (5.3) and (5.4) are represented by the dashed lines.

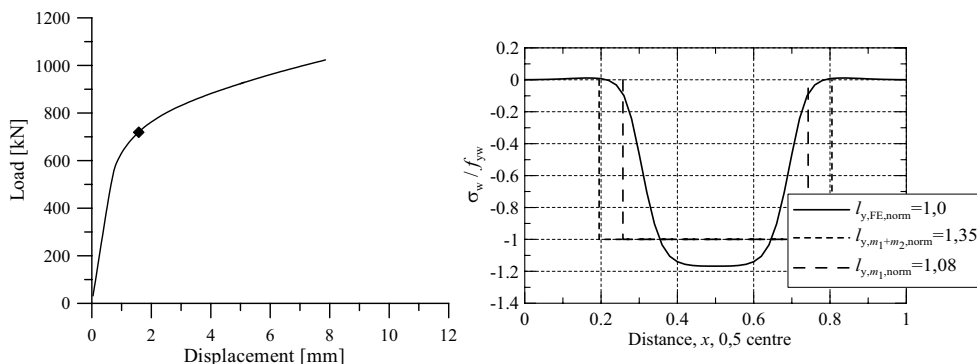


Figure 5.4 Load-web deformation curve (left) and vertical stress distribution in the web plate (right) for the FE-analysis *YRIf*. The right part of the figure was taken when the load-web deformation have reached the diamond in the left figure. The dashed lines in the right figure represents the assumed stress distribution according to Equations (5.3) and (5.4).

The section *YR1d* is shown in Figure 5.5. Also for this case a clearly better prediction of the stress state is obtained by using a l_y without m_2 . Further, as can be seen the load-web deformation curve has a more sudden change in inclination compared to the *YR1f*, which is explained by the thinner flanges used in the model *YR1d*.

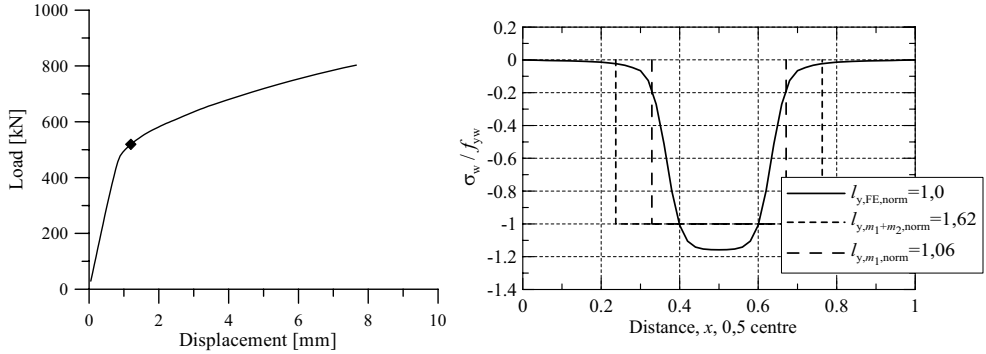


Figure 5.5 Load-web deformation curve (left) and vertical stress distribution in the web plate (right) for the FE-analysis *YR1d*. The right part of the figure was taken when the load-web deformation have reached the diamond in the left figure. The dashed lines in the right figure represents the assumed stress distribution according to Equations (5.3) and (5.4).

As mentioned earlier, the yield resistance depends on the deformation limit. If the deformations are allowed to increase then subsequently the length of the participating web will increase. Nevertheless, very large deformations and stresses are needed to get an l_y corresponding to l_y including m_2 . Depending on the geometry of the section stresses in the vicinity of the ultimate tensile strength are needed. If the results in Table 5.1 are considered, the average values for \bar{l}_{y,m_1+m_2} and \bar{l}_{y,m_1} are 1,48 and 1,05 respectively and the deviation from 1, according to Equation (5.9), are 0,48 and 0,067 respectively.

$$\bar{x}_{\text{error}} = \frac{\sum |\bar{l}_y - 1|}{19} \quad (5.9)$$

The same behaviour as shown in Figure 5.4 and Figure 5.5 was also found for the other 17 cases and hence, it was concluded that m_2 should be removed from the expression for l_y . This means that the yield resistance should be determined according to the model Roberts and Newark (1997) proposed for direct yielding, i.e. according to Equation (5.3) where the load spread through the flange is included. This is also supported by Davaine et al. (2004) who studied longitudinally stiffened bridge girders subjected to patch loading by means of a large number of FE-analyses. Davaine et al. could not find any justification for a participating part of the web at the outer plastic hinges and also proposed that m_2 should be set to zero.

5.3 Proposed design procedure

As a consequence of the change in yield resistance in the previous section, compared to EN 1993-1-5, some other modifications in the design procedure have to be done. The basic equations for the design procedure are given here as basis for the work presented later in this section.

As shown in the previous section, the yield resistance should be determined as

$$F_y = f_{yw} \cdot t_w \cdot \left(s_s + 2 \cdot t_f \cdot \left(1 + \sqrt{\frac{f_{yf} \cdot b_f}{f_{yw} \cdot t_w}} \right) \right) \quad (5.10)$$

from which the resistance is given by

$$F_R = \chi_F \cdot F_y \quad (5.11)$$

where χ_F is the reduction factor relating the slenderness to the resistance. This reduction factor had to be modified to fit the modified yield resistance. To determine the reduction factor, the slenderness, $\bar{\lambda}_F$, is required

$$\bar{\lambda}_F = \sqrt{\frac{F_y}{F_{cr}}} \quad (5.12)$$

which involves the critical load,

$$F_{cr} = k_F \cdot \frac{\pi^2 \cdot E}{12 \cdot (1 - \nu^2)} \cdot \frac{t_w^3}{h_w} \quad (5.13)$$

The critical load can be determined in several ways, e.g. by means of hand calculations, numerical methods or purpose developed softwares. From the designers point of view, numerical methods are not suitable and therefore that will not be considered here but they are of course possible to use. In here focus will be on methods suited for hand calculations, such as proposed by Lagerqvist (1994). As a complement, the newly developed software *EBPlate*, by Galéa and Martin (2006) will be included in the investigation as well.

Lagerqvist (1994) used a buckling coefficient, k_F , in Equation (5.13) according to

$$k_F = 5,3 + 1,9 \cdot \left(\frac{h_w}{a} \right)^2 + 0,4 \cdot \sqrt[4]{\frac{b_f \cdot t_f^3}{h_w \cdot t_w^3}} \quad (5.14)$$

when evaluating his resistance model. However, Lagerqvist suggested a simplified k_F for design which is the same expression as the one implemented in EN 1993-1-5 (2006), i.e.

$$k_F = 6 + 2 \cdot \left(\frac{h_w}{a} \right)^2 \quad (5.15)$$

As shown by the parametric study in Section 4.4, the design model implemented in EN 1993-1-5, could catch the variation in loaded length in a good manner even though the simplified k_F according to Equation (5.15) was used. The difference between Equation (5.14) and Equation (5.15) is very small but both equations will be evaluated here.

The reduction factor, χ_F , must be modified and it was decided herein to not use the reduction factor by Lagerqvist as basis. Instead, the proposal, originally by Müller (2003) and later included in Annex B of EN 1993-1-5, with a little bit more flexibility is used, see Equations (2.12) and (2.13).

Equations (2.12) and (2.13) are rewritten with the subscripts used for patch loading according to

$$\chi_F = \frac{1}{\varphi_F + \sqrt{\varphi_F^2 - \bar{\lambda}_F}} \quad (5.16)$$

and

$$\varphi_F = \frac{1}{2} \cdot (1 + \alpha_F \cdot (\bar{\lambda}_F - \bar{\lambda}_{F0}) + \bar{\lambda}_F) \quad (5.17)$$

in which α_F is an imperfection factor and $\bar{\lambda}_{F0}$ is the plateau length. These two factors will be calibrated to fit the test results in the best possible way.

The test data that was used for this evaluation consists of 382 tests collected by Lagerqvist, nine tests performed by Lagerqvist, one test by Raoul et al. (1990), four tests by Shahabian and Roberts (2000), five tests by Unosson (2003) and one test by Kuhlmann and Seitz (2004), all displayed in Appendix C, and the three tests presented in this study. From the total of 405 tests some were excluded for different reasons, e.g. when the value of f_{yw} was uncertain, when the definition of the ultimate load was unclear and so on. The following tests, with test label following the numbering in Appendix C, were excluded:

1 test: 2005 was excluded because h_w was uncertain.

30 tests: 2012-2022 and 2116-2134 were excluded since they were performed on hot-rolled section which is not of interest here.

16 tests: 2151-2167 were excluded since f_{yw} and f_{yf} are uncertain.

- 88 tests: 2200-2287 were expelled because it is the results from “the first or second loading cycle closely to ultimate load”, i.e. uncertainties in F_u .
- 6 tests: 2330-2332 and 2339-2341 were left out because it is questionable how the connection between the web and the flange was made with such a thin web.
- 1 test: 2366 was excluded because the load was applied through a wooden beam which makes it unclear how this influence the girder behaviour.
- 3 tests: 2381-2383 were left out since it was a study of interaction with shear which was not handled in this thesis.
- 5 tests: 2398-2402 were excluded because it was tests on girders made of stainless steel.

Now, 255 tests remains of which 186 have $M_E/M_R \leq 0,4$. The bending moment resistance, M_R , was calculated according to EN 1993-1-1 (2005) or EN 1993-1-5 (2006) depending on cross section class. Those 186 tests were used to calibrate the reduction factor and Figure 5.6 shows the relation F_u/F_y as a function of $\bar{\lambda}_F$. As expected F_u/F_y decrease with increasing $\bar{\lambda}_F$. In Figure 5.6 the reduction factor proposed herein are shown for comparison with the test data. The best fit was obtained with

$$\begin{cases} \alpha_F = 0,5 \\ \bar{\lambda}_{F0} = 0,6 \end{cases}$$

Further, it was decided herein to keep the simplified k_F as this work is aiming at a procedure that should be used by designers and hence a simple format is desirable. Hence, the $\bar{\lambda}_F$ in Figure 5.6 was determined using k_F from Equation (5.15). Though, statistics for both k_F will be shown later in this section. Equation (5.16) is a continuous function that starts just below 1,5 ($\bar{\lambda}_F = 0$), as can be seen in Figure 5.6. However, after some discussions within the project ComBri (2007) it was proposed to cut the curve at 1,2 as shown by the dashed line in Figure 5.6, instead of 1,0 to still utilize more of the strength of the stocky girders. Nevertheless, the test results show that it might not be necessary to cut the curve at all. The reduction factor with α_F and $\bar{\lambda}_{F0}$ as above becomes

$$\chi_F = \frac{1}{\varphi_F + \sqrt{\varphi_F^2 - \bar{\lambda}_F}} \leq 1,2 \quad (5.18)$$

with

$$\varphi_F = \frac{1}{2} \cdot (1 + 0,5 \cdot (\bar{\lambda}_F - 0,6) + \bar{\lambda}_F) \quad (5.19)$$

The tests performed at Luleå University of Technology by Lagerqvist (1994) and by the author of this thesis are highlighted in Figure 5.6 and as can be seen those tests have a low variation compared to the total test data base. The explanation for this is not obvious but these tests are performed under similar conditions and all data concerning the tests are known, which is not always the case for tests collected from papers.

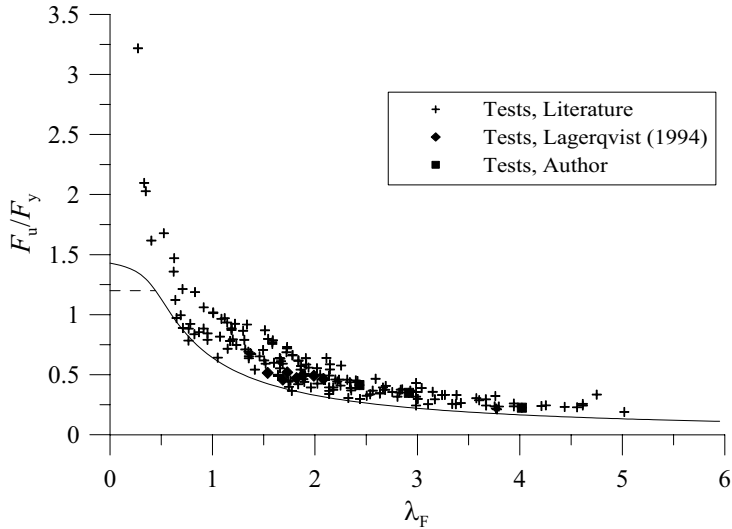


Figure 5.6 F_u/F_y as a function of $\bar{\lambda}_F$ for 186 tests with $M_E/M_R \leq 0,4$ together with the proposed reduction factor, Equation (5.18), k_F according to Equation (5.15).

Figure 5.7 shows the relation F_u/F_R as a function of $\bar{\lambda}_F$, where F_R was calculated according to

$$F_R = \chi_F \cdot F_y \quad (5.20)$$

with χ_F according to Equation (5.18) and F_y according to Equation (5.10). As can be seen in Figure 5.7 the scatter is substantial, though considered as normal compared to other investigations in the field. The scatter can partly be explained by the fact that the model for prediction of the resistance is rather simple compared to the complexity of the problem. Further, it can also partly come from the fact that a large number of tests from many different laboratories are put together in one data base. This may end up in systematic differences, e.g. different methods for evaluating the yield strength. The advantage with a large amount of test data that normally is valuable can be turned to a disadvantage when the tests have been performed by many different research groups. It is reasonable to believe that some test results are more reliable than others, but since most of the information regarding the tests is hard to get and is seldom described in detail in the published papers, i.e. there might be information missing that could influence the calculated resistance, it is difficult to find ground for exclusions of individual tests. Examples of information given in papers that could be missing are; how was f_y

defined, what was the stiffness of the loading plate used to introduce the concentrated force or whether the girder was used for more than one test, e.g. test on both flanges.

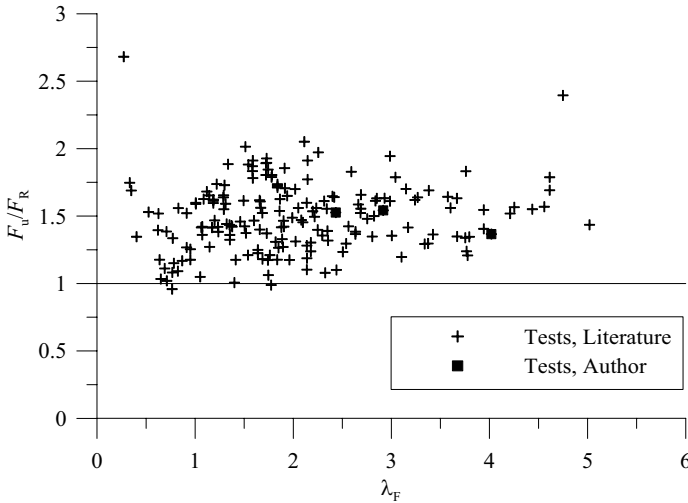


Figure 5.7 F_u/F_R as a function of $\bar{\lambda}_F$ for 186 tests with $M_E/M_R \leq 0,4$.

The statistics for F_u/F_R for the 186 tests with $M_E/M_R \leq 0,4$ are shown in Table 5.2 for different ways of calculating F_{cr} . The difference between the different k_F considered are very small, though a little less variation for the simplified k_F . For the case when F_{cr} was determined through the software *EBPlate* the variation is slightly higher compared to the others but in this case only 119 of the tests could be used due to limitations in the software when it comes to h_w and a/h_w . However, the differences between the three methods are small.

Table 5.2 Comparison of statistics for F_u/F_R between different methods of determining F_{cr} for 186 tests and 119 tests for *EBPlate*.

	F_{cr} acc. to Eq. (5.13) and (5.15)	F_{cr} acc. to Eq. (5.13) and (5.14)	F_{cr} from <i>EBPlate</i>
Mean	1,50	1,45	1,49
Standard deviation	0,257	0,272	0,275
Coefficient of variation	0,172	0,188	0,185
Upper 5-percent fractile	1,93	1,91	1,94
Lower 5-percent fractile	1,07	1,00	1,03

The tests found in the literature contain a number of tests with very odd cross section dimensions. Lääne (2003) made a survey on composite bridges in Switzerland and found out

that the bridge girder dimensions in general were within the limits $0,35 < A_f/A_{tot} < 0,45$ and $0,30 < A_w/A_{tot} < 0,40$. If the most odd sections are removed from the test data base according to the limitations given by Lääne not many tests will be left. Instead, those limits were extended to $0,25 < A_f/A_{tot} < 0,55$ and $0,20 < A_w/A_{tot} < 0,50$. Further, also the test girders with flanges outside the interval $10 < b_f/t_f < 30$ were excluded as these are no realistic flanges for normal girders. With these limitations more realistic cross sections were obtained and now, only 60 tests remains and the statistics for these tests are shown in Table 5.3.

Table 5.3 Comparison of statistics for F_u/F_R between different methods of determining F_{cr} for 60 realistic cross sections and 37 tests for EBPlate.

	F_{cr} acc. to Eq. (5.13) and (5.15)	F_{cr} acc. to Eq. (5.13) and (5.14)	F_{cr} from EBPlate
Mean	1,49	1,42	1,43
Standard deviation	0,188	0,189	0,219
Coefficient of variation	0,126	0,133	0,154
Upper 5-percent fractile	1,81	1,74	1,79
Lower 5-percent fractile	1,18	1,11	1,07

The variation decrease significantly when only the tests with realistic cross sections are taken into account and the difference between the different methods are still small.

In Figure 5.8 F_u/F_R as a function of s_s/h_w are shown for the 186 tests with small bending moments. In addition the FE-results from the parametric study regarding loaded length are shown as well. The results from the parametric study form an almost horizontal line in the figure, which indicates that the model can take care of the variation in loaded length in a good manner. Regarding the test results no other tendency can be found and again it is noted that the limitation $s_s \leq h_w$ in EN 1993-1-5 is not to high, in fact it seems like it could be increased. However, the three test results with $s_s > h_w$ have an s_s equal to a , which probably influence the ultimate load.

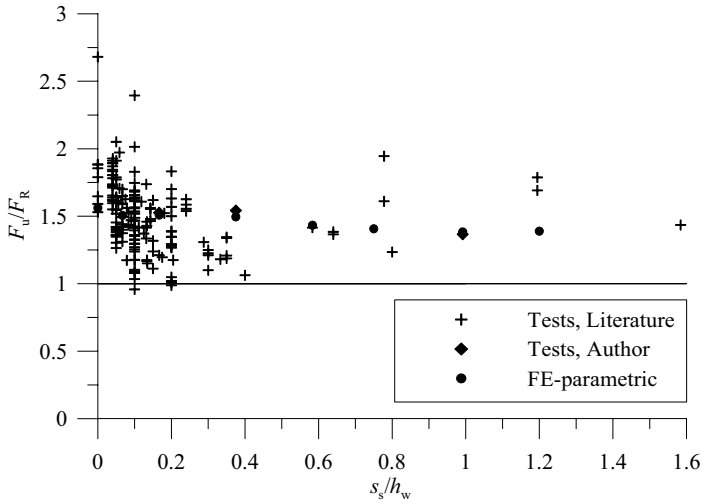


Figure 5.8 F_u/F_R as a function of s_s/h_w for 186 tests together with the FE-results from the parametric study.

Figure 5.9 shows F_u/F_R as a function of s_s/a for the 186 tests with small bending moments together with the FE-results from the parametric study. It can be seen that the results with $s_s/a = 1$ are in the high end of the scatter, which might be due to the fact that some of the applied load goes directly into the vertical stiffeners at the supports.

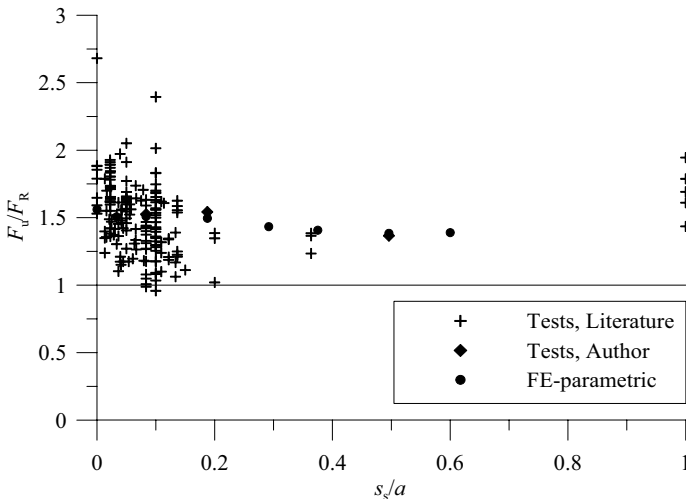


Figure 5.9 F_u/F_R as a function of s_s/a for 186 tests together with the FE-results from the parametric study.

F_u/F_R as a function of M_E/M_R for 255 tests is shown in Figure 5.10 with F_R according to the proposal herein. Together with the tests also the interaction equation according to

EN 1993-1-5, see Equation (5.21), is displayed. As can be seen Equation (5.21) gives a reasonably safe prediction of the influence from bending moment for the tests.

$$\frac{F_E}{F_R} + 0,8 \cdot \frac{M_E}{M_R} \leq 1,4 \quad (5.21)$$

Still, together with Equation (5.21), the conditions $F_E/F_R \leq 1$ and $M_E/M_R \leq 1$ should also be fulfilled.

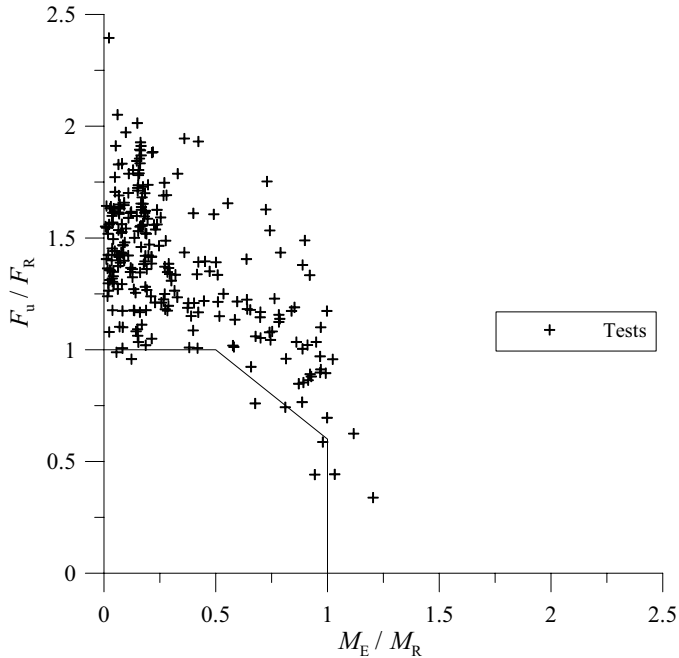


Figure 5.10 F_u/F_R as a function of M_E/M_R for the 255 tests.

The interaction expression, Equation (5.21), shown in Figure 5.10, has only a small number of tests on the unsafe side. It is concluded that even though the procedure for determining the patch loading resistance was modified the interaction expression can be kept as it is, i.e. as Equation (5.21).

To sum up this section the proposed equations for design of an I-girder subjected to patch loading is given here shortly. First, determine the yield resistance, F_y , as

$$F_y = f_{yw} \cdot t_w \cdot \left(s_s + 2 \cdot t_f \cdot \left(1 + \sqrt{\frac{f_{yf} \cdot b_f}{f_{yw} \cdot t_w}} \right) \right) \quad (5.22)$$

The critical load is given by

$$F_{cr} = k_F \cdot \frac{\pi^2 \cdot E}{12 \cdot (1 - \nu^2)} \cdot \frac{t_w^3}{h_w} \quad (5.23)$$

with

$$k_F = 6 + 2 \cdot \left(\frac{h_w}{a}\right)^2 \quad (5.24)$$

Now, the slenderness is calculated according to

$$\bar{\lambda}_F = \sqrt{\frac{F_y}{F_{cr}}} \quad (5.25)$$

and the reduction factor, χ_F , is obtained as

$$\chi_F = \frac{1}{\varphi_F + \sqrt{\varphi_F^2 - \bar{\lambda}_F}} \leq 1,2 \quad (5.26)$$

with

$$\varphi_F = \frac{1}{2} \cdot (1 + 0,5 \cdot (\bar{\lambda}_F - 0,6) + \bar{\lambda}_F) \quad (5.27)$$

Finally, the design resistance is given by

$$F_{Rd} = \chi_F \cdot F_y / \gamma_{M1} \quad (5.28)$$

in which γ_{M1} is a partial factor for the resistance that will be determined in the next section.

5.4 Statistical evaluation of the proposed design procedure

A statistical evaluation of the proposed design model for patch loading was carried out by means of the recommendations provided in EN 1990 Annex D (2002), see Appendix E.

The evaluation presented here was derived with the assumption of a log-normal distribution of the variables. The variations used in the statistical evaluation for the geometrical properties and the yield strength were

$$V_{rt} = 0,08 \text{ (geometry and yield strength)}$$

$$V_{f_y} = 0,07 \text{ (yield strength)}$$

which were used also by Müller (2003).

Figure 5.11 shows a plot of r_c as a function of $r_t = F_R$ for 186 tests. The mean value of the correction factor and the coefficient of variation for the error term become

$$b = 1,497$$

$$V_{\delta} = 0,176$$

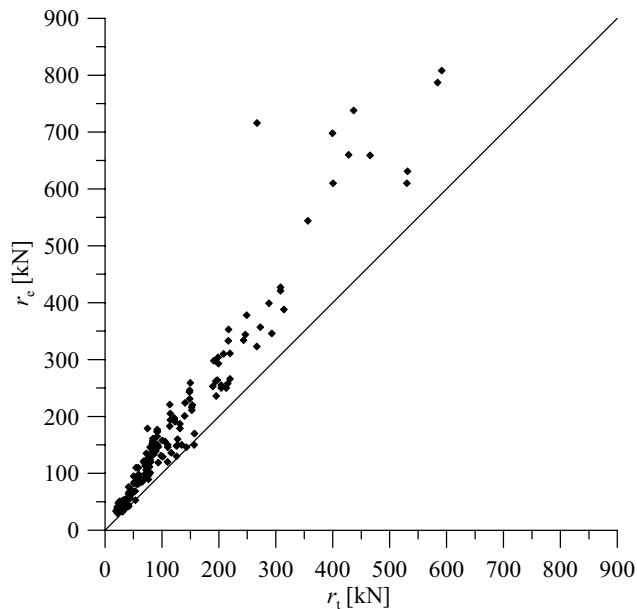


Figure 5.11 Test results r_c as a function of prediction r_t for 186 tests.

The partial factor for the resistance becomes

$$\gamma_M = 1,308$$

and the corrected partial factor that should be applied to the resistance using nominal values of the basic variables is

$$\gamma_M^* = 1,057$$

However, it seems a bit unfair that this method for establishment of the partial factor for the resistance does not take into account if the variations are on the safe side or not. Instead all deviations are taken as random. If the most conservative test is taken out, with $F_u/F_R = 2,68$, $\gamma_M^* = 1,044$ that can be approximated to 1,0.

Further, as mentioned in Section 5.3 there are a lot of tests with very odd cross section dimensions. If only the 60 tests with realistic cross section dimensions are taken into account the results from the evaluation change dramatically according to

$$b = 1,493$$

$$V_\delta = 0,135$$

$$\gamma_M^* = 0,945$$

Based on the different calibrations it is proposed that γ_{M1} can be approximated to 1,0 which is the recommended value for buildings. Moreover, the recommended value of 1,1 for bridges is proposed to be lowered to 1,0 as well.

5.5 Comparison with other models

For comparison F_u/F_R for the 186 tests with $M_E/M_R \leq 0,4$ were determined according to EN 1993-1-5 (2006). F_u/F_R as a function of $\bar{\lambda}_F$ are shown in Figure 5.12 and the statistics are shown in Table 5.4 together with the results from the proposed model. It is clear that the design procedure in EN 1993-1-5 is conservative but also the variation as seen in Table 5.4 is high compared to the proposed model. The reason for the increasing ratio F_u/F_R with increasing slenderness, in Figure 5.12, is explained by the modified reduction factor compared to the one proposed by Lagerqvist (1994), Equation (5.29). Further, Lagerqvist did not have any restrictions regarding m_2 for low values on the slenderness and no limitations regarding l_y , i.e. $l_y \leq a$, as implemented in EN 1993-1-5.

The original proposal by Lagerqvist is also added in Table 5.4 for comparison. It is easily seen in Table 5.4 that the design procedure by Lagerqvist has the lowest mean and variation by far.

However, the model by Lagerqvist contains the parameter m_2 , which according to the numerical study carried out in this thesis is not relevant.

$$\chi_F = \frac{0,47}{\bar{\lambda}_F} + 0,06 \leq 1 \tag{5.29}$$

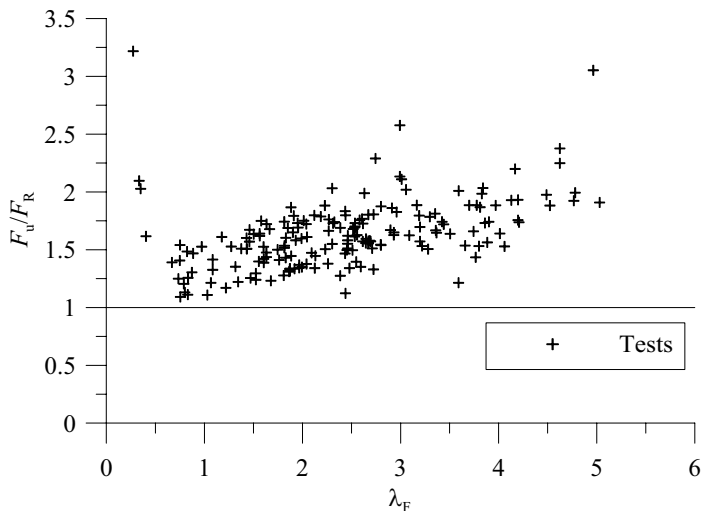


Figure 5.12 F_u/F_R as a function of $\bar{\lambda}_F$ for the 186 tests with $M_E/M_R \leq 0,4$. F_R according to EN 1993-1-5.

Also the evaluation of the design model by Roberts and Newark (1997) is shown in Table 5.4. As can be seen that model is in the same region as the proposed design procedure and the model in EN 1993-1-5, considering the mean and variation. Though, it has a somewhat low value on the lower 5-percent fractile which should be aimed at 1 or above. Furthermore, the method proposed by Roberts and Newark includes a safety factor which could be changed to raise the mean and consequently the lower 5-percent fractile but then the variation increases as well.

Table 5.4 Comparison of F_u/F_R for 186 tests with $M_E/M_R \leq 0,4$ between proposal and EN 1993-1-5.

	Proposal	EN 1993-1-5	Lagerqvist (1994)	Roberts et al. (1997)
Mean	1,50	1,63	1,28	1,41
Standard deviation	0,257	0,299	0,173	0,294
Coeff, of variation	0,172	0,183	0,135	0,209
Upper 5-percent fractile	1,93	2,13	1,57	1,90
Lower 5-percent fractile	1,07	1,13	0,993	0,920

5.6 Concluding remarks

Considering the first part of the design procedure, the yield resistance, the numerical study performed herein shows that the assumption of a fictitious T-section at the outer plastic hinges, see Figure 2.13, proposed by Lagerqvist, is doubtful. If the web contribution, m_2 , is removed from the yield resistance the agreement with the numerical study is good and hence, the m_2 parameter is herein proposed to be removed.

The modification of the yield resistance resulted in a new calibration of the reduction factor, χ_F . It was chosen to use the type of curve given in Annex B of EN 1993-1-5 for the new reduction factor, which comes from a proposal by Müller (2003). The idea from Müller was to introduce general reduction factors through the definition of the slenderness parameter, λ , from load multipliers used to define the plastic resistance and the critical load, respectively. If the different reduction factors for plate buckling are compared it turns out that patch loading clearly fall below the others. However, with the change in yield resistance proposed here, the reduction factor for patch loading will be lifted and then the reduction factors are more harmonized, although not completely. This is shown in Figure 5.13 where the proposed reduction factor are shown together with the reduction factor in EN 1993-1-5 for patch loading, plate buckling and shear buckling, respectively. The reduction factor for shear buckling shown, is the one for non-rigid end posts. The aim from Müller was to have one reduction factor for all plate buckling problems but that will not be appropriate from an economic point of view.

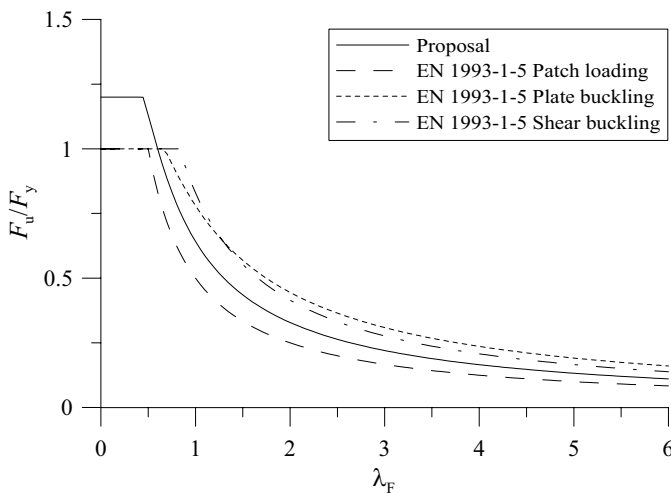


Figure 5.13 Comparison of different reduction factors.

The proposal is closer to the plate buckling curve, which on the other hand is a little too high. Clarin (2004) carried out a large number of stub column tests on square hollow sections made of high strength steel, with nominal f_y from 420 - 1100 MPa. The results clearly showed that the plate buckling or Winter curve is too high for welded sections. Further, Clarin also put together

a large amount of similar tests with lower f_y and found the same behaviour also for those. The only tests on welded specimens that fall above the Winter curve were stress relieved. Further, Veljkovic and Johansson (2001) performed FE-studies of plates with and without residual stresses and concluded that the Winter curve is more suitable for plates without significant residual stresses or for plates that are stress relieved.

The proposed design procedure gives less variation and lower mean compared to the existing procedure in EN 1993-1-5. However, the proposal by Lagerqvist (1994) still has the lowest mean and variation but the herein proposed procedure does describe the actual stress distribution in the web, when subjected to concentrated forces, more correctly. Further, there is still a substantial scatter in the results as can be seen in Figure 5.7.

The proposed design procedure had an average of $m = 1,50$, a standard deviation of $s = 0,26$ and a coefficient of variation of $V = 0,17$ when compared to 186 tests with small bending moment. This must be seen as normal when it comes to patch loading and the complexity of the problem. It was experienced here that the advantage of a large number of tests could be turned into a disadvantage when tests from several research groups are put together into one large data base as mentioned earlier. However, if only the tests performed at Luleå University of Technology are considered, i.e. the tests by Lagerqvist and the tests presented in this thesis, the variation decrease substantially. These tests are performed following the same principles and all data regarding the tests are known. For this group $m = 1,39$, $s = 0,11$ and $V = 0,08$ using the reduction factor calibrated against all 186 tests with small bending moments.

The expression for interaction between patch loading and bending moment according to EN 1993-1-5 (2006) was found applicable also for the herein proposed patch loading resistance. No further work considering the interaction between patch loading and shear was conducted in this work but Kuhlmann and Braun (2007) showed that their interaction equation, see Section 2.3.4, together with the proposed patch loading resistance fits well to the available test and numerical results.

Finally, the proposed design procedure was calibrated versus test results according to Annex D of EN 1990 (2002). From this statistical evaluation it is proposed that the partial safety factor, γ_{M1} , should be set to 1,0.

6 BRIDGE LAUNCHING - A SERVICEABILITY LIMIT STATE

6.1 General

For long bridges, bridges high over ground or bridges over water, i.e. when the bridge is either too heavy to lift into position or it is impossible for other reasons, a very common method to erect the bridge girders is to launch it from one or both ends, see Figure 6.1. This means that sections manufactured at the workshop are welded together on ground and then pushed out over launching shoes into the final position. A launching nose is usually placed in the front of the bridge girder to both get it up on the next support and also to decrease the bending moment and support reaction in the girder at the launching shoe.

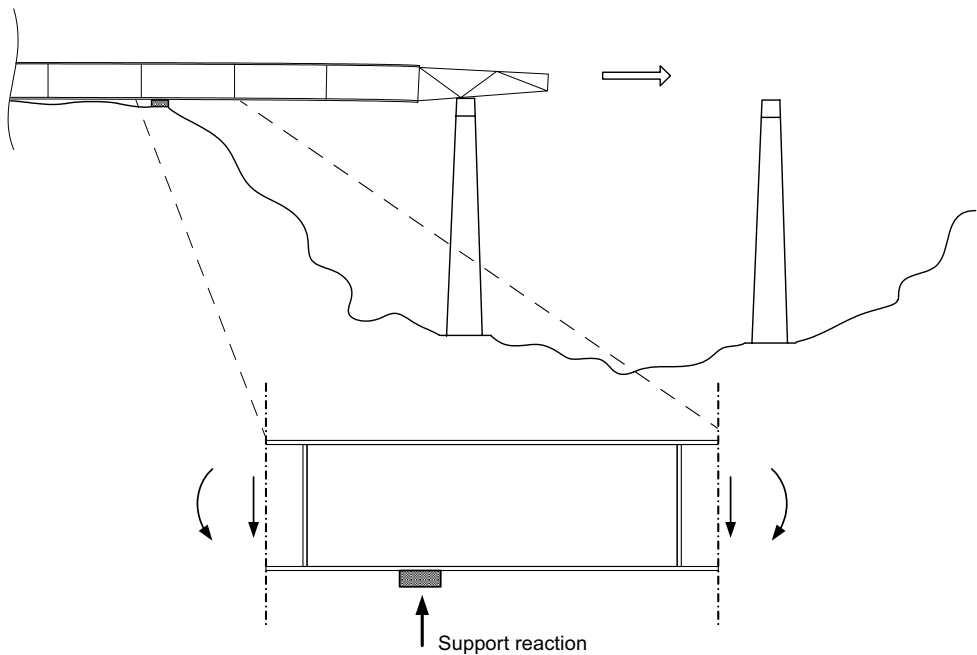


Figure 6.1 Launching of a bridge girder and load situation.

For a steel bridge girder, the problem concerning resistance to patch loading occurs during launching of the girder. Referring to Figure 6.1, the lower flange is subjected to a concentrated force from the launching shoe, along which the girder travels. Further, just before the launching nose reaches the next support, also large bending moments are present. A section of the girder can be subjected to several repeated travelling concentrated forces when passing over a number of

supports during launching. These concentrated forces can be of the magnitude that governs the web thickness and even a small increase of the web thickness can add a substantial amount of steel. Therefore, it is important to find a suitable criterion for the serviceability limit state for bridge launching.

In the following a brief review on bridge launching can be found as well as a numerical study regarding travelling loads on a bridge girder section. Based on the numerical study a simple serviceability criterion is proposed for bridge launching.

6.2 Bridge launching

Launching is a very common method to erect steel and composite bridges. Large pre-fabricated sections are welded together on ground, usually behind the abutment, in position for launching. After welding of the sections the girders are pushed out over the launching shoes into position. The launching can either be a step wise procedure or the entire girder is launched at once, depending on the length of the bridge, the size of the construction site behind the abutment and the delivery of the pre-fabricated sections. Further, the entire bridge girder can be launched from one side or one part from each abutment. In order to reduce the bending moment and support reaction at the launching shoe a launching nose is usually attached in front of the bridge girder. The launching nose usually consists of a steel truss with low weight. An example of a bridge launching with a launching nose is displayed in Figure 6.2.



Figure 6.2 Bridge launching with a launching nose in the front, outside Sollefteå in Sweden.

In general a combination of a wire system and hydraulic jacks are used to push and hold the girders during launching, see Figure 6.3. The bridge girder and wire system shown in Figure 6.3 are from the new rail way bridge over Nätraån just south of Örnsköldsvik in the north part of Sweden. The wire system in the middle of the photo are used to push the bridge while the wire in the left part of the figure are used to hold the bridge in the longitudinal direction. It is common, if the girder is launched in a downward inclination, that as soon as the friction is

overcome the girder will slide by itself and only needs to be hold back. It is a large weight that travels over the supports and hard to stop and therefore a wire system is needed to hold the bridge at a suitable speed.



Figure 6.3 Wire system used to both hold and push the bridge girder over Nätraån in the north part of Sweden.

The launching shoes or bearings were earlier mainly of the roller type, i.e. the bearing contained two or more rollers on which the girder travelled. Lately, at least in Sweden, the slide bearings are more common according to Bergholtz (1994). The advantages with slide bearings are a better introduction of the load into the web and that the size of the slide bearing are less compared to roller bearings according to Raoul and Davaine (2006). The slide bearings can be of two types, a temporary slide bearing or a modified permanent bearing. One example of a slide bearing is shown in Figure 6.4. The top plate normally has a large curvature to fit to the deformations of the girder. As can be seen the shoe is tiltable around an axis perpendicular to the launching direction. On top of the slide plate some kind of low friction material are applied, e.g. a Teflon film. Further, a lubricant can also be used to decrease the friction.



Figure 6.4 Launching shoe of the slide bearing type at Nätraån, Sweden.

There are also other types of bearings without any sliding. The progression of the bridge is then obtained by a jack system, such system was used for launching of the Millau viaduct in France, or by a track, which is a Japanese technique, according to Raoul and Davaine (2006).

The advantages with launching compared to for example erection with cranes are that no scaffold is needed under the bridge, which enables traffic under the bridge if that is the case. Further, if the bridge spans over water scaffolding may not be possible anyway and it is also preferably to perform all welding on ground under weather protection.

Bridge launching can be performed with either only the girders, girders together with the form work, girders with form work and reinforcement or girders with the concrete already in place. The latter is favourable since it allows for casting at ground under weather protection. However, in some cases a weather protection can be used for the casting also after launching, see Figure 6.5.



Figure 6.5 Weather protection for casting of concrete after launching, Nätraån, Sweden.

The disadvantage with launching of a composite bridge, including the concrete deck, is the large increase of the self weight and subsequently that the support reaction and bending moment that the girder web must resist will increase.

6.3 Numerical study

During launching of a bridge girder, the girder is subjected to a support reaction from the launching shoe together with a bending moment. The size of these loads depends on the self weight of the girder and the span length. The worst case arise when the girder is in the position directly before the launching nose gets up on the next support. If the bridge is long this could be repeated several times for a girder section in the worst position, assuming the distance between the supports is equal.

When the girder is subjected to the loads shown in Figure 6.1 the web may deflect laterally as the support reaction or patch load travels along the section. As the patch load travels over the stiffener and the section is unloaded the web deformations will decrease to some extent. This

process is repeated until the girder is in its final position, maybe up to ten times and therefore it is of importance that the remaining deformation or buckle is kept small. How small can be discussed but it should not increase for every repeated loading. The increase of the remaining buckle is of course related to the plastic deformations, i.e. plastic strains in the web. Hence, the aim with this study is to find a criterion that keeps the girder elastic and subsequently that limits the increase of the remaining buckle after several loadings. This follows the recommendations in EN 1993-2 (2003) that the behaviour should be reversible.

To find such criterion a number of non-linear FE-analyses were carried out on 13 different girder sections. The section geometries are primarily based on the tests performed in this thesis, see Section 3. This is due to the possibility to verify the model in terms of mesh density and boundary conditions. In addition some other girder dimensions were studied to expand the base of results for the evaluation of the serviceability criterion.

Once again all pre- and post-processing were conducted with ABAQUS CAE version 6.6 and the calculations were performed with ABAQUS/Standard version 6.6.

6.3.1 Finite element model and method

The geometry and boundary conditions of the studied girder section are shown in Figure 6.6. All dimensions are given in Table 6.1 together with a girder label. The ends of the web were modelled as very stiff to simulate vertical stiffeners, i.e. no actual stiffeners were included in the model. Further, the ends of the loaded flange were constrained to move equally in the 2-direction according to the coordinate system in Figure 6.6, symbolizing the support from vertical stiffeners. At the corners of the web plate, boundary conditions were applied to prevent out of plane disablement. Finally, vertical boundary conditions were applied in the centre of gravity and on one side also in the 3-direction to prevent horizontal movements.

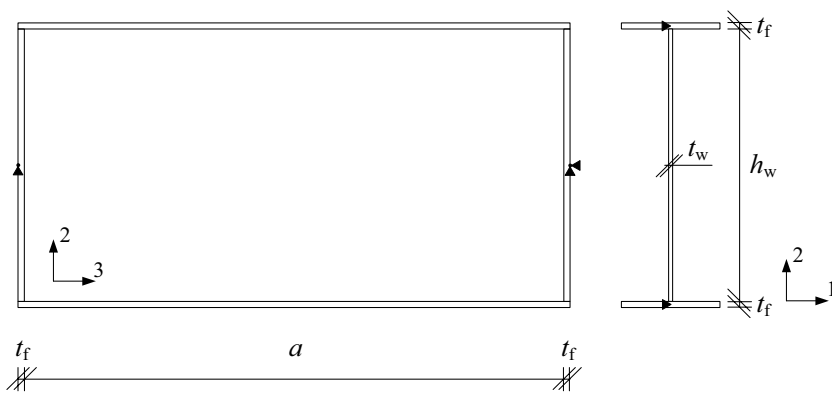


Figure 6.6 Geometry of the analysed girder sections together with applied boundary conditions.

The girder labels in Table 6.1 follows a system where *SLS* means serviceability limit state, the next figure is the ratio h_w/t_w and the *i* is an internal label for different analyses on the specific girder section. For some of the girders additional codes are attached to the labels. Those are *w8*, which stands for a $h_w = 800$ mm and *F30* or *F40*, which corresponds to a different flange thickness and finally *LS* that stands for Large Scale, i.e. the girder sections were scaled up to investigate if there are any scaling effects.

Table 6.1 Girder section geometries and labels.

Label	h_w [mm]	t_w [mm]	h_w/t_w	b_f [mm]	t_f [mm]	a [mm]
<i>SLS80i</i>	1200	15	80	450	20	2400
<i>SLS80i-w8</i>	800	10	80	450	20	2400
<i>SLS80i-F30</i>	1190	15	80	450	30	2400
<i>SLS100i</i>	1200	12	100	450	20	2400
<i>SLS100i-F30</i>	1190	12	99	450	30	2400
<i>SLS100i-F40</i>	1180	12	98	450	40	2400
<i>SLS100i-w8</i>	800	8	100	450	20	2400
<i>SLS100i-LS</i>	2000	20	100	750	33,3	4000
<i>SLS125i</i>	1200	9,6	125	450	20	2400
<i>SLS150i</i>	1200	8	150	450	20	2400
<i>SLS150i-LS</i>	2000	13,3	150	750	33,3	4000
<i>SLS175i</i>	1200	6,86	175	450	20	2400
<i>SLS200i</i>	1200	6	200	450	20	2400

The FE-model was assembled up side down compared to the real launching situation in such a way that the upper flange is compressed due to the bending moment and loaded by concentrated forces. The analyses were performed in several steps. First, a buckling analysis of each section was carried out to get the eigenmode used as initial imperfection. The maximum magnitude of this imperfection was taken as $h_w/200$ which again is the recommended value in Annex C of EN 1993-1-5 (2006). Secondly, a non-linear analysis that contains 12 steps was conducted for each individual analysis according to Figure 6.7 and the list below.

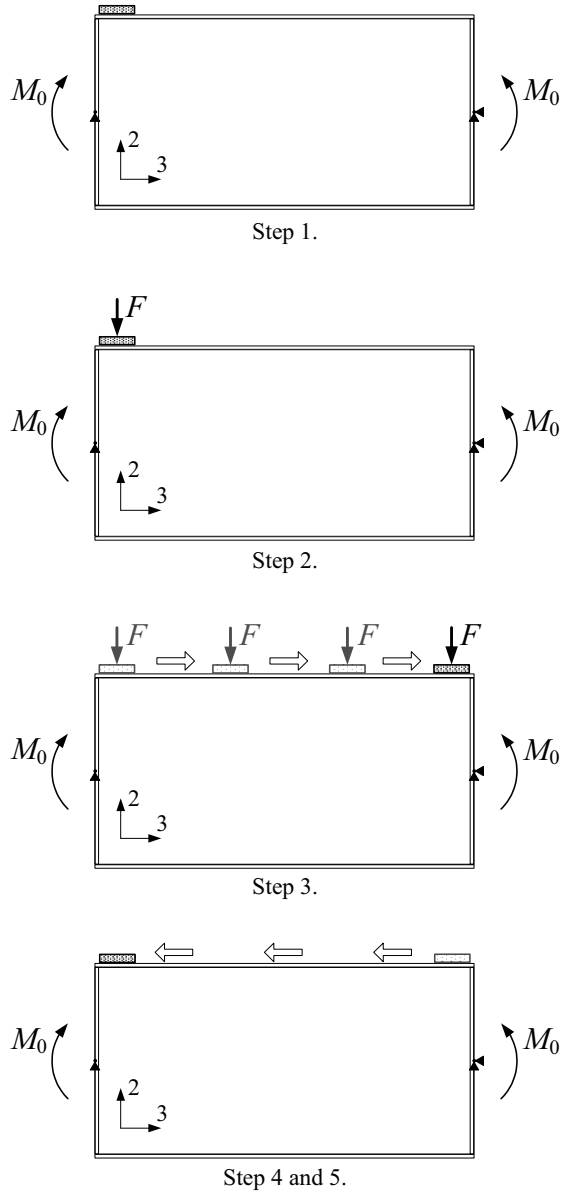


Figure 6.7 Description of the different steps of the non-linear analyses.

1. A bending moment is applied incrementally to the section and then held constant.
2. The load on the loading plate is applied incrementally.
3. The loading plate travels along the girder in small steps with a constant load.
4. When the loading plate has reached the other end of the girder it is unloaded.
5. The loading plate is moved back to the starting point without any load on it.

6. Step 2 is repeated.
7. Step 3 is repeated.
8. Step 4 is repeated.
9. Step 5 is repeated.
10. Step 2 is repeated.
11. Step 3 is repeated.
12. Step 4 is repeated.

It was assumed that if the remaining buckle did not increase after three loadings it would not after more loading either. Moreover, it was observed during the analyses that when the effective plastic strains in the mid-plane of the web were zero, the remaining buckle was kept constant.

The FE-models of the girder sections consists of shell elements of the type S4R, as in the other FE-studies in this thesis. To model the load transfer from the launching shoe into the girder in the most realistic way a loading plate with the ratio $s_y/a = 0,083$ was used. This means that for all analyses except the large scale models a loading plate with $s_s = 200$ mm was used and subsequently for the large scale models a loading plate with $s_s = 333$ mm was used. The loading plates were modelled with solid elements, C3D8R, and the load was applied as a concentrated force in the mid point of the loading plate. All nodes along the mid-line of the loading plate were constrained to move equally in the vertical direction, the 2-direction in Figure 6.8, as the mid-point. Further, boundary conditions were applied to the loading plate in direction 1 along the symmetry line to prevent movements in that direction. To model the contact problem between the loading plate and the upper flange, contact surfaces were defined in between the lower surface of the loading plate and the upper surface of the flange. Figure 6.8 shows the FE-model at the start of an analysis together with a schematic drawing of the loading plate. Approximately the same element size was used for all models and corresponds to the size used in the earlier numerical studies, i.e. in Section 4.

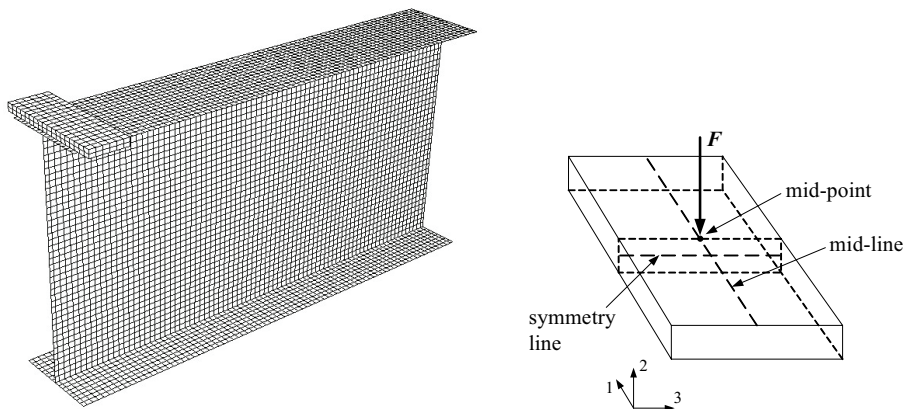


Figure 6.8 Finite element mesh of girder section when the loading plate is located at the starting position (left) and explanation of the details of the loading plate (right).

Further, a friction coefficient, μ , has to be specified between the loading plate and the loaded flange. According to Granath (1998) who carried out tests with a launching shoe similar to the one shown in Figure 6.4, the friction coefficient, μ , varied between 0,1 and 0,2. In here, both $\mu = 0,1$ and 0,2 was tested without any significant differences. Following this observation, an $\mu = 0,15$ was used in the simulations.

The material properties used in the model are the same as used in the numerical simulations of the tests, i.e. corresponding to a S355 steel grade, and the material model used was an isotropic hardening rule together with a von Mises yield surface.

6.3.2 Results from the numerical study

Before the somewhat complex analyses described above were carried out, the ultimate loads of the girders were determined both with respect to patch loading and bending moment separately, see Table 6.2. These loads, $F_{u,FE}$ and $M_{u,FE}$, were then used as reference values of the resistance in the analyses with travelling load. $F_{u,FE}$ and $M_{u,FE}$ were determined on the girders using the same FE-model and method as described in Section 6.3.1 apart from the travelling load, instead a prescribed vertical displacement of the flange at mid-span was used to introduce the load to the girder. The ultimate load for the test presented in this thesis, P200, was 544 kN, which should be compared to the SLS200 FE-analysis, i.e. 540 kN. Hence, it was concluded that the FE-model was reasonable and that the results are trustworthy. The resistance to patch loading in the ultimate limit state, F_R , in column four are according to the proposal presented in Section 5.3 and the bending resistance, M_R , are determined according to EN 1993-1-1 (2005) or EN 1993-1-5 (2006) depending on cross section class.

As can be seen in Table 6.2 the ratio $F_{u,FE}/F_R$ falls in line with what is expected. However, $M_{u,FE}/M_R$ was expected to be closer to unity for some of the different girders. One explanation for this behaviour is how the moment is applied to the girder. For simplicity it was chosen to apply the moment as a force couple acting on the flanges corresponding to a moment according to Figure 6.7. Looking at the stresses in the girder it can be seen that except for the part closest to the ends of the girder there is a nice stress pattern but closest to the ends the stresses are concentrated to the flanges. This induce flange buckling close to the ends in the vicinity of $M_{u,FE}$. Further, if *SLS100i* and *SLS100i-LS* are compared it can be seen that they show of almost exactly the same $F_{u,FE}/F_R$ and $M_{u,FE}/M_R$, which indicates that there are no scale effects involved.

Table 6.2 Data from the FE-analyses of the different girders together with patch loading resistance according to the proposal herein and bending resistance according to Eurocode 3.

Label	$F_{u,FE}$ [kN]	F_R [kN]	$F_{u,FE}/F_R$	$M_{u,FE}$ [kNm]	M_R [kNm]	$M_{u,FE}/M_R$
<i>SLS80i</i>	2331	1901	1,23	4435	5058	0,88
<i>SLS80i-w8</i>	1349	1084	1,24	2932	2909	1,01
<i>SLS80i-F30</i>	2660	2177	1,22	7405	6884	1,08
<i>SLS100i</i>	1644	1271	1,29	4363	4811	0,91
<i>SLS100i-F30</i>	1857	1457	1,27	6936	6645	1,04
<i>SLS100i-F40</i>	2000	1624	1,23	9310	8450	1,10
<i>SLS100i-w8</i>	943	722	1,31	2858	2838	1,01
<i>SLS100i-LS</i>	4527	3529	1,28	20330	22255	0,91
<i>SLS125i</i>	1148	846	1,36	4197	4417	0,95
<i>SLS150i</i>	850	605	1,40	4170	4225	0,99
<i>SLS150i-LS</i>	2371	1672	1,42	19476	19532	1,00
<i>SLS175i</i>	664	456	1,46	4157	4108	1,01
<i>SLS200i</i>	540	356	1,52	4123	4031	1,02

A total of 39 different analyses with travelling load were carried out according to Table 6.3. The main parameter varied within each girder section was the load level F_{FE} . However, a few analyses with higher M_E was conducted to verify that the levels obtained was suitable. The idea was to find a load level $F_{FE,sls}$ for each girder section where the remaining lateral web deformations did not grow for each load passage. As this level is hard to know in advance several analyses had to be performed on each section to find the suitable load level. Furthermore, M_E in Table 6.3 was determined when the load plate was located at mid-span according to

$$M_E = M_0 + \frac{F_{FE} \cdot a}{4} \quad (6.1)$$

in which M_0 is the constant bending moment applied in the beginning of the analysis, see Figure 6.7.

Table 6.3 Patch loading and bending moment levels used in the analyses with travelling load. Bold figures indicates load levels that are acceptable, i.e. no plastic strains are produced at this load level.

Label	F_{FE} [kN]	$F_{FE}/F_{u,FE}$	F_{FE}/F_R	M_E [kNm]	$M_E/M_{u,FE}$	M_E/M_R
<i>SLS80a</i>	1049	0,45	0,55	2529	0,57	0,50
<i>SLS80b</i>	979	0,42	0,51	2527	0,57	0,50
<i>SLS80a-w8</i>	675	0,50	0,62	1467	0,50	0,50
<i>SLS80b-w8</i>	742	0,55	0,68	1468	0,50	0,50
<i>SLS80a-F30</i>	1197	0,45	0,55	3465	0,47	0,50
<i>SLS80b-F30</i>	1117	0,42	0,51	3451	0,47	0,50
<i>SLS100a</i>	1069	0,65	0,84	2204	0,51	0,46
<i>SLS100b</i>	986	0,60	0,78	2153	0,49	0,45
<i>SLS100c</i>	904	0,55	0,71	2103	0,48	0,44
<i>SLS100d</i>	822	0,50	0,65	2203	0,51	0,46
<i>SLS100e</i>	718	0,52²	0,64²	3092	0,71	0,64
<i>SLS100f</i>	592	0,53²	0,63²	3956	0,91	0,82
<i>SLS100g</i>	871	0,53	0,69	2233	0,51	0,46
<i>SLS100h</i>	732	0,57 ²	0,69 ²	3369	0,77	0,70
<i>SLS100a-F30</i>	929	0,50	0,64	3322	0,48	0,50
<i>SLS100b-F30</i>	1022	0,55	0,70	3323	0,48	0,50
<i>SLS100a-F40</i>	1000	0,50	0,62	4225	0,45	0,50
<i>SLS100b-F40</i>	1100	0,55	0,68	4226	0,45	0,50
<i>SLS100c-F40</i>	1070	0,54	0,66	4223	0,45	0,50
<i>SLS100a-w8</i>	472	0,50	0,65	1428	0,50	0,50
<i>SLS100b-w8</i>	519	0,55	0,72	1432	0,50	0,50
<i>SLS100c-w8</i>	641	0,68	0,89	1431	0,50	0,50
<i>SLS100d-w8</i>	566	0,60	0,78	1430	0,50	0,50
<i>SLS100e-w8¹</i>	519	0,55	0,72	1432	0,50	0,50
<i>SLS100f-w8</i>	594	0,63	0,82	1432	0,50	0,50
<i>SLS100a-LS</i>	2265	0,50	0,64	11132	0,55	0,50
<i>SLS125a</i>	689	0,60	0,81	2208	0,53	0,50
<i>SLS150a</i>	629	0,74	1,04	2064	0,49	0,49
<i>SLS150b</i>	553	0,65	0,91	2087	0,50	0,49
<i>SLS150c</i>	465	0,65²	0,91²	2918	0,70	0,69
<i>SLS150d</i>	578	0,68	0,96	2115	0,51	0,50
<i>SLS150e</i>	486	0,69²	0,96²	2960	0,71	0,70
<i>SLS150a-LS</i>	1612	0,68	0,96	9758	0,50	0,50
<i>SLS150b-LS</i>	1588	0,66	0,94	9760	0,50	0,50

Label	F_{FE} [kN]	$F_{FE}/F_{u,FE}$	F_{FE}/F_R	M_E [kNm]	$M_E/M_{u,FE}$	M_E/M_R
<i>SLS175a</i>	465	0,70	1,02	2079	0,50	0,51
<i>SLS175b</i>	391	0,70²	1,02²	2876	0,69	0,70
<i>SLS175c</i>	478	0,72	1,05	2057	0,49	0,50
<i>SLS200a</i>	405	0,75	1,14	1865	0,45	0,46
<i>SLS200b</i>	389	0,72	1,09	1855	0,45	0,46

¹ initial imperfection of $h_w/133$ instead of the usual $h_w/200$

² the ratios have been recalculated to take into account the interaction with bending moment according to Equation (6.2), $F_{FE}/F_{u,FE}$ with $M_E/M_{u,FE}$ and F_{FE}/F_R with M_E/M_R

The bold figures in Table 6.3 indicates that at these load levels no increasing lateral web deformations occurred and no plastic membrane strains were produced during the analyses. It can be seen in Table 6.3 that in some cases the acceptable load level for large bending moments are higher compared to the same analysis with smaller bending moments, see e.g. *SLS100f* and *SLS100g*. For the cases with bending moment ratios higher than 0,5, F_R has been recalculated according to

$$F_{R, \text{int}} = F_R \cdot \left(1,4 - 0,8 \cdot \frac{M_E}{M_R} \right) \quad (6.2)$$

using $M_E/M_{u,FE}$ for the ratio $F_{FE}/F_{u,FE}$ and M_E/M_R for the ratio F_{FE}/F_R .

For all analyses the lateral web deformation at the mid-length section along a line in the vertical direction were plotted initially, after the moment was applied, when the loading plate was localized at mid-length and after the load passage when unloaded. This is also shown for the second and third load passage. In Figure 6.9 and Figure 6.10 the lateral web deformations are displayed for *SLS100b* and *SLS100d*, respectively. Figure 6.9 clearly indicates growing buckles for each load passage and this would not be a recommended load level for the serviceability limit state in launching situations. After three passages the remaining maximum amplitude of the lateral deformation have grown from the initial 6 mm to 8 mm, which is no large buckle and it can be discussed if the girder behaviour will change due to that. However, the buckle will probably keep on growing if the girder is subjected to additional load passages and then it might be more critical.

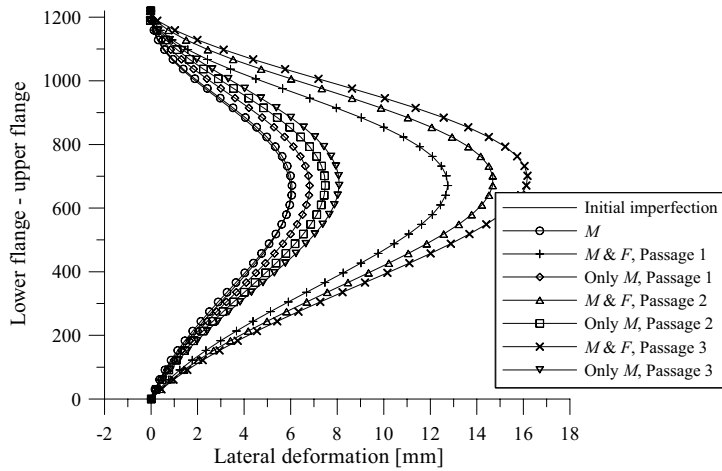


Figure 6.9 Lateral deformation of the web at mid-length section for SLS100b. Load level used in the analysis was $0,60F_{u,FE}$.

Also for the load level in SLS100c, i.e. $0,55F_{u,FE}$, the remaining buckle are increasing even though the increase is smaller compared to SLS100b, only around 0,6 mm after three passages. Still, plastic strains are produced during the loading, which is not suitable. When the load level was decreased further as in SLS100d no plastic strains were developed and the remaining lateral deformations of the web were constant after each new load passage, see Figure 6.10. Hence, it was concluded that this was an appropriate load level that keeps the deformations in the elastic range.

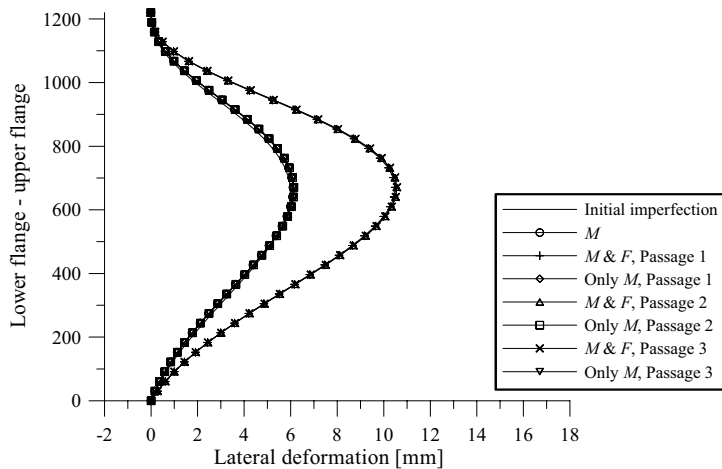


Figure 6.10 Lateral deformation of the web at mid-length section for SLS100d. Load level used in the analysis was $0,50F_{u,FE}$.

When the web slenderness was increased to $h_w/t_w = 150$, i.e. *SLS150*, the relative load level could be increased compared to *SLS100*, without development of plastic strains and the remaining buckle stayed constant for every new load passage. The fact that *SLS150* could resist a higher relative load level was expected due to the higher slenderness. This means that at ultimate load the *SLS150* will fail at a lower stress level compared to the yield strength of the web material. Considering *SLS100* on the other hand the stresses in the web will get higher and plastic deformations will develop earlier in relation to the ultimate load compared to *SLS150* and therefore the relative load level is lower.

Figure 6.11 show how the buckles develop at mid-length for the *SLS150d* girder, i.e. with a load level of $0,68F_{u,FE}$. *SLS150e* shows the same behaviour as *SLS150d*, which indicates that this load level is adequate also for higher bending moments. Regarding Figure 6.11 the behaviour is satisfactory and not unexpectedly the size of the lateral deformations were larger compared to the *SLS100* girder. The small difference in lateral deformation when the loading plate was situated approximately at mid-length of the section, the curves with both *M* and *F* in Figure 6.11, is explained by the fact that the position of the loading plate was not exactly the same. However, the lateral deformations when the girder is unloaded, i.e. only loaded with the applied constant bending moment, are constant and not increasing after several load passages.

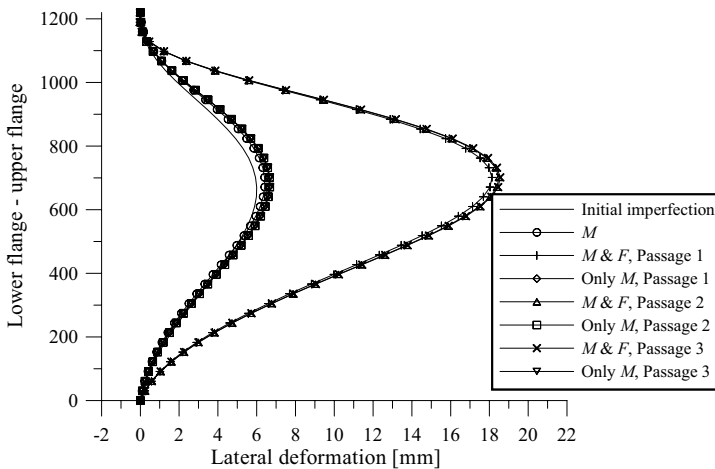


Figure 6.11 Lateral deformation of the web at mid-length section for *SLS150d*. Load level used in the analysis was $0,68F_{u,FE}$.

In order to limit the size of this Section the outcome of the other analyses are not shown in figures, only in tables. Regarding the large scale girders, they have the same behaviour as their corresponding smaller girders. Further, it should be mentioned that the different load levels were chosen by trial and error, i.e. if it was concluded that a level was too high it was changed to a lower until the residual deformation stayed constant. This means that there might be a level in between the one that was established as appropriate and the slightly higher level that was not

acceptable. However, these FE-analyses are very time consuming and further studies are needed for a more exact level but the levels presented here are on the safe side. It would also be interesting to verify the results with experimental tests.

6.4 Proposed criteria for bridge launching

The aim with this study was to find a criterion that can be used when a bridge girder is launched into position. The criterion proposed here works when the load is travelling along the girder but would also work for a stationary load, i.e. a load that are only introduced at mid-span without any horizontal movements. For the latter case it would be on the safe side. This conclusion is based on simulations performed with a stationary load applied and removed three times, similar to the procedure described for the travelling load simulations. This was only carried out for the *SLS100* and *SLS150*, but both girders could carry higher loads without increase of the remaining lateral web deformations. Hence, it was concluded that a moving load is worse compared to a stationary load, in terms of residual deformations.

As can be seen in the literature review on serviceability limit state for patch loading, Section 2.4, not many references can be found in this area. The only actual criterion found was the one presented by Granath (2000), see Equations (2.123) - (2.126).

The basic serviceability requirement is that the behaviour should be repeatable and therefore it is proposed here that the membrane strains should be elastic. This limit criterion makes sure that the growth of the lateral web deformations is limited and will be constant even for repeated travelling loads. The main idea was to keep the serviceability criterion as simple as possible and therefore a basic equation is proposed according to

$$F_{R,sls} = \chi_{F,sls}(\bar{\lambda}_F) \cdot F_R \quad (6.3)$$

in which $\chi_{F,sls}(\bar{\lambda}_F)$ is a function that reduces the resistance compared to the earlier proposed ultimate resistance, F_R . In other words, instead of developing a completely different expression for $F_{R,sls}$ that includes all variables that is related to the resistance as in Granath (2000), those variables are taken into account by F_R and only the slenderness, $\bar{\lambda}_F$, will govern the relation between $F_{R,sls}$ and F_R .

The data from the numerical study on girder sections subjected to a travelling repeated load serves as a basis for the calibration of $\chi_{F,sls}(\bar{\lambda}_F)$. Table 6.4 shows $\bar{\lambda}_F$ and the final acceptable load levels, $F_{FE,sls}$, in relation to $F_{u,FE}$ and the proposed F_R for the different sections.

Table 6.4 Slenderness and relation between $F_{FE,sls}/F_{u,FE}$ and $F_{FE,sls}/F_R$ for different girder sections.

Label	$\bar{\lambda}_F$	$F_{FE,sls}/F_{u,FE}$	$F_{FE,sls}/F_R$
<i>SLS80b</i>	0,863	0,42	0,51
<i>SLS80a-w8</i>	1,14	0,50	0,62
<i>SLS80b-F40</i>	0,973	0,42	0,51
<i>SLS100d</i>	1,11	0,50	0,65
<i>SLS100a-F30</i>	1,26	0,50	0,64
<i>SLS100c-F40</i>	1,38	0,54	0,66
<i>SLS100d-w8</i>	1,46	0,60	0,78
<i>SLS100a-LS</i>	1,11	0,50	0,64
<i>SLS125a</i>	1,43	0,60	0,81
<i>SLS150d</i>	1,75	0,68	0,96
<i>SLS150a-LS</i>	1,76	0,66	0,94
<i>SLS175c</i>	2,09	0,72	1,05
<i>SLS200b</i>	2,43	0,72	1,09

One fact to consider in the serviceability limit state is that the design load is 1,0g whereas for the ultimate limit state it is 1,35g, which gives the ratio 0,74 between the loads at SLS and ULS respectively. Furthermore, the serviceability criterion do not need the same safety margin as in the ultimate limit state and therefore, $\chi_{F,sls}(\bar{\lambda}_F)$ will be evaluated against F_R and not $F_{u,FE}$. This means that a check in the ultimate limit state should be sufficient for all cases where the relative load level, $F_{FE,sls}/F_R$, is above 0,74. However, as the partial factors for the design loads might change in the codes the criterion proposed here will not be limited to 0,74. Instead, $F_{R,sls}$ is limited to never exceed F_R .

A simple linear format of $\chi_{F,sls}(\bar{\lambda}_F)$ according to Equation (6.4) fits rather well to the results as can be seen in Figure 6.12 where $F_{FE,sls}/F_R$ as a function of $\bar{\lambda}_F$ are shown together with Equation (6.4).

$$\chi_{F,sls}(\bar{\lambda}_F) = 0,05 + 0,44 \cdot \bar{\lambda}_F \leq 1 \tag{6.4}$$

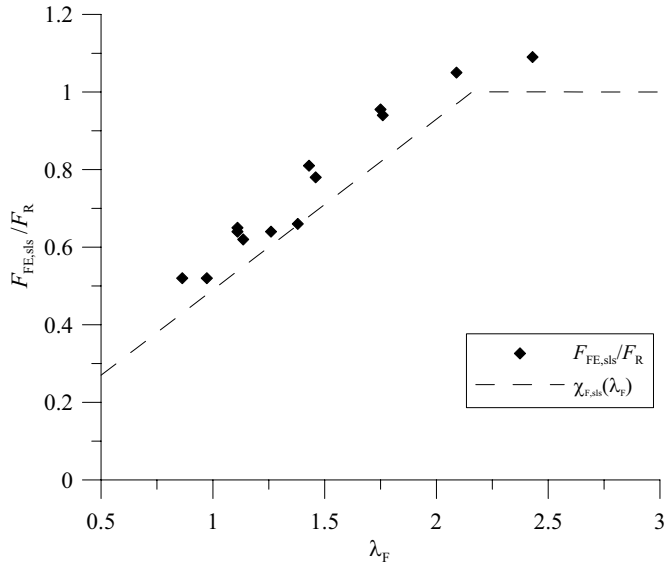


Figure 6.12 $F_{FE,sls}/F_R$ as a function of $\bar{\lambda}_F$ together with Equation (6.4).

The proposed serviceability criterion is only calibrated against FE-analyses and must therefore be seen as somewhat preliminary. A verification against experimental data would be valuable but there are no data available. Moreover, the criterion is based on FE-analyses with only one type and size of loading plate or launching shoe, i.e. a flat plate. However, it is assumed that different loaded lengths, s_{sl} , could be handled by F_R . Further, it is common that the launching shoe is curved with a very large radius to better fit to the deformations of the loaded flange, especially when large girders are launched and the loads are high and one way to limit the concentrated forces from the launching shoe is to increase its length, i.e. s_{sl} . If a very stiff, long and flat launching shoe is used, the girder might rest only on the edges of the shoe and then instead of a long distributed load it will turn into two very concentrated forces and that is not desirable. On the other hand, the plate used in the study herein was not that stiff, 40 mm thick and material properties corresponding to a mild steel with $f_y = 235$ MPa. Furthermore, the load corresponds to a line load at the mid-line of the loading plate, as shown in Figure 6.8. This means that the loading plate could deform to fit the deformations of the flange. In addition, when studying the stress pattern in the web directly under the load plate the largest vertical stresses were concentrated under the middle of the plate, i.e. there were no signs of stress concentrations in the web under the edges of the plate.

In Figure 6.13 $F_{R,sls}$ proposed herein according to Equations (6.3) and (6.4) are compared to the acceptable load levels from the FE-analyses, $F_{FE,sls}$. In addition the criterion proposed by Granath (2000) is shown as well. The trend considering the proposal by Granath is not

satisfactory with an average of $m = 1,19$ and a coefficient of variation of $V = 0,23$. The proposed criterion gives a better prediction with $m = 1,13$ and $V = 0,057$.

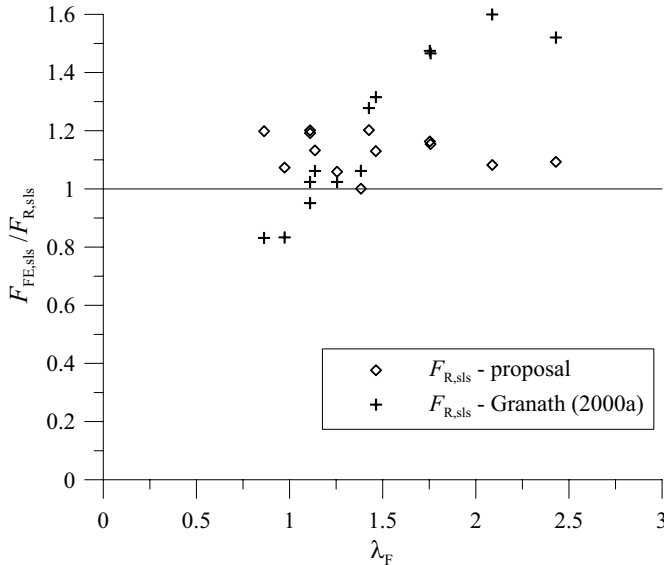


Figure 6.13 Comparison between the serviceability criterion proposed herein and the one proposed by Granath (2000).

6.5 Concluding remarks

It is believed that the proposed serviceability criterion can serve as a useful tool for the designer. The criterion is based on a number of realistic FE-analyses with a travelling patch load. The parameters varied in the analyses were; h_w , t_w , t_f , M_E and of course the load level. The overall geometry was chosen to fit with the tests performed in this thesis in order to make it possible to verify the FE-model in terms of element size and boundary conditions. Further, the launching shoe/loading plate was included in the FE-model instead of directly apply the load as concentrated forces in the nodes of the flange as in Granath et al. (2000). This difference gave the flange the opportunity to rotate without restraint when the loading plate has passed except at the ends of the section. Under the loading plate, when loaded, the flange is forced to be horizontal. In the simulations performed by Granath et al. with travelling loads it is not clear how the rotational constraint of the flange was dealt with. However, the approach used herein is the most realistic in the author’s opinion.

The requirement for the serviceability criterion proposed was to limit the remaining lateral deformations of the web, which corresponds to the criteria of only allowing elastic membrane strains in the web. After launching, when the bridge is in position, the girder section will presumably not be subjected to any concentrated forces. Instead, depending on position in the bridge it will be subjected to sagging or hogging bending moments and shear forces. From the

criterion proposed herein, not allowing plastic membrane strains, it follows that the web depth is kept and hence, the section modulus W is not affected.

In general, when it comes to a real launching, if the distance between the supports are equal it is possible to decrease the support reaction and the bending moment during launching through the length of the launching nose. Nevertheless, if the supports are unevenly distributed this is not always possible but in this case it is not likely that some section of the bridge girder are in the worst position in every new span. Hence, every bridge launching depends on the conditions at site and must be evaluated by the designer. The criterion proposed here can be used in either case and always on the safe side but might be conservative for some cases.

One thing that definitely could be of interest to study a little further is how different loaded lengths affect the serviceability limit state. Herein it was assumed that the variation in s_g was taken care of by F_R , which is a fair assumption but it could be worth to investigate further.

Further, it is always desirable to have experimental results for verification of numerical simulations. It would be very interesting to perform some tests on small girders with a travelling load.

7 DISCUSSION AND CONCLUSIONS

7.1 Discussion

The ultimate resistance of girders subjected to patch loading has drawn attention from many different researchers all over the world as can be seen in the literature review in Section 2.3, where only a part of the total amount of published research is presented. Further, it was early established that the web thickness is the most important parameter for the resistance. Most of the resistance models presented are divided into two criteria, one for yielding and one for buckling of the web although the test results do not show any clear distinction between those two. The work presented by Lagerqvist (1994) was a step forward on this point because the resistance model proposed included only one check independent of cross section. The resistance model proposed by Lagerqvist was harmonized with the approach for other buckling problems including a yield resistance F_y , a critical buckling load F_{cr} that together with F_y gave the slenderness $\bar{\lambda}_F$ and finally, a reduction factor that relates F_y to F_R . This approach gives a smooth and continuous transition from yielding to buckling. However, in the design model in EN 1993-1-5 (2006) it was decided to slightly modify the model by Lagerqvist both with respect to the yield resistance and the reduction factor. The first change does unfortunately create a discontinuity in the resistance because the yield resistance when $\bar{\lambda}_F$ is below 0,5 is smaller compared to the yield resistance when $\bar{\lambda}_F$ is above 0,5. This means that according to EN 1993-1-5 a section with $\bar{\lambda}_F = 0,49$ might have a lower resistance compared with a section with $\bar{\lambda}_F = 0,51$ even though the latter has a reduction factor below 1 multiplied with the yield resistance. The second change, considering the reduction factor, creates a bias for underprediction with increasing slenderness, see Figure 5.12.

The resistance model in ultimate limit state proposed here is a continuation and modification of the work presented by Lagerqvist (1994). The assumption that a part of the web contributes to the plastic moment resistance of the outer hinges in the flange could not be verified by the numerical investigation considering the yield resistance. This supports the conclusion by Davaine et al. (2004) who, based on a numerical study of typical bridge girders, suggested that the parameter m_2 should be set to zero. The consequence of $m_2 = 0$ is that the yield resistance will decrease and subsequently that a new calibration of the reduction factor is needed. The new reduction factor proposed herein is based on the format used by Müller (2003) who intended to establish a general reduction factor that should work for all different plate buckling problems. This approach was later included in Annex B in EN 1993-1-5 (2006). However, the original curve by Müller with the imperfection factor $\alpha = 0,34$ and the plateau length $\bar{\lambda}_0 = 0,8$ might give

an overestimation of the patch loading resistance, in the slenderness range between 0,7 and 2,5 according to Figure 7.1. Instead, the best fit to the test results available is obtained with $\alpha = 0,5$ and $\bar{\lambda}_0 = 0,6$. Further, it is shown by the test results on stocky girder webs that the ultimate load is clearly higher than the yield resistance and hence, it is proposed to allow the reduction factor to continue up to 1,2. Moreover, as the yield resistance was changed and proposed to be determined equally for all $\bar{\lambda}_F$, the discontinuity in EN 1993-1-5 is removed.

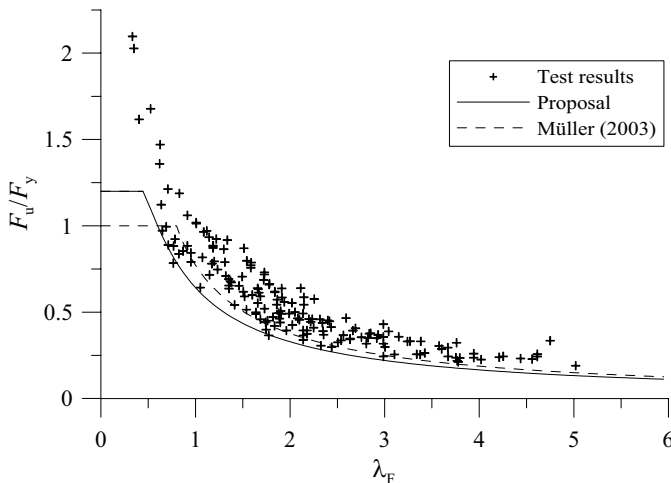


Figure 7.1 Comparison of the herein proposed reduction factor and the reduction factor by Müller (2003) together with test results.

As the derivation of the reduction factor is empirical it is important to check if the essential parameters are reasonably represented by the proposed design model. In Appendix D and in Section 5.3 such checks are displayed but they showed no significant bias. However, the design procedure proposed still show a substantial scatter even though it is less compared to the existing procedure in EN 1993-1-5. One thing that affects the accuracy of the procedure is that the test results are taken from many different sources and put together in one data base. This may end up in systematic differences, for example different methods for evaluating the yield strength or if one girder is used for more than one test, e.g. tests on both flanges.

Clarín (2007) carried out a study on plate buckling, including both local buckling and patch loading of longitudinally stiffened girder webs. The study shows that the herein proposed reduction factor fits well also for the case with longitudinal stiffeners. Further, Clarín (2007) also show that the test results considering local buckling both performed by Clarín (2004) and by others seems to fit to this reduction factor as well. However, it should be noted that the stub column tests generally used for tests regarding local buckling, usually contains large welds compared to bridge girders. That might influence the results, as the residual stress distribution will be more significant compared to e.g. bridge girders where the welds are very small compared to the plates.

The study herein also contains tests and numerical analyses of the influence from the loaded length on the patch loading resistance. This is important for bridge launching because the simplest way to increase the resistance is to increase the length of the launching shoe. ENV 1993-1-1 (1992) had a limitation that s_s/h_w should not be taken as larger than 0,2 while the rules in EN 1993-1-5 (2006) had a limitation of 1. The results in this thesis indicates that this limit can be increased further, at least up to 1,2. There is though a lack of test data with such long loaded lengths and it would therefore be very interesting to perform a numerical investigation verified by tests on girders with for example $a/h_w = 4$ and s_s up to $3h_w$. Such investigation could provide information regarding failure mode and if it still corresponds to a patch loading failure or if column like behaviour will occur, which might significantly reduce the resistance.

Considering the few tests with $s_s = a$, they do not show any significant difference in resistance compared to the tests with shorter loaded lengths. However, they are in the high end of the scatter, which indicates that the resistance model for patch loading, with the mechanism model as basis, can be used on the safe side also for this type of loading, even though it can be discussed whether it is a patch load or not.

When it comes to steel bridge girders, the problem concerning patch loading resistance occurs during launching of the girder. Further, bridge launching involves a travelling concentrated load from the launching shoe, which can be repeated several times for each section depending on length and number of supports. As these concentrated forces can be of the magnitude that governs the web thickness it would be desirable to have a criterion in the serviceability limit state. The only criterion found in the literature is the one proposed by Granath (2000), which is based on stationary loadings and the limit criterion was that the effective stress on the web surface is not allowed to pass the yield strength of the material. This seems a bit conservative since bending of the web might give stresses of the magnitude of the yield stress while the membrane stresses still are below the yield strength, which would give a reversible behaviour. However, as can be seen in Figure 6.13 the proposal by Granath overestimates the resistance in some cases, which is explained by the fact that the serviceability criterion was based on stationary loadings.

The serviceability criterion herein is instead formulated such that no effective plastic membrane strains are allowed in the web. From the results of the FE-analyses presented in this thesis this was found as a suitable criterion which gave no increasing buckles in the web. Further, the criterion proposed herein is based on realistic FE-analyses performed in several steps using contact surfaces in between the loading plate and the loaded flange. The loading plate is travelling along the girder from one side to the other three times in order to verify whether the lateral deformations of the web are increasing after each passage or not.

A total of 13 different girder sections were analysed to find a load level $F_{FE,sls}$ that gives reversible behaviour. It was found from these analyses that the acceptable load levels did follow

the slenderness, $\bar{\lambda}_F$, of the sections so that for low $\bar{\lambda}_F$ the load level was significantly lower than the design resistance in ultimate limit state, F_R , but for higher $\bar{\lambda}_F$ the difference was not as large. With this in mind a simple criterion is proposed based on F_R multiplied with a function $\chi_{F,sls}(\bar{\lambda}_F)$, i.e. instead of developing a completely different expression for $F_{R,sls}$ that includes all variables that is related to the resistance, those are taken into account by F_R and only $\bar{\lambda}_F$ will govern the relation between $F_{R,sls}$ and F_R . This seems like a fair assumption but there are still questions that need some further studies, e.g. the influence from different loaded lengths was not investigated even though it is assumed to be covered by F_R .

Further, the proposed criterion considering the serviceability limit state are only based on numerical results and it is always desirable to have experimental results for verification of the model. It would be very interesting to perform some tests for verification of the model on small girders with a travelling load passing a few times over the girder.

The serviceability criterion proposed here was developed to fit the results from FE-analyses on girders subjected to travelling patch loading. However, it was found that travelling loads are worse compared to stationary loads when it comes to remaining lateral deformations of the web, i.e. the criterion can be used for stationary loadings as well though it will be conservative for such cases.

7.2 Conclusions

The following conclusions are drawn from the work presented:

- The three patch loading tests with varied loaded length was conducted successfully and falls in the middle of the scatter if compared to other tests found in the literature.
- The numerical calibration versus tests show good agreement with respect to deformations and ultimate load. The parametric study performed with the same FE-model together with the test results supports the definition of the loaded length in EN 1993-1-5 (2006), i.e. for more than one loading plate the centre-to-centre distance between the outer plates plus the load spread through the plates should be used as s_g .
- The numerical study considering the yield resistance clearly implies that the contribution from the web to the bending moment resistance of the outer plastic hinges in the mechanism model should be neglected. This means that the yield resistance should be determined as in EN 1993-1-5 but with the parameter m_2 set to zero, i.e. according to the model proposed by Roberts and Newark (1997) for direct yielding.
- The proposed design procedure, with a reduction factor in the same format as used by Müller (2003), gives a prediction of the ultimate load from tests with less scatter compared to the design model implemented in EN 1993-1-5.
- Based on the statistical evaluation of the proposed design procedure according to Annex D of EN 1990 (2002) the partial safety factor $\gamma_{M1} = 1,0$ is proposed.
- The simple serviceability limit state criterion developed for bridge launching fits well to the FE-results and should work as a useful tool for the bridge designer.

7.3 Future work

During the work with this thesis a number of questions have appeared. It was stated herein that no signs indicates that the limitation in EN 1993-1-5 for s_s/h_w is insufficient, at least not for the available test results and FE-results. Instead, the results show that the limit could be somewhat increased. However, there are no tests or FE-analyses, known by the author, that really can support that no limitation is needed. For this it would be interesting to perform FE-analyses and tests with larger aspect ratios and longer loaded lengths. For instance, $a/h_w = 4$ and an s_s from h_w to $3h_w$, which could serve as basis for new conclusions considering this matter, i.e. if the usual buckling pattern will turn into column like behaviour or not.

Further, the knowledge considering the influence from bending moment on the patch loading resistance could definitely be improved. For this a test serie covering the entire interaction surface would be beneficial. As it looks today the interaction formulas are very influenced by what design models that are used.

The design procedure proposed herein for patch loading needs to be verified also considering opposite and end patch loading. However, there is a lack of test data considering opposite patch loading on welded girders in the literature, which would be valuable for such evaluation. Further, also rolled sections should be included in the design procedure.

Considering the serviceability limit state there are a need for some further investigations. It would be very interesting to verify the FE-analyses with some tests with travelling loads. This is a challenge but it should be possible to perform such tests on small girders with a load travelling over a few supports. Further, the FE-analyses carried out in this thesis were performed with a constant loaded length. This matter could be studied with a few analyses using different lengths on the loading plate for verification of the proposed serviceability limit criterion.

REFERENCES

- ABAQUS (2006). *ABAQUS Standard User's Manual*, ver. 6.6, ABAQUS, Inc.
- Bergfelt, A. and Hövik, J. (1968). Thin-walled deep plate girders under static loads, Final report, *IABSE Congress*, New York, 465-477
- Bergfelt, A. (1971). Studies and tests on slender plate girders without stiffeners - Shear strength and local web crippling, *Proceedings, IABSE Colloquium, London*, 67-83
- Bergfelt, A. (1976). The behaviour and design of slender webs under partial edge loading, *International conference on steel plated structures*, Dowling, P. J., Harding, J. E., Frieze, P. A., eds., Imperial College, London, Crosby Lockwood Staples, 486-502
- Bergfelt, A. (1979). *Patch loading on a slender web - Influence of horizontal and vertical web stiffeners on the load carrying capacity*, Chalmers University of Technology, Dept. of Structural Engineering, Div. of Steel and Timber Structures, publ. S 79:1, Göteborg
- Bergfelt, A. (1983). *Girder web stiffening for patch loading*, Chalmers University of Technology, Dept. of Structural Engineering, Div. of Steel and Timber Structures, publ. S 83:1, Göteborg
- Bergholtz, A. (1994). *Lansering av brobalkar av stål - Lokal intryckning över stöd*, publ. S 94:7, Avd. för Stål- och Träbyggnad, Chalmers tekniska högskola, Göteborg
- Bossert, T. W. and Ostapenko, A. (1967). *Buckling and ultimate loads for plate girder web plates under edge loading*, Report No. 319.1, Fritz Engineering Laboratory, Dept. of Civil Engineering, Lehigh University, Bethlehem, Pa.
- BSK 99 (1999). *Boverkets handbok om stålkonstruktioner* (The Swedish design code for steel structures), Boverket, Sweden
- Carolin, A., Olofsson, T. and Täljsten, B. (2004). Photographic strain monitoring for Civil Engineering, *The second International Conference on FRP Composites in Civil Engineering*, Adelaide, Australia
- Clarín, M. (2004). *High Strength Steel - Local buckling and residual stresses*, Licentiate thesis 2004:54, Luleå University of Technology, ISRN: LTU-LIC--04/54--SE
- Clarín, M. (2007). *Plate buckling resistance - Patch loading of longitudinally stiffened webs and local buckling*, Doctoral thesis 2007:31, Luleå University of Technology, ISRN: LTU-DT--07/31--SE
- ComBri (2007). *Competitive Steel and Composite Bridges by Improved Steel Plated Structures, Final Report*, RFCS Contract No. RFS-CR-03018

- Davaine, L., Raoul, J. and Aribert, J. M. (2004). Patch load resistance of longitudinally stiffened bridge girder, *Steelbridge 2004, International Symposium on Steel Bridges*, Millau, France
- Davaine, L. and Aribert, J. M. (2005). Launching of steel girder bridge, *Proceedings of the fourth European conference on Steel and Composite Structures, Eurosteel 2005*, Maastricht, Netherlands
- Drdacky, M. and Novotny, R. (1977). Partial edge load-carrying capacity tests of thick plate girder webs, *Acta Technica CSAV*, **87**, 614-620
- Drdacky, M. (1986). Limit states of steel plate girder webs under patch loading, *Proceedings, Regional Colloquium on Stability of Steel Structures*, Ivanyi M. ed., Tihany, Hungary, 687-694
- Edlund, B. (1988). Buckling and failure modes in slender plate girders under patch loading, *Der Metallbau im Konstruktiven-Ingenieurbau (K-I)*, Karlsruhe, Germany, 461-469
- Elgaaly, M. (1983). Web design under compressive edge loads, *Engineering Journal*, AISC, **20**, 4th Q., 153-171
- EN 1990 (2002). *Eurocode - Basis of structural design*, CEN, European Committee for Standardization, Brussels, Belgium
- EN 1993-1-1 (2005). *Eurocode 3: Design of steel structures, Part 1.1: General rules and rules for buildings*, CEN, European Committee for Standardization, Brussels, Belgium
- EN 1993-1-5 (2006). *Eurocode 3: Design of steel structures, Part 1.5: Plated structural elements*, CEN, European Committee for Standardization, Brussels, Belgium
- EN 1993-2 (2003). *Eurocode 3: Design of steel structures, Part 2: Steel bridges*, CEN, European Committee for Standardization, Brussels, Belgium
- EUR 20344 EN (2002). *Partial safety factors for resistance of steel elements to EC3 and EC4 - Calibration of various steel products and failure criteria, Final report*, European Commission, Luxembourg
- Galéa, Y. and Martin, P. O. (2006). EBPlate - Elastic buckling of plates: Presentation manual of EBPlate, *RFCS contract RFCS-CR-03018, ComBri-Report- CTICM-005*, CTICM, France
- Gozzi, J., Olsson, A. and Talja, A. (2004). Cold-formed stainless steel profiles subjected to bending and concentrated forces - Test results, numerical modelling and design guidance, *Proceedings of the 10th Nordic Steel Construction Conference*, Copenhagen, Denmark
- Graciano, C. and Johansson, B. (2003). Resistance of longitudinally stiffened I-girders subjected to concentrated loads, *Journal of Constructional Steel Research*, **59**, 561-586
- Granath, P. (1998). Distribution of support reaction against a steel girder on a launching shoe, *Journal of Constructional Steel Research*, **47**, 245-270

-
- Granath, P. (2000). Serviceability limit state of I-shaped steel girders subjected to patch loading, *Journal of Constructional Steel Research*, **54**, 387-408
- Granath, P., Thorsson, A. and Edlund, B. (2000). I-shaped steel girders subjected to bending moment and travelling patch loading, *Journal of Constructional Steel Research*, **54**, 409-421
- Granholm, C. A. (1960). *Tests on girders with extremely thin web plates* (in Swedish), Report 202, Inst. för Byggnadsteknik, Göteborg
- Herzog, M. A. M. (1986). Die Krüppellast von Blechträger- und Walzprofilstegen, *Stahlbau*, **55**(3), 87-88
- Herzog, M. A. M. (1992). Web crippling with bending and shear of thin-walled plate girders, *Journal of Constructional Steel Research*, **22**, 87-97
- Johansson, B. and Lagerqvist, O. (1995). Resistance of plate edges to concentrated forces, *Journal of Constructional Steel Research*, **32**, 69-105
- Johansson, B., Maquoi, R. and Sedlacek, G. (2001). New design rules for plated structures in Eurocode 3, *Journal of Constructional Steel Research*, **57**, 279-311
- von Kármán, T., Sechler, E. E. and Donnel, L. H. (1932). The strength of thin plates in compression, *Transactions ASME*, APM 54-5, 53-57
- Khan, M. Z. and Walker, A. C. (1972). Buckling of plates subjected to localized edge loading, *The Structural Engineer*, **50**, No. 6, June, 225-232
- Khan, M. Z. and Johns, K. C. (1975). Buckling of web plates under combined loadings, *Journal of the Structural Division*, Proceedings, ASCE, **101**, No. ST10, October, 2079-2092
- Khan, M. Z., Johns, K. C. and Hayman, B. (1977). Buckling of plates with partially loaded edges, *Journal of the Structural Division*, Proceedings, ASCE, **103**, No. ST3, March, 547-558
- Kuhlmann, U. and Seitz, M. (2004). Longitudinally stiffened girder webs subjected to patch loading, *Steelbridge 2004, International Symposium on Steel Bridges*, Millau, France
- Kuhlmann, U. and Braun, B. (2007). Combined Shear- and Patch Loading: Numerical studies and development of an interaction equation, *RFCS contract RFCS-CR-03018, ComBri-Report-USTUTT-002*, Universität Stuttgart, Germany
- Kutmanová, I. and Skaloud, M. (1992). Ultimate limit state of slender steel webs subjected to (i) constant and (ii) repeated partial edge loading, *Journal of Constructional Steel Research*, **21**, 147-162
- Lagerqvist, O. (1994). *Patch loading - Resistance of steel girders subjected to concentrated forces*, Doctoral thesis 1994:159D, Luleå University of Technology, ISRN: HLU-TH-T-159-D--SE
- Lagerqvist, O. and Johansson, B. (1996). Resistance of I-girders to Concentrated loads, *Journal of Constructional Steel Research*, **39**, 87-119

- Lääne, A. (2003). *Post-critical behaviour of composite bridges under negative moment and shear*, Thesis no. 2889(2003), Lausanne EPFL, Switzerland
- Maquoi, R. and Rondal, J. (1986). From thick to thin or from thin to thick?, *Proceedings IABSE Colloquium, Thin-Walled Metal Structures in Buildings*, Stockholm
- Müller, C. (2003). *Zum Nachweis ebener Tragwerke aus Stahl gegen seitliches Ausweichen*, Stahlbau, RWTH Aachen, Heft 47, ISBN 3-8322-1574-3
- Novak, P. and Skaloud, M. (1973). Incremental collapse of thin webs subjected to cyclic concentrated loads, *Preliminary report, IABSE symposium*, Lisbon, 179-184
- Olsson, A. (2001). *Stainless Steel Plasticity -Material modelling and structural applications-*, Doctoral thesis 2001:19, Luleå University of Technology, ISRN: LTU-DT--01/19--SE
- Raoul, J., Schaller, I. and Theillout, J. -N. (1990). Tests of buckling of panels subjected to in-plane patch loading, *Proceedings, Contact Loading and Local Effects in Thin-walled Structures, IUTAM symposium*, Prague, 173-183
- Raoul, J., Spinassas, I. and Virlogeux, M. (1991). Étude par éléments finis d'une âme soumise à une charge locale dans son plan, *Construction Metallique*, No. 1, 29-40
- Raoul, J. and Davaine, L. (2006). I-girder launching: Influence of load eccentricity, *RFCS contract RFCS-CR-03018, ComBri-Report- SETRA-001*, SETRA, France
- Ren, T. and Tong, G. S. (2005). Elastic buckling of web plates in I-girders under patch and wheel loading, *Engineering Structures*, **27**, 1528-1536
- Roberts, T. M. and Rockey, K. C. (1978). Méthod pour prédire la charge de ruine d'une poutre a ame mince soumise a une charge simi-répartie dans le plan de l'ame, *Construction Metallique*, No. 3, 3-13
- Roberts, T. M. and Rockey, K. C. (1979). A mechanism solution for predicting the collapse loads of slender plate girders when subjected to in-plane patch loading, *Proc. Instn Civ. Engrs*, Part 2, **67**, 155-175
- Roberts, T. M. (1981). Slender plate girders subjected to edge loading, *Proc. Instn Civ. Engrs*, Part 2, **71**, 805-819
- Roberts, T. M. and Chong, C. K. (1981). Collapse of plate girders under edge loading, *ASCE, Jour. Struct. Div.*, ST8, **107**, 1503-1509
- Roberts, T. M. and Markovic, N. (1983). Stocky plate girders subjected to edge loading, *Proc. Instn Civ. Engrs*, Part 2, **75**, 539-550
- Roberts, T. M. and Coric, B. (1988). Collapse of plate girders subjected to patch loading, *Miscellany Dedicated to the 65th Birthday of Academician Professor Dr. Nicola Hajdin, N. Naerlovic-Veljkovic ed.*, University of Belgrade, Belgrade, 203-209
- Roberts, T. M. and Newark, A. C. B. (1997). Strength of webs subjected to compressive edge loading, *Journal of Structural Engineering*, **123**(2), 176-183

-
- Rockey, K. C. and Bagchi, D. K. (1970). Buckling of plate girder webs under partial edge loadings, *International Journal of Mechanical Science*, **12**, 61-76
- Rockey, K. C. and El-Gaaly, M. A. (1971). Ultimate strength of plates when subjected to in-plane patch loading, *Proceedings, IABSE Colloquium*, London, 401-407
- Shahabian, F. and Roberts, T. M. (1999). Buckling of slender web plates subjected to combinations of in-plane loading, *Journal of Constructional Steel Research*, **51**, 99-121
- Shahabian, F. and Roberts, T. M. (2000). Combined Shear-and-Patch loading of plate girders, *Journal of Structural engineering*, **126**(3), 316-321
- Shimizu, S., Yabana, H. and Yoshida, S. (1989). A new collapse model for patch-loaded web plates, *Journal of Constructional Steel Research*, **13**, 61-73
- Skaloud, M. and Novak, P. (1972). Post-buckling behaviour and incremental collapse of webs subjected to concentrated loads, *Proceedings, IABSE, 9th Congress*, Amsterdam, 101-110
- Skaloud, M. and Drdacky, M. (1975). Ultimate load design of webs of steel plated structures - Part 3 Webs under concentrated loads (in Czech), *Staveb. Casopis*, **23**, C3, Veda Bratislava, 140-160
- Spinassas, I., Raoul, J. and Virlogeux, M. (1990). Parametric study on plate girders subjected to patch loading, *Proceedings, Contact Loading and Local Effects in Thin-walled Structures, IUTAM symposium*, Prague, 192-203
- Tryland, T., Hopperstad, O. S. and Langseth, M. (1999). Steel girders subjected to concentrated loading - Validation of numerical simulations, *Journal of Constructional Steel Research*, **50**, 199-216
- Ungermann, D. (1990). *Bemessungsverfahren für vollwand- und kastenträger unter besonderer berücksichtigung des stegverhaltens*, Stahlbau, RWTH Aachen, Heft 17, ISSN 0722-1037
- Unosson, E. (2003). *Patch loading of stainless steel girders - Experiments and finite element analyses*, Licentiate thesis 2003:12, Luleå University of Technology, ISRN: LTU-LIC-03/12--SE
- Veljkovic, M. and Johansson, B. (2001). Design for buckling of plates due to direct stress, *Proceedings of the 9th Nordic Steel Construction Conference*, Helsinki, Finland
- Winter, G. (1947). Strength of thin steel compression flanges, *Transactions ASCE*, **112**, 527-544
- Zetlin, L. (1955). Elastic instability of flat plates subjected to partial edge loads, *Proceedings, ASCE, Vol. 81, Separate paper No. 795*, 1-24
- Zoetemeijer, P. (1980). *The influence of normal-, bending- and shear stresses on the ultimate compression force exerted laterally to European rolled sections*, Report 6-80-5, Facultiet der Civiele Techniek, Technische Universiteit Delft, Delft

APPENDIX A UNIAXIAL COUPON TESTS

Specimens were taken in both the rolling and the transverse direction. All uniaxial tests were performed under deformation control. The small notch in the curves, in the strain hardening stage, come from a speed change during testing. Stresses are engineering stresses. The results from the uniaxial tests are presented in Table A.1 and Figure A.1 - Figure A.4.

Table A.1 Results from the uniaxial coupon tests. L - rolling direction and T - transverse direction. F - flange and stiffener material and W - web material.

Test	f_y [MPa]	f_u [MPa]	A_5 [%]	mean f_y	mean f_u
F20L1	360	519	42	354	519
F20L2	349	521	41		
F20L3	354	518	41		
F20T1	356	521	40	354	521
F20T2	352	520	40		
F20T3	355	522	41		
W6L1	375	541	30	371	542
W6L2	369	541	29		
W6L3	369	544	30		
W6T1	395	542	29	394	543
W6T2	395	544	29		
W6T3	393	545	29		

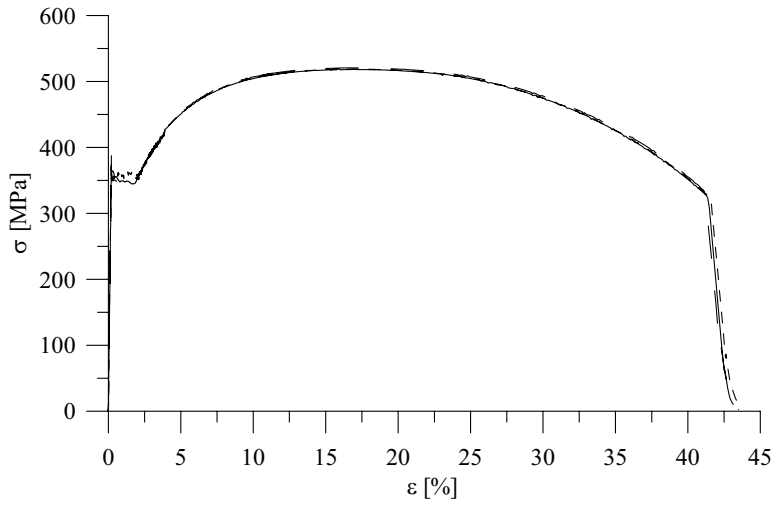


Figure A.1 Stress - strain relation for the three tests on 20 mm thick material along the rolling direction, F20L1-3.

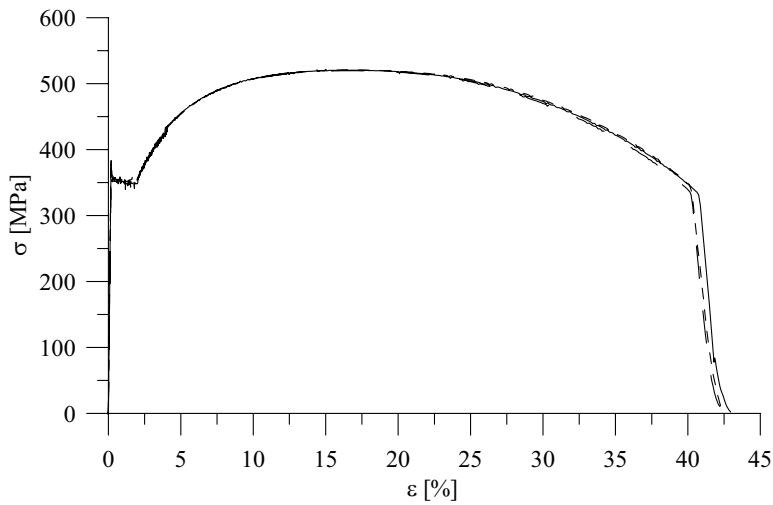


Figure A.2 Stress - strain relation for the three tests on 20 mm thick material transverse the rolling direction, F20T1-3.

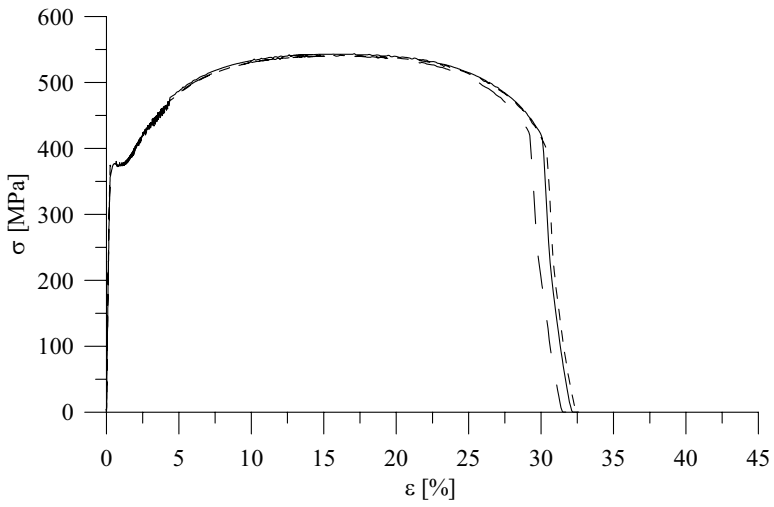


Figure A.3 Stress - strain relation for the three tests on 6 mm thick material along the rolling direction, W6L1-3.

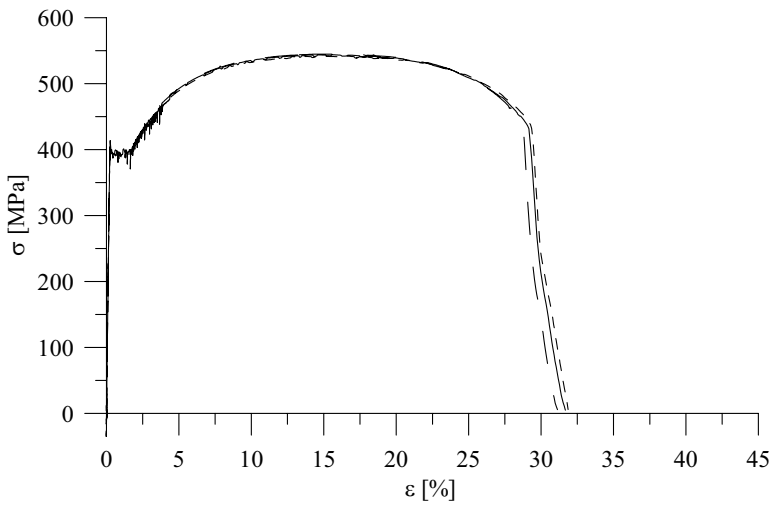


Figure A.4 Stress - strain relation for the three tests on 6 mm thick material transverse the rolling direction, W6T1-3.

APPENDIX B PATCH LOADING TESTS

B.1 Measured girder dimensions

Mean values of the measured geometries of the tested girders are shown in Table B.1. Index u stands for the upper flange and l for the lower flange, respectively.

Table B.1 Measured geometry of the tested girders.

Girder	h_w [mm]	t_w [mm]	b_{fl} [mm]	t_{fl} [mm]	b_{fu} [mm]	t_{fu} [mm]	a [mm]
P200	1198	5,9	446	20,0	449	20,0	2401
P700	1200	5,9	450	20,0	450	20,0	2400
P1440	1200	5,9	450	20,0	450	20,0	2400

B.2 Strain gauge layout on girder webs

Strains were measured at the girder webs in the three tests performed. The strain gauge layout are shown in Figure B.1 - Figure B.3.

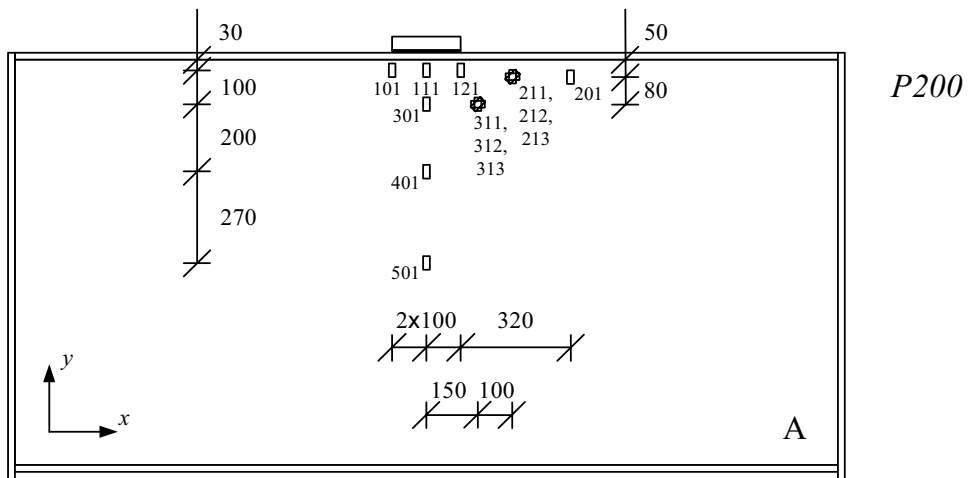


Figure B.1 Positions, orientation and labelling of strain gauges attached to side A of girder P200. Strain gauges were placed in the same positions on side B as well. Strains ϵ_x , ϵ_y and γ_{xy} are presented in accordance with the shown coordinate system.

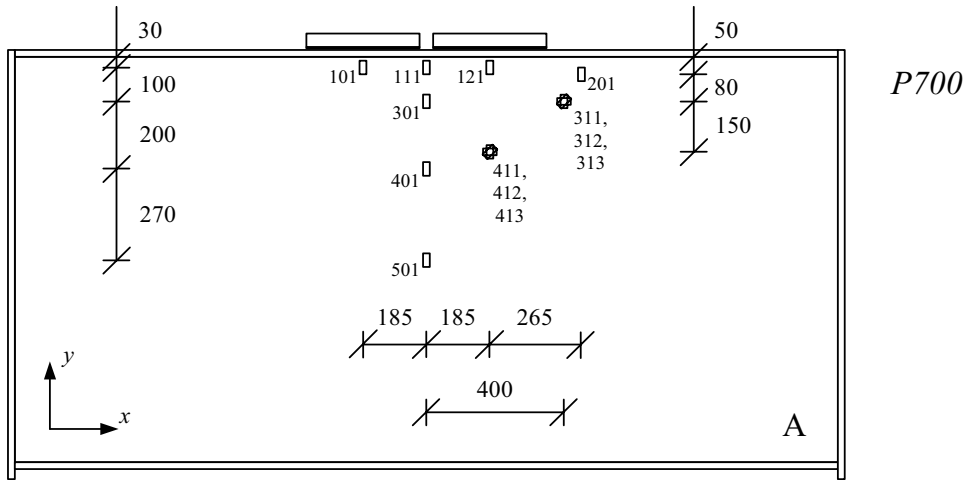


Figure B.2 Positions, orientation and labelling of strain gauges attached to side A of girder P700. Strain gauges were placed in the same positions on side B as well. Strains ε_x , ε_y and γ_{xy} are presented in accordance with the shown coordinate system.

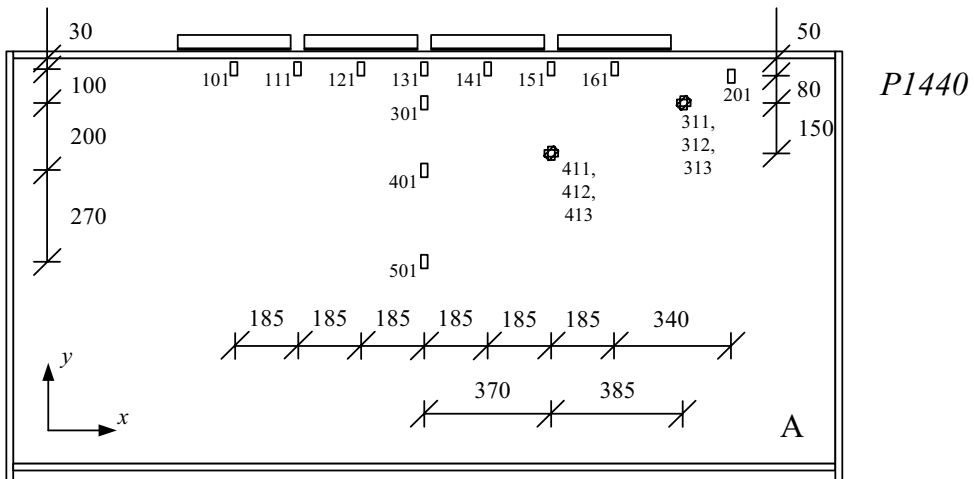


Figure B.3 Positions, orientation and labelling of strain gauges attached to side A of girder P1440. Strain gauges were placed in the same positions on side B as well. Strains ε_x , ε_y and γ_{xy} are presented in accordance with the shown coordinate system.

B.3 Force - strain curves for the P200 test

Force - strain curves for the P200 test are shown in Figure B.4 - Figure B.7. Vertical membrane strains, ε_y , from the uniaxial strain gauges along a vertical line under the load, i.e. at positions 111, 301, 401 and 501, are shown in Figure B.4. The vertical membrane strains along the flange,

i.e. at positions 101, 111, 121 and 201, are shown in Figure B.5. All strains are displayed in relation to the yield strain $\varepsilon_{\text{yield}} = 2550 \mu\text{m/m}$.

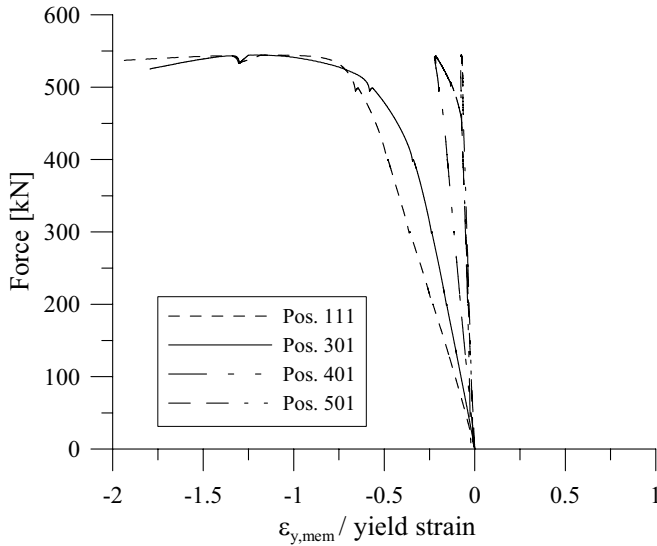


Figure B.4 Force - membrane strain curves for the strain gauges placed on a vertical line under the load.

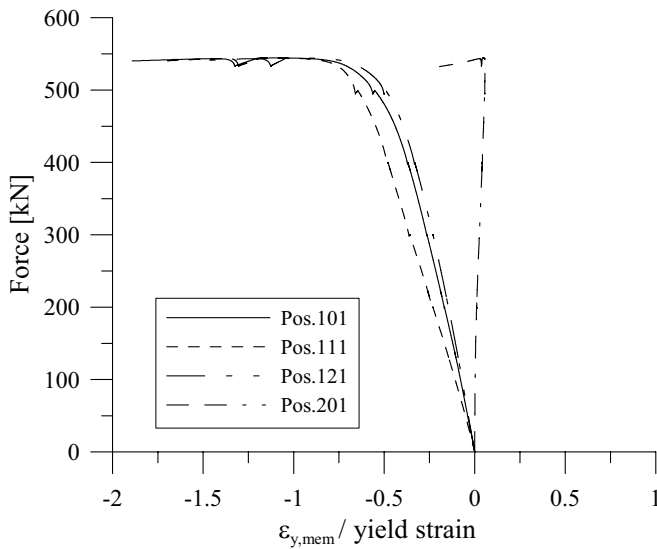


Figure B.5 Force - membrane strain curves for the strain gauges placed along the loaded flange.

Figure B.6 and Figure B.7 shows the strain measurements from the triaxial strain gauges, i.e. position 211, 212 and 213 as well as 311, 312 and 313, respectively.

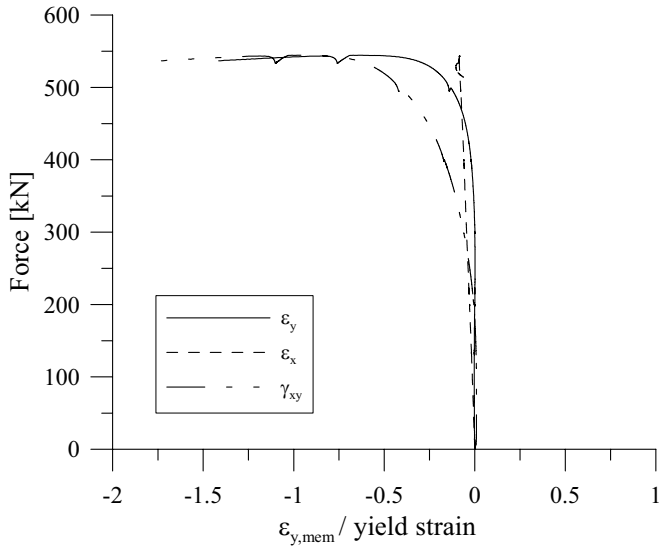


Figure B.6 Force - membrane strain curves for the positions 211-213.

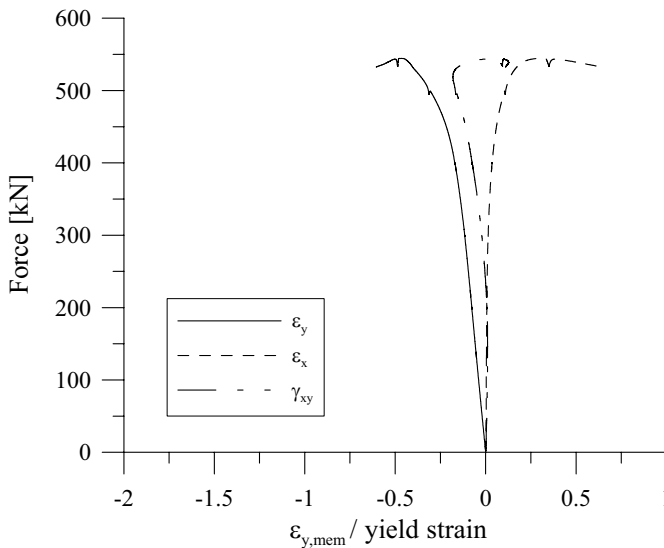


Figure B.7 Force - membrane strain curves for the positions 311-313.

B.4 Force - strain curves for the P700 test

Vertical membrane strains, ε_y , from the uniaxial strain gauges along a vertical line under the load, i.e. at positions 111, 301, 401 and 501, are shown in Figure B.8. The vertical membrane strains along the flange, i.e. at positions 101, 111, 121 and 201, are shown in Figure B.9.

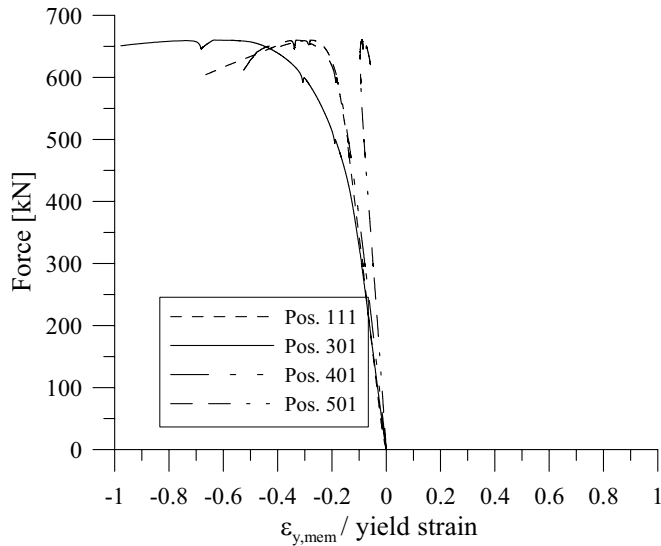


Figure B.8 Force - membrane strain curves for the strain gauges placed on a vertical line under the load.

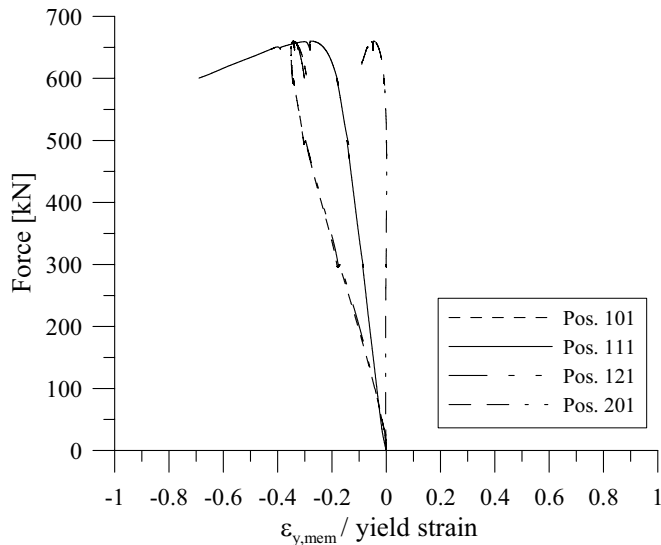


Figure B.9 Force - membrane strain curves for the strain gauges placed along the loaded flange.

Figure B.10 and Figure B.11 shows the strain measurements from the triaxial strain gauges, i.e. position 311, 312 and 313 as well as 411, 412 and 413, respectively.

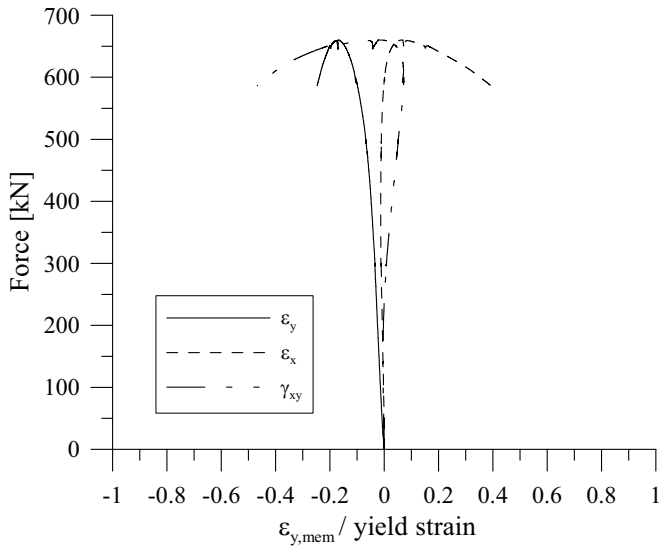


Figure B.10 Force - membrane strain curves for the positions 311-313.

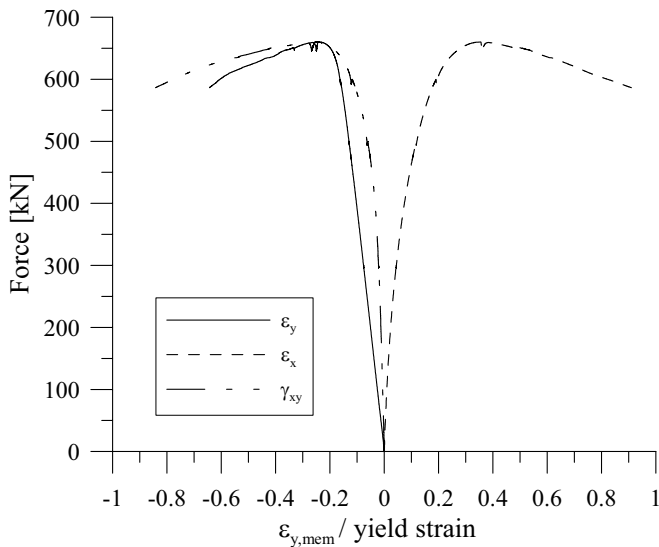


Figure B.11 Force - membrane strain curves for the positions 411-413.

B.5 Force - strain curves for the P1440 test

Vertical membrane strains, ε_y , from the uniaxial strain gauges along a vertical line under the load, i.e. at positions 131, 301, 401 and 501, are shown in Figure B.12. The vertical membrane strains along the flange, i.e. at positions 101, 111, 121, 131, 141, 151, 161 and 201, are shown in Figure B.13.

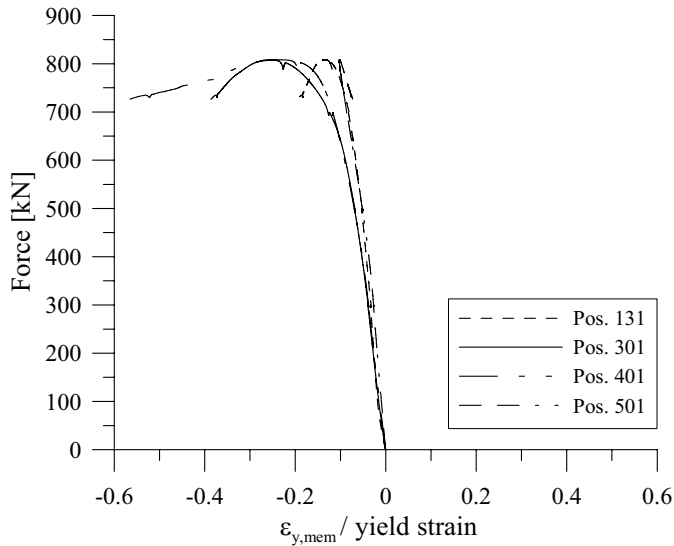


Figure B.12 Force - membrane strain curves for the strain gauges placed on a vertical line under the load.

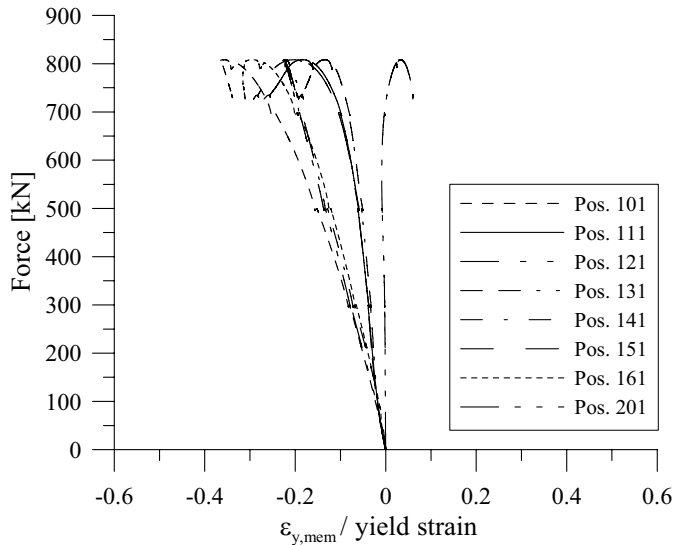


Figure B.13 Force - membrane strain curves for the strain gauges placed along the loaded flange.

Figure B.14 and Figure B.15 shows the strain measurements from the triaxial strain gauges, i.e. position 311, 312 and 313 as well as 411, 412 and 413, respectively.

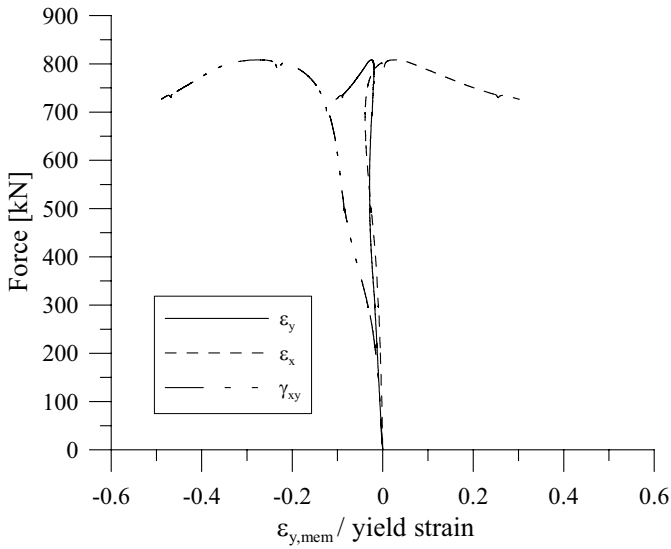


Figure B.14 Force - membrane strain curves for the positions 311-313.

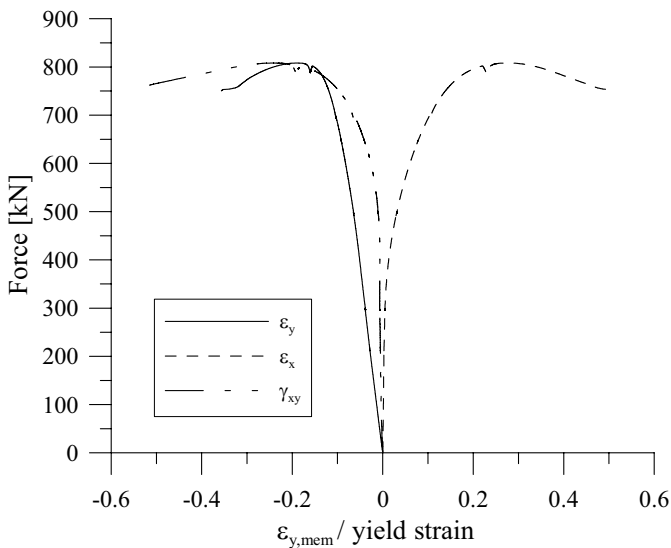


Figure B.15 Force - membrane strain curves for the positions 411-413.

APPENDIX C DATA FROM TESTS BY OTHERS

Appendix C contains all tests included in the evaluation of the design procedure and follows the numbering from Lagerqvist (1994) and from the original source. The tests excluded from the data base collected by Lagerqvist, e.g. tests on rolled sections, are not shown here. Further, the tests found after 1994 are added in the end of this Appendix with a number following the numbering from Lagerqvist. In the table title the full reference is shown as some of them are not included in the reference list.

Table C.1 Bamm, D., Lindner, J. and Voss, R.-P. (1983). Traglastversuche an ausgesteiften trägerauflagern, *Stahlbau*, **52**(10), 296-300

Nr	Nr in ref	t_w mm	h_w mm	f_{yw} MPa	t_f mm	b_f mm	f_{yf} MPa	a mm	s_s mm	F_u kN	M_s kNm
2001	77	8,0	558	305	16,0	150	427	1840	37.5	652	300
2002	78	8,0	558	305	16,0	150	427	1840	75	610	281
2003	79	8,0	558	305	8,0	300	305	1840	75	525	242
2004	80	8,0	558	286	16,0	150	427	1840	75	625	288

Table C.2 Granholm, C. A. (1960). *Tests on girders with extremely thin web plates* (in Swedish), Report 202, Inst. för Byggnadsteknik, Göteborg

Nr	Nr in ref	t_w mm	h_w mm	f_{yw}^a MPa	t_f mm	b_f mm	f_{yf}^a MPa	a mm	s_s mm	F_u kN	M_s kNm
2005	A9	2,2	580 ^a	275	9,0 ^a	180 ^a	343	2000	120	44,1	22
2006	E21	4,6	580	275	9,0	180	343	8000	120	170	339
2007	E23	4,6	580	275	9,0	180	343	8000	0	178	354
2008	E31	3,1	580	275	9,0	180	343	8000	120	91,2	182
2009	34	3,1	580	275	9,0	180	343	8000	0	83,4	313
2010	E36	3,1	580	275	9,0	180	343	8000	0	106	257
2011	E43	3,1	580	275	10,0	200	343	8000	0	105	210

^a uncertain value

Table C.3 Galea, Y., Godart, B., Radouant, I. and Raoul, J. (1987). Tests of buckling of panels subjected to in-plane patch loading, *Proceedings, ECCS Colloquium, Stability of Plate and Shell Structures, Dubas, P., Vandepitte D., eds., 6-8 April, Ghent, Belgium, 65-71*

Nr	Nr in ref	t_w mm	h_w mm	f_{yw} MPa	t_f mm	b_f mm	f_{yf} MPa	a mm	s_s^a mm	F_u kN	M_s kNm
2023	P1	6	1274	276	40	230	250	1800	690	530	2040

^a four rollers with 230 mm centre distance

Table C.4 Scheer, J., Liu, X. L., Falke, J. and Peil, U. (1988). Traglastversuche zur lasteinleitung an I-förmigen geschweissten biegeträgern ohne steifen, *Stahlbau, 57(4), 115-121*

Nr	Nr in ref	t_w mm	h_w mm	f_{yw} MPa	t_f mm	b_f mm	f_{yf} MPa	a mm	s_s mm	F_u kN	M_s kNm
2024	A11	3,72	800	341	20,2	200	363	2300	280	176	925
2025	A12	3,73	800	341	20,2	200	363	2300	280	9,6	1204
2026	A13	3,73	800	341	20,3	201	363	2300	280	228	622
2027	A14	3,72	800	341	20,3	200	363	2300	280	139	1102
2028	A15	4,14	800	352	20,3	199	363	2300	280	217	922
2029	A16	3,74	800	341	20,3	200	363	2300	140	178	943
2030	A17	3,73	800	341	20,3	199	363	2300	140	201	556
2031	A21	3,75	800	341	30,3	298	329	2300	280	236	916
2032	A22	3,77	800	341	30,2	300	329	2300	280	264	716
2033	A23	3,75	800	341	30,1	301	329	2300	280	244	1302
2034	A24	3,74	800	341	30,3	301	329	2300	280	262	397
2035	A25	3,73	800	341	30,2	301	329	2300	280	205	1656
2036	A26	3,74	800	341	30,4	299	329	2300	140	238	1243
2037	A27	4,14	800	352	30,1	299	329	2300	140	258	702
2038	B11	6,27	800	329	20,4	201	335	1700	280	439	1156
2039	B12	5,97	800	328	20,4	201	335	1700	140	397	1051
2040	B13	6,13	800	325	20,2	201	327	2700	280	469	1219
2041	B21	5,08	800	332	30,4	299	329	2300	280	309	2421
2042	B22	5,11	800	332	30,2	300	329	2300	280	357	1854
2043	B23	5,09	800	332	30,1	300	329	2300	280	396	1047
2044	C11	7,35	800	378	20,3	201	363	2300	280	544	1412
2045	C12	7,33	800	378	20,3	198	363	2300	280	267	1450

Nr	Nr in ref	t_w mm	h_w mm	f_{yw} MPa	t_f mm	b_f mm	f_{yf} MPa	a mm	s_s mm	F_u kN	M_s kNm
2046	C13	7,31	800	378	20,2	200	363	2300	280	375	1574
2047	C14	7,33	800	378	20,2	200	363	2300	280	204	1698
2048	C15	6,42	800	373	20,1	199	363	2300	280	572	859
2049	C21	7,41	800	378	30,9	299	329	2300	280	806	2072
2050	C22	7,4	800	378	30,3	301	329	2300	280	314	2466
2051	C23	7,46	800	378	30,3	299	329	2300	280	623	2378
2052	C24	7,45	800	378	30,2	298	329	2300	280	500	2581
2053	C25	6,34	800	373	30,2	300	329	2300	280	631	951

Table C.5 Shimizu, S., Yoshida, S. and Okuhara, H. (1987). An experimental study on patch-loaded web plates, *Proceedings, ECCS Colloquium, Stability of Plate and Shell Structures, Dubas, P., Vandepitte D., eds., 6-8 April, Ghent, Belgium, 85-94*

Nr	Nr in ref	t_w mm	h_w mm	f_{yw} MPa	t_f mm	b_f mm	f_{yf}^a MPa	a mm	s_s mm	F_u kN	M_s kNm
2054	AL-1	6	1000	319	9	300	320	1000	300	332	747
2055	AL-2	6	1000	320	9	300	320	1000	500	355	799
2056	AS-1	6	1000	320	9	300	320	1000	300	353	529
2057	AS-2	6	1000	325	9	300	320	1000	500	480	720
2058	BL-1	6	1000	340	9	300	320	600	180	274	616
2059	BL-2	6	1000	405	9	300	320	600	300	352	792
2060	BL-2C	6	1000	365	9	300	320	600	300	326	733
2061	BS-1	6	1000	320	9	300	320	600	180	356	533

^a uncertain value

Table C.6 Oxfort, J. and Gauger, H. -U. (1989). Beultraglast von Vollwandträgern unter Einzellasten, *Stahlbau*, **58**(11), 331-339

Nr	Nr in ref	t_w mm	h_w mm	f_{yw} MPa	t_f mm	b_f mm	f_{yf} MPa	a mm	s_s mm	F_u kN	M_s kNm
2062	V1	11,8	1300	215	38,3	302	195	2000	100	888	2334
2063	V2	7,7	1300	339	38,1	261	329	2000	100	663	2975

Table C.7 Dubas, P. and Tschamper, H. (1990). Stabilité des ames soumises à une charge concentrée et à une flexion globale, *Construction Metallique*, No. 2, 25-39

Nr	Nr in ref	t_w mm	h_w mm	f_{yw} MPa	t_f mm	b_f mm	f_{yf} MPa	a mm	s_s mm	F_u kN	M_s kNm
2064	T01-1	4,0	990	360	10,0	150	281	2400	40	120	450
2065	T01-2	4,0	990	360	10,0	150	281	1800	40	177	80
2066	T01-3	4,0	990	360	10,0	150	281	1800	40	174	78
2067	T01-5	4,0	990	360	10,0	150	274	1800	40	173	78
2068	T01-6	4,0	990	360	10,0	150	274	1800	40	165	74
2069	T02-1	4,0	990	349	8,0	150	293	2400	40	134	309
2070	T02-2	4,0	990	349	8,0	150	293	1800	40	157	71
2071	T02-3	4,0	990	349	8,0	150	293	1800	40	154	69
2072	T02-5	4,0	990	349	8,0	150	298	1800	40	150	67
2073	T02-6	4,0	990	349	8,0	150	298	1800	40	161	72
2074	T03-1	5,0	990	317	8,0	150	294	2400	40	107	466
2075	T03-2	5,0	990	317	8,0	150	294	1800	40	196	88
2076	T03-3	5,0	990	317	8,0	150	294	1800	40	194	87
2077	T03-5	5,0	990	317	8,0	150	294	1800	40	197	89
2078	T03-6	5,0	990	317	8,0	150	294	1800	40	197	89
2079	VT01-1	3,8	1000	369	8,35	150	293	2480	240 ^a	125	305
2080	VT01-2	3,8	1000	369	8,35	150	293	1760	40	146	64
2081	VT01-3	3,8	1000	369	8,35	150	293	1760	240 ^a	193	85
2082	VT01-4	3,8	1000	369	8,45	150	327	2480	240 ^a	124	466
2083	VT01-5	3,8	1000	369	8,45	150	327	1760	240 ^a	191	84
2084	VT01-6	3,8	1000	369	8,45	150	327	1760	40	146	64
2085	VT02-1	3,8	1000	352	11,9	100	292	2480	40	97	356
2086	VT02-2	3,8	1000	352	11,9	100	292	1760	40	143	63
2087	VT02-3	3,8	1000	352	11,9	100	292	1760	40	145	64
2088	VT02-4	3,8	1000	352	11,9	100	292	2480	40	125	310
2089	VT02-5	3,8	1000	352	11,9	100	292	1760	40	144	63
2090	VT03-1	5,2	1000	305	12,0	150	286	2480	40	140	668
2091	VT03-2	5,2	1000	305	12,0	150	286	1760	40	259	114
2092	VT03-3	5,2	1000	305	12,0	150	286	1760	240 ^a	353	155
2093	VT03-5	5,2	1000	305	12,0	150	277	1760	40	231	102

Nr	Nr in ref	t_w mm	h_w mm	f_{yw} MPa	t_f mm	b_f mm	f_{yf} MPa	a mm	s_s mm	F_u kN	M_s kNm
2094	VT03-6	5,2	1000	305	12,0	150	277	1760	240 ^a	333	146
2095	VT04-1	5,2	1000	300	12,0	150	279	2480	240 ^a	187	588
2096	VT04-2	5,2	1000	300	12,0	150	279	1760	40	243	107
2097	VT04-3	5,2	1000	300	12,0	150	279	1760	640 ^b	421	185
2098	VT04-4	5,2	1000	300	12,0	150	284	2480	640 ^b	292	628
2099	VT04-5	5,2	1000	300	12,0	150	284	1760	40	246	108
2100	VT04-6	5,2	1000	300	12,0	150	284	1760	640 ^b	427	188
2101	VT05-1	5,0	800	292	8,4	150	300	2480	40	114	382
2102	VT05-2	5,0	800	292	8,4	150	300	1760	40	179	79
2103	VT05-3	5,0	800	292	8,4	150	300	1760	240 ^a	250	110
2104	VT05-5	5,0	800	292	8,4	150	300	1760	40	187	82
2105	VT05-6	5,0	800	292	8,4	150	300	1760	240 ^a	255	112
2106	VT06-1	5,0	800	301	12,0	150	291	2480	40	172	364
2107	VT06-2	5,0	800	301	12,0	150	291	1760	40	211	93
2108	VT06-3	5,0	800	301	12,0	150	286	1760	240 ^a	266	117
2109	VT06-4	5,0	800	301	12,0	150	286	2480	240 ^a	217	455
2110	VT06-5	5,0	800	301	12,0	150	286	1760	40	216	95
2111	VT06-6	5,0	800	301	12,0	150	291	1760	640 ^b	388	171

^a two 40 mm steel plates with 200 mm centre distance

^b four 40 mm steel plates with 200 mm centre distance

Table C.8 Höglund, T. (1991). Local buckling of steel bridge girder webs during launching, *Proceedings, Nordic Steel Colloquium, Odense, Denmark*, 531-535

Nr	Nr in ref	t_w mm	h_w mm	f_{yw} MPa	t_f mm	b_f mm	f_{yf} MPa	a mm	s_s mm	F_u kN	M_s kNm
2112	1	4,9	830	422	10,0	200	355	3150	170 ^a	250	197
2113	5	4,9	830	422	10,0	200	355	3150	0 ^b	224	176

^a two rollers with 170 mm centre distance

^b one roller

Table C.9 Dogaki, M., Kishigami, N. and Yonezawa, H. (1991). Ultimate strength analysis of plate girder webs under patch loading, *Proceedings, ICSAS 91, Singapore, 192-201*

Nr	Nr in ref	t_w mm	h_w mm	f_{yw} MPa	t_f mm	b_f mm	f_{yf} MPa	a mm	s_s mm	F_u kN	M_s kNm
2114	1	3,2	900	255	5,0	80	308	900	90	110	25
2115	2	6,0	900	306	5,0	80	308	900	90	298	67

Table C.10 Drdacky, M. and Novotny, R. (1977). Partial edge load-carrying capacity tests of thick plate girder webs, *Acta Technica CSAV, 87, 614-620*

Nr	Nr in ref	t_w mm	h_w mm	f_{yw} MPa	t_f mm	b_f mm	f_{yf} MPa	a mm	s_s mm	F_u kN	M_s kNm
2135	TTG1	3,97	300	285	10,0	49	269	300	30	130	10
2136	TTG2	4,0	300	270	9,9	50	288	300	30	148	11
2137	TTG3	4,01	300	281	15,9	50	265	300	30	170	13
2138	TTG4	3,97	450	267	10,0	49	267	450	45	120	14
2139	TTG6	3,96	450	249	15,8	50	265	450	45	150	17
2140	TTG7	3,57	600	257	10,0	50	274	600	60	140	21
2141	TTG8	3,63	600	282	10,1	50	279	600	60	148	22
2142	TTG9	3,67	600	306	16,0	49	282	600	60	150	22
2143	TTG'1	3,97	300	285	10,0	49	269	300	45	150	11
2144	TTG'2	4,0	300	270	9,9	50	288	300	60	146	11
2145	TTG'3	4,01	300	281	15,9	49	265	300	30	150	11
2146	TTG'4	3,97	450	267	10,0	49	267	450	60	136	15
2147	TTG'6	3,96	450	249	15,8	50	265	450	45	160	18
2148	TTG'7	3,57	600	257	10,0	50	274	600	30	119	18
2149	TTG'8	3,63	600	282	10,1	50	279	600	45	138	21
2150	TTG'9	3,67	600	306	16,0	49	282	600	60	146	22

Table C.11 Bergfelt, A. (1979). *Patch loading on a slender web - Influence of horizontal and vertical web stiffeners on the load carrying capacity*, Chalmers University of Technology, Dept. of Structural Engineering, Div. of Steel and Timber Structures, publ. S 79:1, Göteborg, Tab. A1:3

Nr	Nr in ref	t_w mm	h_w mm	f_{yw} MPa	t_f mm	b_f mm	f_{yf} MPa	a mm	s_s mm	F_u kN	M_s kNm
2151 ^a	B12	2,0	300	330	6,0	100	285	2400	180	66	39
2153 ^a	B13	2,0	400	275	8,0	100	285	2400	180	54	32
2154 ^a	B14	2,0	400	275	8,0	100	285	2400	180	59	36
2155 ^a	B15	2,0	500	275	10,0	100	285	2400	180	54	33
2156 ^a	B16	2,0	500	275	10,0	100	285	2400	180	55	33
2157 ^a	B18	2,0	600	275	12,0	100	285	2900	180	62	45
2158 ^a	B17	2,0	600	275	12,0	100	285	2900	0	54	39
2159 ^a	B19	2,0	700	275	15,0	100	285	3500	180	55	48
2160 ^a	B20	2,0	700	275	15,0	100	285	3500	0	56	49
2161 ^a	B21	3,4	700	295	10,0	250	275	9800	0	115	282
2162 ^a	“	3,4	700	295	10,0	250	275	9800	0	113	276
2163 ^a	“	3,4	700	295	10,0	250	275	9800	0	101	248
2164 ^a	“	3,4	700	295	10,0	250	275	9800	0	117	286
2165 ^a	B22	3,4	700	295	10,0	250	275	9800	100	120	294
2166 ^a	“	3,4	700	295	10,0	250	275	9800	100	116	285
2167 ^a	B23	3,4	700	295	10,0	250	275	9800	200	121	297
2168	B1	3,26	700	325	6,1	150	347	9400 ^b	0	95	57
2169	B2	3,26	700	325	6,1	150	347	9400 ^b	100	106	64
2170	B3	3,26	700	325	8,5	200	235	9400 ^b	0	110	66
2171	B4	3,26	700	325	8,5	200	235	9400 ^b	100	122	73
2172	B5	3,26	700	325	10,1	250	243	9400 ^b	0	121	72
2173	B6	3,26	700	325	10,1	250	243	9400 ^b	100	133	80
2174	B7	3,26	700	325	11,9	250	232	9400 ^b	0	135	81
2175	B8	3,26	700	325	11,9	250	232	9400 ^b	100	139	84
2176	B9	3,26	700	325	15,3	300	305	9400 ^b	0	151	91
2177	B10	3,26	700	325	15,3	300	305	9400 ^b	100	156	94

^a uncertain material data according to Bergfelt

^b span length 2,4 m

Table C.12 Bergfelt, A. (1979). *Patch loading on a slender web - Influence of horizontal and vertical web stiffeners on the load carrying capacity*, Chalmers University of Technology, Dept. of Structural Engineering, Div. of Steel and Timber Structures, publ. S 79:1, Göteborg, ser. A, B, R, Tab. 1

Nr	Nr in ref	t_w mm	h_w mm	f_{yw} MPa	t_f mm	b_f mm	f_{yf} MPa	a mm	s_s mm	F_u kN	M_s kNm
2178	R1	2,05	800	266	15,5	300	295	800	40	60	12
2179	R12	2,05	800	266	15,5	300	295	800	40	66	13
2180	R3	2,0	800	266	5,07	120	285	800	40	38	7,6
2181	R32	2,0	800	266	5,07	120	285	800	40	41	8,2
2182	A11	2,12	800	300	15,4	300	295	2500	40	64	8
2183	A13	2,12	800	300	15,4	300	295	1200	40	66	20
2184	A21	3,03	800	245	12,0	250	265	2500	40	84	17
2185	A23	3,03	800	245	12,0	250	265	1200	40	85	26
2186	A31	2,08	680	354	5,05	120	290	2200	40	47,1	56
2187	A33	2,08	680	354	5,05	120	290	1020	40	50,7	13
2188	B8	2,07	800	285	5,03	120	290	800	40	48	9,6
2189	B6	2,07	600	285	5,03	120	290	800	40	42	8,4
2190	B4	2,07	400	285	5,03	120	290	800	40	48	9,6
2191	B3	2,07	300	285	5,03	120	290	800	40	49	9,8
2192	B41	2,07	400	285	5,03	120	290	400	40	53	5,3
2193	B31	2,07	300	285	5,03	120	290	400	40	51	5,1
2194	B83	2,9	800	328	12,4	250	298	800	40	121	24
2195	B63	2,9	600	328	12,4	250	298	800	40	120	24
2196	B43	2,9	400	328	12,4	250	298	800	40	119	24
2197	A15	2,12	800	300	15,4	300	295	600	40	84	13
2198	A25	3,03	800	245	12,0	250	265	600	40	96,8	14
2199	A35	2,08	680	354	5,05	120	290	510	40	51,5	6,6

Table C.13 Bergfelt, A. (1979). *Patch loading on a slender web - Influence of horizontal and vertical web stiffeners on the load carrying capacity*, Chalmers University of Technology, Dept. of Structural Engineering, Div. of Steel and Timber Structures, publ. S 79:1, Göteborg, Tab. A1:1

Nr	Nr in ref	t_w mm	h_w mm	f_{yw} MPa	t_f mm	b_f mm	f_{yf} MPa	a mm	s_s mm	F_u^a kN	M_s kNm
2200	IaBp	3,26	700	332	6,0	150	354	2400	100	106	64
2201	IaBae	3,26	700	332	6,0	150	354	1400	0	95,2	33
2202	IaCe	3,26	700	332	8,0	200	240	2400	0	110	66
2203	IaFp	3,26	700	332	8,0	200	240	2400	100	101	61
2204	IaCu,p	3,26	700	332	10,0	250	248	2400	100	134	81
2205	IaGu,e	3,26	700	332	10,0	250	248	2400	0	121	72
2206	IaDp	3,26	700	332	12,0	250	237	2400	100	99,1	59
2207	IaGe	3,26	700	332	12,0	250	237	2400	0	135	81
2208	IaEp	3,26	700	332	15,0	300	311	2400	100	155	93
2209	IaHce	3,26	700	332	15,0	300	311	2400	0	151	91
2210	IaH2e	3,26	700	332	15,0	300	311	2400	0	150	90
2211	IaBu,p	3,26	700	332	10,0	250	248	9400	100	128	302
2212	IaEu,e	3,26	700	332	10,0	250	248	9400	0	102	240
2213	Ib1e	3,26	700	332	6,0	152	279	9400	0	62,8	148
2214	Ib3p	3,26	700	332	6,0	152	279	9400	100	86,8	204
2215	Ib5e	3,26	700	332	6,0	152	279	2400	0	90,3	54
2216	Ib6p	3,26	700	332	6,0	152	279	2400	50	98,1	59
2217	Ic1e	2,91	700	310	6,0	150	294	9400	0	58,9	138
2218	Ic4e	2,91	700	310	5,9	151	294	2400	0	65,7	39
2219	Ic5p	2,91	700	310	5,9	151	294	2400	100	81,4	49
2220	II1e	3,05	700	309	12,1	251	815	2400	0	107	64
2221	II2p	3,08	700	305	8,2	200	705	2400	100	83,4	50
2222	II3e	3,08	700	305	6,8	151	788	2400	0	67,7	41
2223	II4e	2,9	700	600	6,8	152	788	2400	0	113	68
2224	II5e	2,9	700	600	8,1	200	705	2400	0	135	81
2225	II7e	2,9	700	600	2,9	100	600	2400	0	55,4	33
2226	III1e	2,1	500	355	3,9	151	288	2400	0	39,7	24
2227	III2e	2,1	500	355	8,6	203	328	2400	0	57,9	35
2228	III3e	2,1	500	355	9,8	253	269	2400	0	66,7	40

Nr	Nr in ref	t_w mm	h_w mm	f_{yw} MPa	t_f mm	b_f mm	f_{yf} MPa	a mm	s_s mm	F_u^a kN	M_s kNm
2229	III4e	2,1	500	355	5,9	151	282	2400	0	47,6	29
2230	III5p	2,1	500	355	8,6	203	323	2400	100	63,3	38
2231	III6p	2,1	500	355	3,9	151	288	2400	100	53,5	32
2232	III7p	2,1	500	355	9,9	253	269	2400	100	63,8	38
2233	III8p	2,1	500	355	5,9	151	282	2400	100	59,8	36
2234	III9p	2,1	500	355	5,9	150	282	9600	100	40,7	98
2235	III10e	2,1	500	355	6	151	282	9600	0	41,7	100
2236	IV1e	5,83	700	329	5,9	151	289	2400	0	178	107
2237	IV2e	5,83	700	329	8,7	203	328	2400	0	244	147
2238	IV3e	5,83	700	329	11,6	251	248	2400	0	280	168
2239	IV4e	5,83	700	329	17,7	355	263	2400	0	363	218
2240	IV5p	5,83	700	329	8,7	202	328	2400	100	291	175
2241	IV6p	5,83	700	329	11,7	253	248	2400	100	343	206
2242	IV7p	5,83	700	329	18,3	350	274	2400	100	417	250
2243	IV14p	5,83	700	329	11,7	251	248	2400	100	356	214
2244	IV17e	5,83	700	329	11,7	251	250	9600	0	212	509

^a test results from the first loading cycle close to ultimate load

Table C.14 Bergfelt, A. (1979). *Patch loading on a slender web - Influence of horizontal and vertical web stiffeners on the load carrying capacity*, Chalmers University of Technology, Dept. of Structural Engineering, Div. of Steel and Timber Structures, publ. S 79:1, Göteborg, Tab. A1:2

Nr	Nr in ref	t_w mm	h_w mm	f_{yw} MPa	t_f mm	b_f mm	f_{yf} MPa	a mm	s_s mm	F_u^a kN	M_s kNm
2245	IaBe	3,26	700	332	6,0	150	354	2400	0	95,2	57
2246	IaCp	3,26	700	332	8,0	200	240	2400	100	122	73
2247	IaFe	3,26	700	332	8,0	200	240	2400	0	101	61
2248	IaCu,e	3,26	700	332	10,0	250	248	2400	0	121	72
2249	IaGu,p	3,26	700	332	10,0	250	248	2400	100	132	79
2250	IaDe	3,26	700	332	12,0	250	237	2400	0	117	70
2251	IaGp	3,26	700	332	12,0	250	237	2400	100	139	84
2252	IaEe	3,26	700	332	15,0	300	311	2400	0	153	92

Nr	Nr in ref	t_w mm	h_w mm	f_{yw} MPa	t_f mm	b_f mm	f_{yf} MPa	a mm	s_s mm	F_u^a kN	M_s kNm
2253	IaH2p	3,26	700	332	15,0	300	311	2400	100	158	95
2254	IaBu,e	3,26	700	332	10,0	250	248	9400	0	118	277
2255	IaEu,p	3,26	700	332	10,0	250	248	9400	100	118	277
2256	II1p	3,05	700	308	12,1	251	815	2400	100	108	65
2257	II2e	3,08	700	305	8,2	200	705	2400	0	78,5	47
2258	II3p	3,08	700	305	6,8	151	788	2400	100	70,6	42
2259	II4p	2,9	700	600	6,8	152	788	2400	100	126	76
2260	II5p	2,9	700	600	8,1	200	705	2400	100	140	84
2261	II6e	2,9	700	600	12,1	250	815	2400	0	149	89
2262	II6p	2,9	700	600	12,1	250	815	2400	100	158	95
2263	II7p	2,9	700	600	2,9	100	600	2400	100	59,8	36
2264	II7b,e	3,03	700	316	2,9	100	600	400	0	63,3	6,3
2265	II7b,p	3,03	700	316	2,9	100	600	400	100	80,9	8,1
2266	II8e	3,08	700	305	8,1	201	705	9600	0	88,3	212
2267	II9e	2,9	700	600	6,6	151	788	9600	0	73,6	177
2268	II11e	2,9	700	600	8,1	201	705	9600	0	99,1	238
2269	II51p	2,11	500	355	3,94	151	288	2400	100	45,1	27
2270	II52p	2,11	500	355	8,58	203	328	2400	100	59,8	36
2271	II53p	2,09	500	355	9,83	253	269	2400	100	69,7	42
2272	II54p	2,09	500	355	5,86	151	282	2400	100	52,5	32
2273	II55e	2,12	500	355	8,62	203	323	2400	0	56,9	34
2274	II56e	2,12	500	355	3,94	151	288	2400	0	43,2	26
2275	II57e	2,1	500	355	9,98	253	269	2400	0	58,9	35
2276	II58e	2,11	500	355	5,9	151	282	2400	0	40,2	24
2277	II59e	2,09	500	355	5,88	150	282	9600	0	39,7	95
2278	II510p	2,12	500	355	5,98	151	282	9600	100	43,9	105
2279	IV1p	5,83	700	329	5,93	151	289	2400	100	240	144
2280	IV1e	5,83	700	329	5,93	151	289	2400	0	169	101
2281	IV2p	5,83	700	329	8,66	203	328	2400	100	29	176
2282	IV3p	5,83	700	329	11,6	251	248	2400	100	324	194
2283	IV4p	5,83	700	329	17,7	355	263	2400	100	376	225

Nr	Nr in ref	t_w mm	h_w mm	f_{yw} MPa	t_f mm	b_f mm	f_{yf} MPa	a mm	s_s mm	F_u^a kN	M_s kNm
2284	IV5e	5,83	700	329	8,69	202	328	2400	0	215	129
2285	IV6e	5,83	700	329	11,7	253	248	2400	0	235	141
2286	IV7e	5,83	700	329	18,3	350	274	2400	0	373	224
2287	IV14e	5,83	700	329	11,7	251	248	2400	0	274	164

^a test results from the second, or later, loading cycle close to ultimate load

Table C.15 Bergfelt, A. (1983). *Girder web stiffening for patch loading*, Chalmers University of Technology, Dept. of Structural Engineering, Div. of Steel and Timber Structures, publ., S 83:1, Göteborg

Nr	Nr in ref	t_w mm	h_w mm	f_{yw}^a MPa	t_f mm	b_f mm	f_{yf} MPa	a mm	s_s mm	F_u kN	M_s kNm
2288	324	2,0	300	207	6,1	100	277	2400	40	39,8	24
2289	325	2,0	300	207	6,1	100	277	900	40	34,1	7,7
2290	326	2,0	300	207	6,1	100	277	900	120	38,3	8,6
2291	624	2,0	600	206	6,1	100	284	2400	40	35	21
2292	625	2,0	600	206	6,1	100	284	900	40	31	7
2293	626	2,0	600	206	6,1	100	284	900	120	37,5	8,4
2294	424	2,0	400	205	12,2	100	278	3000	40	40,7	30
2295	425	2,0	400	205	12,2	100	278	1100	40	36,9	10
2296	426	2,0	400	205	12,2	100	278	1100	120	42,1	12
2297	824	2,0	800	205	12,1	100	277	3000	40	41,9	31
2298	825	2,0	800	205	12,1	100	277	1100	40	40,5	11
2299	826	2,0	800	205	12,1	100	277	1100	120	46,5	13
2300	827	2,0	800	206	12,3	250	273	3000	40	38,2	29
2301	828	2,0	800	206	12,3	250	273	1100	40	41,4	11
2302	829	2,0	800	206	12,3	250	273	1100	120	41,4	11
2303	837	3,0	800	215	12	250	268	3000	40	81,5	61
2304	838	3,0	800	215	12	250	268	1100	40	90,7	25
2305	839	3,0	800	215	12	250	268	1100	120	92,5	25

^a $\sigma_{0,2}$

Table C.16 Skaloud, M. and Novak, P., data taken from Roberts, T. M. and Rockey, K. C. (1979). A mechanism solution for predicting the collapse loads of slender plate girders when subjected to in-plane patch loading, *Proc. Instn Civ. Engrs*, Part 2, **67**, 155-175

Nr	Nr in ref	t_w mm	h_w mm	f_{yw} MPa	t_f mm	b_f mm	f_{yf} MPa	a mm	s_s mm	F_u kN	M_s kNm
2306 ^a	TG1	2,5	1000	298	5,5	160	342	1000	100	51,5	13
2307	TG2	2,5	1000	299	10,1	200	253	1000	100	63,8	16
2308	TG3	2,5	1000	251	16,2	200	266	1000	100	68,7	17
2309	TG4	2,5	1000	254	20,2	200	231	1000	100	88,3	22
2310 ^b	TG5	2,5	1000	289	30,5	250	261	1000	100	179	45
2311 ^b	TG6	3,0	1000	290	6,3	160	294	2000	100	81,9	41
2312	TG7	3,0	1000	297	10	200	253	2000	100	98,1	49
2313	TG8	3,0	1000	308	16,6	200	266	2000	100	118	59
2314	TG9	3,0	1000	300	19,8	200	231	2000	100	126	63
2315 ^b	TG10	3,0	1000	299	30	250	261	2000	100	147	74
2316 ^b	TG11	3,0	1000	290	6,3	160	294	2000	200	93,2	47
2317	TG12	3,0	1000	297	10	200	253	2000	200	118	59
2318	TG13	3,0	1000	308	16,6	200	266	2000	200	132	66
2319	TG14	3,0	1000	300	19,8	200	231	2000	200	152	76
2320 ^b	TG15	3,0	1000	299	30	250	261	2000	200	158	79
2321 ^b	STG12	2,0	500	243	6	50	294	500	50	37,3	4,7
2322 ^b	STG34	2,0	500	243	16,2	45	261	500	50	54	6,8
2323 ^b	STG56	2,0	500	243	24,6	50	225	500	50	76	9,5
2324 ^b	STG78	2,0	500	280	5	50	294	1000	100	35,6	8,9
2325 ^b	STG910	2,0	500	280	15,9	45	261	1000	100	49,3	12
2326 ^b	STG1112	2,0	500	280	24,8	60	225	1000	100	56,4	14

^a average of three tests

^b average of two tests

Table C.17 Bagchi, D. K. and Rockey K. C., data from Roberts, T. M. and Rockey, K. C. (1979). A mechanism solution for predicting the collapse loads of slender plate girders when subjected to in-plane patch loading, *Proc. Instn Civ. Engrs*, Part 2, **67**, 155-175

Nr	Nr in ref	t_w mm	h_w mm	f_{yw} MPa	t_f mm	b_f mm	f_{yf} MPa	a mm	s_s mm	F_u kN	M_s kNm
2327	BR1	3,25	635	250	12,7	152	250	660	75	141	23
2328	BR2	3,25	635	250	12,7	152	250	864	50	124	27
2329	BR3	3,25	635	250	12,7	152	250	1270	50	89,4	28

Table C.18 Roberts, T. M. (1981). Slender plate girders subjected to edge loading, *Proc. Instn Civ. Engrs*, Part 2, **71**, 805-819

Nr	Nr in ref	t_w mm	h_w mm	f_{yw} MPa	t_f mm	b_f mm	f_{yf} MPa	a mm	s_s mm	F_u kN	M_s kNm
2330	A1-3	0,99	250	193	3,05	149	221	600	50	9,02	1,4
2331	A1-7	0,99	250	193	6,75	149	279	600	50	11,5	1,7
2332	A1-12	0,99	250	193	11,8	149	305	600	50	27,8	4,2
2333	A2-3	2,12	250	224	3,05	149	221	600	50	32,6	4,9
2334	A2-7	2,12	250	224	6,75	149	279	600	50	42,2	6,3
2335	A2-12	2,12	250	224	11,8	149	305	600	50	52,8	7,9
2336	A3-3	3,05	250	221	3,05	149	221	600	50	79,7	12
2337	A3-7	3,05	250	221	6,75	149	279	600	50	101	15
2338	A3-12	3,05	250	221	11,8	149	305	600	50	129	19
2339	B1-3	0,99	500	192	3,05	149	221	600	50	8,45	1,3
2340	B1-7	0,99	500	192	6,75	149	279	600	50	10,8	1,6
2341	B1-12	0,99	500	192	11,8	149	305	600	50	28,8	4,3
2342	B2-2	2,12	500	224	3,05	149	221	600	50	34,1	5,1
2343	B2-7	2,12	500	224	6,75	149	279	600	50	37,9	5,7
2344	B2-12	2,12	500	224	11,8	149	305	600	50	44,2	6,6
2345	B2-20	2,12	500	224	20,1	149	305	600	50	84,5	13
2346	B3-3	3,05	500	221	3,05	149	221	600	50	70,6	11
2347	B3-7	3,05	500	221	6,75	149	279	600	50	90,7	14
2348	B3-12	3,05	500	221	11,8	149	305	600	50	111,4	17
2349	B3-20	3,05	500	221	20,1	149	305	600	50	131	20

Nr	Nr in ref	t_w mm	h_w mm	f_{yw} MPa	t_f mm	b_f mm	f_{yf} MPa	a mm	s_s mm	F_u kN	M_s kNm
2350	C2-3	2,12	750	224	3,05	149	221	600	50	30	4,5
2351	C2-7	2,12	750	224	6,75	149	279	600	50	38,4	5,8
2352	C2-12	2,12	750	224	11,8	149	305	600	50	53,0	8
2353	C3-3	3,05	750	221	3,05	149	221	600	50	67,4	10
2354	C3-7	3,05	750	221	6,75	149	279	600	50	81,1	12
2355	C3-12	3,05	750	221	11,8	149	305	600	50	99,6	15

Table C.19 Roberts, T. M. and Coric, B. (1988). Collapse of plate girders subjected to patch loading, *Miscellany Dedicated to the 65th Birthday of Academician Professor Dr. Nicola Hajdin*, Naerlovic-Veljkovic N ed., University of Belgrade, Belgrade, 203-209

Nr	Nr in ref	t_w mm	h_w mm	f_{yw} MPa	t_f mm	b_f mm	f_{yf} MPa	a mm	s_s mm	F_u kN	M_s kNm
2356	D2-2	1,96	380	178	3,05	80	272	760	50	33,6	6,4
2357	D3-6	2,99	380	245	6,25	80	298	760	50	84,1	16
2358	D5-10	4,94	380	292	9,97	100	305	760	50	253	48
2359	D2-3S	1,96	380	178	3,05	80	272	760	50	32	18
2360	D3-6S	3	380	245	6,25	80	298	760	50	84	48

Table C.20 Bossert and Ostapenko (1967), data from Roberts, T. M. and Chong, C. K. (1981). Collapse of plate girders under edge loading, *ASCE, Jour. Struct. Div.*, ST8, 107,1503-1509. *Distributed patch loading.*

Nr	Nr in ref	t_w mm	h_w mm	f_{yw} MPa	t_f mm	b_f mm	f_{yf} MPa	a mm	s_s mm	F_u kN	σ_b/f_{yf}
2361	EG1.1	3,1	914	233	15,9	203	300	711	711	221	0,36
2362	EG1.2	3,1	914	233	15,9	203	300	711	711	125	0,97
2363	EG1.3	3,1	914	233	15,9	203	300	711	711	163	0,79
2364	EG1.4	3,1	914	233	15,9	203	300	711	711	183	0,40
2365	EG2.1	2,9	914	252	15,9	203	300	1092	1092	134	0,70
2366	EG2.2	2,9	914	252	15,9	203	300	1092	1092	254 ^a	0,71
2367	EG2.3	2,9	914	252	15,9	203	300	1092	1092	205	0,33

Nr	Nr in ref	t_w mm	h_w mm	f_{yw} MPa	t_f mm	b_f mm	f_{yf} MPa	a mm	s_s mm	F_u kN	σ_b/f_{yf}
2368	EG2.4	2,9	914	252	15,9	203	300	1092	1092	194	0,28
2369	EG3.1	3,1	914	236	15,9	203	300	1448	1448	201	0,36
2370	EG3.2	3,1	914	236	15,9	203	300	1448	1448	170	0,51

^a load applied through a wooden beam

Table C.21 Roberts, T. M. and Markovic, N. (1983). Stocky plate girders subjected to edge loading, *Proc. Instn Civ. Engrs, Part 2*, **75**, 539-550

Nr	Nr in ref	t_w mm	h_w mm	f_{yw}^a MPa	t_f mm	b_f mm	f_{yf}^a MPa	a mm	s_s mm	F_u kN	M_s kNm
2371	E10-1/1	9,95	500	222	10,0	150	240	500	0	716	90
2372	E10-2/1	9,95	500	247	10,0	150	250	500	100	787	98
2373	E10-1/2	9,95	500	222	10,0	150	240	500	50	698	87
2374	E10-2/2	9,95	500	247	10,0	150	250	500	50	738	92
2375	E6-1/1	6,0	500	253	10,0	150	250	500	0	304	38
2376	E6-1/2	6,0	500	253	10,0	150	250	500	50	378	47
2377	E6-2/1	6,0	500	253	10,0	150	237	500	100	399	50
2378	E6-2/2	6,0	500	253	10,0	150	237	500	50	344	43
2379	F3-1/1	3,01	500	242	5,94	150	308	500	50	89	11
2380	F3-1/2	3,01	500	242	5,94	150	308	500	50	89	11

^a the static yield stress was determined as the stress corresponding to 0,5% strain after the strain has been held constant for 5 minutes

Table C.22 Raoul, J., Schaller, I. and Theillout, J. -N. (1990). Tests of buckling of panels subjected to in-plane patch loading, *Proceedings, Contact Loading and Local Effects in Thin-walled Structures, IUTAM symposium*, Prague, 173-183

Nr	Nr in ref	t_w mm	h_w mm	f_{yw} MPa	t_f mm	b_f mm	f_{yf} MPa	a mm	s_s^a mm	F_u kN	M_s kNm
2384	1	6	1274	362	40	230	286	1780	230	610	271

^a two rollers with 230 mm centre distance

Table C.23 Lagerqvist, O. (1994). Patch loading - Resistance of steel girders subjected to concentrated forces, Doctoral thesis 1994:159D, Luleå University of Technology, ISRN: HLU-TH-T--159-D--SE

Nr	Nr in ref	t_w mm	h_w mm	f_{yw} MPa	t_f mm	b_f mm	f_{yf} MPa	a mm	s_s mm	F_u kN	M_s kNm
2385	A13p	3,8	239,8	830	12,0	118,5	844	1008	40	323	81
2386	A14p	3,8	239,8	830	12,0	118,5	844	1008	80	346	87
2387	A22p	3,8	278,1	830	12,0	119,9	844	1260	80	357	113
2388	A32p	3,9	319,7	832	12,0	120,1	844	1404	40	334	117
2389	A41p	3,8	359,6	832	11,9	120,5	844	1315	40	311	102
2390	A51p	3,8	397,7	830	12,0	120,0	844	1900	40	310	147
2391	A61p	3,8	439,9	830	12,0	120,0	844	1626	40	293	119
2392	A71p	7,9	320,7	762	11,9	120,5	844	1405	40	931	327
2393	A81p	8	400,5	762	12,0	120,4	844	1684	40	929	391

Table C.24 Shahabian, F. and Roberts, T. M. (2000). Combined Shear-and-Patch loading of plate girders, *Journal of Structural engineering*, **126**(3), 316-321

Nr	Nr in ref	t_w mm	h_w mm	f_{yw}^a MPa	t_f mm	b_f mm	f_{yf}^a MPa	a mm	s_s mm	F_u kN	M_s kNm
2394	PG1-1	4,1	600	343	12,5	200	257	600	50	220	33
2395	PG2-1	3,1	900	285	10,2	300	254	900	50	113	25
2396	PG3-1	3,2	600	282	10,1	200	264	900	50	120	27
2397	PG4-1	1,9	500	250	9,9	200	293	1000	50	52	13

^a $\sigma_{0,2}$

Table C.25 Unosson, E. (2003). *Patch loading of stainless steel girders - Experiments and finite element analyses*, Licentiate thesis 2003:12, Luleå University of Technology, ISRN: LTU-LIC--03/12--SE

Nr	Nr in ref	t_w mm	h_w mm	f_{yw}^a MPa	t_f mm	b_f mm	f_{yf}^a MPa	a mm	s_s mm	F_u kN	M_s kNm
2398	Pli 4301:1	4,1	238,3	297	11,8	118,1	285	998	40	176	44
2399	Pli 4301:2	4,1	238,3	297	11,9	118,8	285	996	80	196	49
2400	Pli 4301:3	4,1	316,0	297	11,9	120,1	285	1397	40	168	59
2401	Pli 4301:4	4,1	438,4	297	12,0	121,1	285	1623	40	169	69
2402	Pli 4301:5	8,8	400,9	245 ^b	12,0	120,5	285	1682	40	478	201

^a $R_{p0,2}$

^b From test certificates delivered by the steel mill

Table C.26 Kuhlmann, U. and Seitz, M. (2004). Longitudinally stiffened girder webs subjected to patch loading, *Steelbridge 2004, International Symposium on Steel Bridges*, Millau, France

Nr	Nr in ref	t_w mm	h_w mm	f_{yw}^a MPa	t_f mm	b_f mm	f_{yf}^a MPa	a mm	s_s^b mm	F_u kN	M_s kNm
2403	I	6	1200	367	20	260	396	2400	700	659	395

^a upper yield strength

^b four 100 mm wide loading plates with 200 mm centre distance

APPENDIX D INFLUENCE OF VARIOUS PARAMETERS

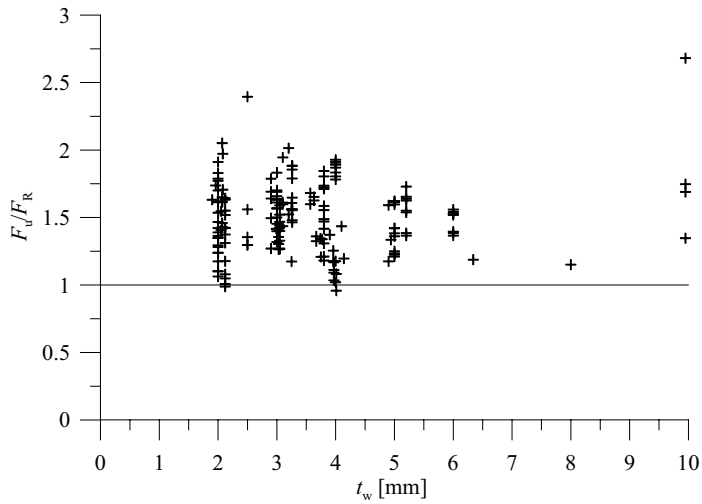


Figure D.1 F_u/F_R as a function of t_w for 184 tests.

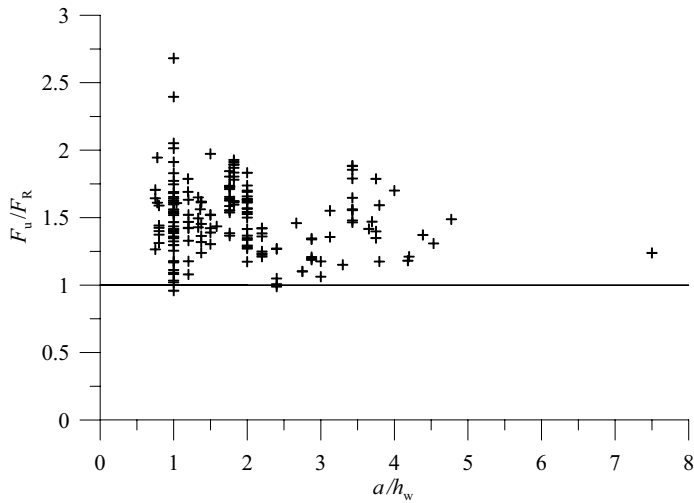


Figure D.2 F_u/F_R as a function of a/h_w for 184 tests.

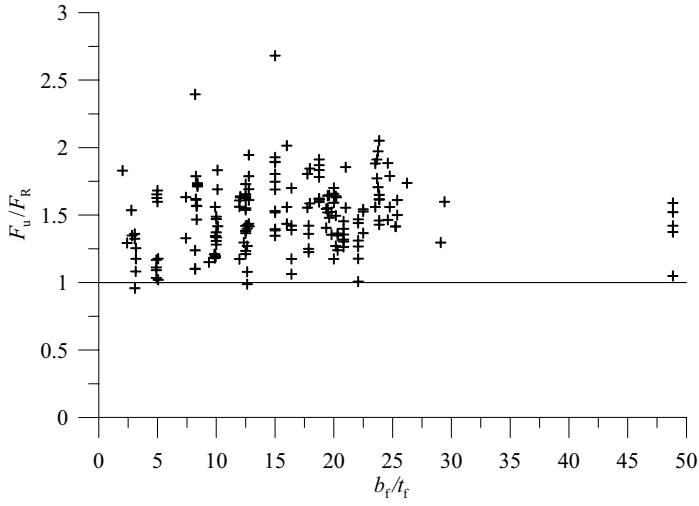


Figure D.3 F_u/F_R as a function of b_f/t_f for 184 tests.

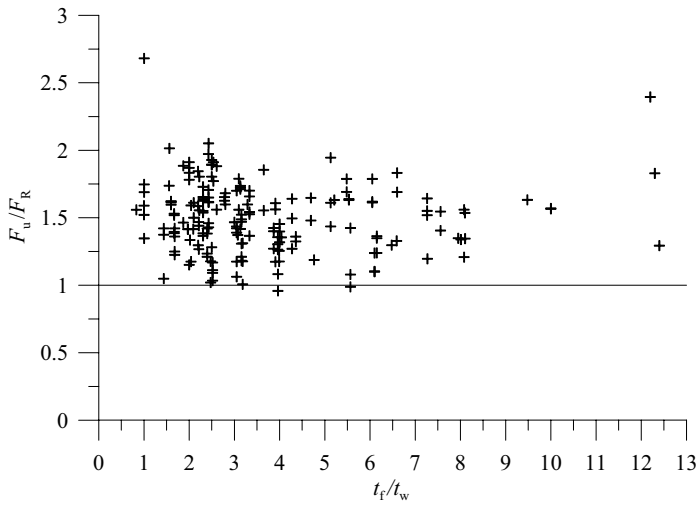


Figure D.4 F_u/F_R as a function of t_f/t_w for 184 tests.

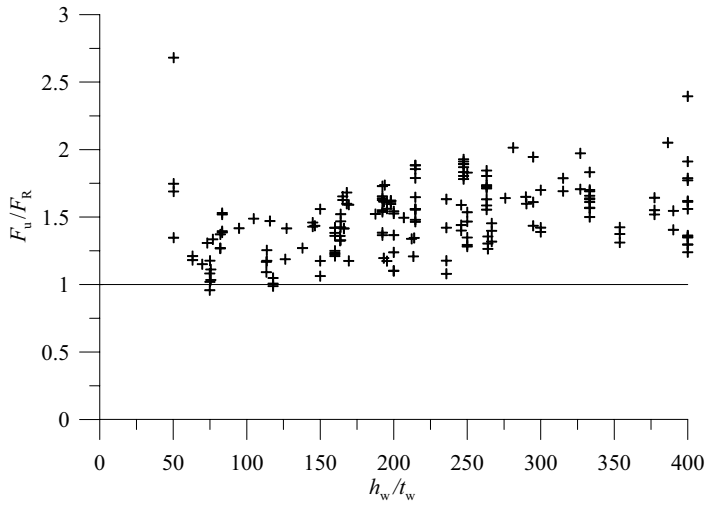


Figure D.5 F_u/F_R as a function of h_w/t_w for 184 tests.

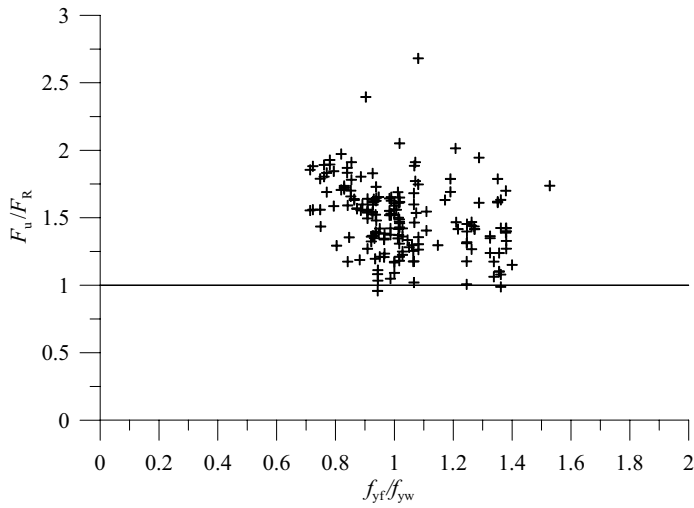


Figure D.6 F_u/F_R as a function of f_{yt}/f_{yw} for 184 tests.

APPENDIX E ANNEX D OF EN 1990 (2002)

Here, the method for determination of the partial factor that should be applied to the resistance according to Annex D of EN 1990 (2002), will be described.

The statistical evaluation is initiated by the determination of a resistance function on the form

$$r_t = g_{rt}(\underline{X}) \quad (\text{E.1})$$

where g_{rt} is the resistance formulae proposed in Equations (5.22) - (5.28). \underline{X} are the relevant basic variables that affect the resistance. In this stage measured values on the variables are used.

The theoretical resistance for each test, r_{ti} , is compared to the test results, r_{ei} , and the mean value of the correction factor b is estimated as the least square best-fit to the results according to

$$b = \frac{\sum r_e \cdot r_t}{\sum r_t^2} \quad (\text{E.2})$$

The probabilistic model for the resistance, r , can be represented as

$$r = b \cdot r_t \cdot \delta \quad (\text{E.3})$$

in which δ is an error term.

The mean value of the theoretical resistance function, calculated using the mean values \underline{X}_m of the basic variables, is obtained from

$$r_m = b \cdot r_t(\underline{X}_m) \cdot \delta = b \cdot g_{rt}(\underline{X}_m) \cdot \delta \quad (\text{E.4})$$

The next step is to estimate the coefficient of variation of the error term, δ . δ_i for each experimental value r_{ei} is determined from

$$\delta_i = \frac{r_{ei}}{b \cdot r_{ti}} \quad (\text{E.5})$$

From the values of δ_i an estimated value for the coefficient of variation of the error, V_δ , is determined with Equations (E.6) - (E.9).

$$\Delta_i = \ln(\delta_i) \quad (\text{E.6})$$

$$\bar{\Delta} = \frac{1}{n} \sum_{i=1}^n \Delta_i \quad (\text{E.7})$$

$$s_{\Delta}^2 = \frac{1}{n-1} \cdot \sum_{i=1}^n (\Delta_i - \bar{\Delta})^2 \quad (\text{E.8})$$

$$V_{\delta} = \sqrt{e^{s_{\Delta}^2} - 1} \quad (\text{E.9})$$

As the resistance function in this case is on the complex form

$$r = b \cdot r_t \cdot \delta = b \cdot g_{rt}(X_1, \dots, X_j) \cdot \delta \quad (\text{E.10})$$

the coefficient of variation, V_{rt} , for the basic variables included in the resistance function is obtained from

$$V_{rt}^2 = \frac{VAR[g_{rt}(X_m)]}{g_{rt}^2(X_m)} \cong \frac{1}{g_{rt}^2(X_m)} \cdot \sum_{i=1}^j \left(\frac{\partial g_{rt}}{\partial X_i} \sigma_i \right)^2 \quad (\text{E.11})$$

However, this gets very extensive and complicated for this case. Instead a fixed conservative value $V_{rt} = 0,08$ according to the research project EUR 20344 EN (2002) and Müller (2003)¹ is used.

The coefficient of variation for the resistance, V_r , is determined as

$$V_r = \sqrt{V_{\delta}^2 + V_{rt}^2} \quad (\text{E.12})$$

and the characteristic resistance, r_k , defined as the 5% fractile is obtained according to

$$r_k = b \cdot g_{rt}(X_m) \cdot e^{(-k_{\infty} Q - 0,5Q^2)} \quad (\text{E.13})$$

where

1. After discussions with Dr. Müller, RWTH, Aachen, Germany, who was involved in EUR 20344 EN (2002) and in his thesis Müller (2003) used $V_{rt} = 0,08$.

$$Q = \sigma_{\ln(r)} = \sqrt{\ln(V_r^2 + 1)} \quad (\text{E.14})$$

and k_∞ is the value of k_n for $n \rightarrow \infty$ $[k_\infty = 1,64]$

The design value of the resistance, r_d , is obtained from

$$r_d = b \cdot g_{\text{rt}}(X_m) \cdot e^{(-k_{d,\infty}Q - 0,5Q^2)} \quad (\text{E.15})$$

where $k_{d,\infty}$ is the value of $k_{d,n}$ for $n \rightarrow \infty$ $[k_{d,\infty} = 3,04]$

The partial factor for the resistance, γ_M , is determined as

$$\gamma_M = \frac{r_k}{r_d} = \frac{e^{(-k_\infty Q - 0,5Q^2)}}{e^{(-k_{d,\infty}Q - 0,5Q^2)}} \quad (\text{E.16})$$

However, instead of the 5% fractile value r_k , a resistance r_n with nominal values for the input variables is used to determine a corrected partial factor, γ_M^* , which is given by

$$\gamma_M^* = \frac{r_n}{r_d} = k_c \cdot \gamma_M \quad (\text{E.17})$$

with

$$k_c = \frac{r_n}{r_k} = \frac{1}{b} \cdot \frac{e^{(-2V_{fy} - 0,5V_{fy}^2)}}{e^{(-k_\infty Q - 0,5Q^2)}} \quad (\text{E.18})$$

Hence, k_c takes into account that f_y is not an average value but a minimum value.

